Interrogation of kinase-mediated signaling pathways to decode human cell division

by

Amber L. Lasek

A dissertation submitted in partial fulfillment of

the requirements for the degree of

Doctor of Philosophy

(Cellular and Molecular Biology)

at the

University of Wisconsin-Madison

2016

Date of final oral examination: November 22nd, 2016

The dissertation is approved by the following members of the Final Oral Committee

Mark Burkard, Associate Professor, Medicine

William Bement, Professor, Zoology

Shigeki Miyamoto, Professor, Oncology

Linda Schuler, Professor, Comparative Biosciences

Beth Weaver, Associate Professor, Cell and Regenerative Biology

Table of Contents

Abbreviations

APC/C-Anaphase Promoting Complex/Cyclosome

AS-Analog Sensitive

ATM-Ataxia Telangiectasia Mutated

ATP- Adenosine Triphosphate

BI- BI2536

CAK- Cdk-Activating Kinase

CDC20-Cell Division Cycle 20

Cdk1- Cyclin-Dependent Kinase 1

CI-Combination Index

CPC-Chromosomal Passenger Complex

DAD-D-box-Activating-Domain

DAPI-4',6-diamidino-2-phenylindole

DFG-Aspartic Acid-Phenylalanine-Glycine (motif)

DNA-Deoxyribonucleic Acid

Dox-Doxorubicin

DRC-Dose-response Curve

DUB- Deubiquitinating Enzyme

Flavo-Flavopiridol

GFP-Green Fluorescent Protein

pH3-Phosphorylated Histone H3

HR-Homologous Recombination

HRD- Histidine-Arginine-Aspartic Acid (motif)

INCENP- Inner Centromere Protein

IPdR- Ropidoxuridine

IUdR-5-iodo-2'-deoxyuridine

KT-Kinetochore

KT-MT-Kintochore-Microtubule

MAP- Mitogen-activated Protein

MAP2K (MAPKK)- Mitogen-activated Protein Kinase Kinase

MAP3K (MAPKKK)- Mitogen-activated Protein Kinase Kinase Kinase

MKLP1- Mitotic Kinesin-like Protein 1

MLN-MLN8237 (Alisertib)

MMR-Mismatch Repair

MPS1- Multipolar Spindle 1

mRNA- Messenger Ribonucleic Acid

MT-Microtubule

NHEJ- Non-Homologous End Joining

Noc-Nocodazole

PBD- Polo-Box Domain

PI- Propidium Iodide

Plk1- Polo-Like Kinase 1

RhoA- Ras Homolog Gene Family, Member A

RNA- Ribonucleic Acid

RNAi- Ribonucleic Acid Interference

siRNA- Small Interfering Ribonucleic Acid

TNBC- Triple-Negative Breast Cancer

WT- Wild Type

Preface

Protein interactions within a living cell are complex and are necessary for transmitting signals quickly and accurately. Kinases provide an important source of regulation and communication. They activate, inactivate, or change the conformation of a protein to alter signaling events and play important roles for triggering and maintaining signaling cascades. These processes are themselves restrained so that they occur at the correct time and place. Due to the complexity of these processes and the need for improved methods, there remain many unresolved questions regarding the interconnectedness of signaling pathways and the extent that posttranslational modifications on kinases play for regulating kinase activity and function.

Many kinases are known to be activated by phosphorylation within its catalytic loop; however, these proteins have multiple sites of modification including additional sites of phosphorylation and ubiquitination. Whether and how much these sites influence the activity and function of the kinase is unresolved. Using analog-specific kinases, I have discovered that Plk1 is not only regulated by the activating phosphorylation within the catalytic loop, T210, but also requires a neighboring site, T214. Additionally, other phosphorylation sites within the catalytic domain, but not in the C-terminal localization domain, redundantly control mitotic functions of Plk1 and cell cycle progression. These results demonstrate the intricacy of signaling to control and regulate Plk1.

Further analysis of the complexity of signaling within a cell is demonstrated by comparing the pathways of two proteins. For a cellular process, involved proteins can act in parallel or overlapping pathways. If they overlap, can moderately perturbing a pathway from multiple directions simultaneously cause a greater response than each individual assault? This idea was used to design a screen between differing therapeutic agents. Many

of the drugs include those that directly target proteins key to signaling pathways, kinases, while others were agents that would activate signaling pathways through error induction, such as mitotic checkpoint signaling activation with nocodazole treatment. Aurora A inhibition was found to potentiate the effect of a Plk1 inhibitor, a pan-Cdk inhibitor, and DNA damage response inducer, IUdR.

Overall, this work expands the knowledge of and provides insight into the way that signaling networks function within the cell. It reveals that Plk1, and likely other kinases, are regulated not only by a single T-loop residue but also others including redundant phosphorylations. Also, the screen demonstrates that multiple kinases or kinase mediated pathways can be targeted concurrently to elicit a larger response.

Chapter 1: Background

Amber L. Lasek

Protein Interactions and Signaling

Cell processes depend on signaling networks and cascades to transmit information and to progress the cell cycle when appropriate. These processes need to be efficient and are facilitated by enzymes that alter the activities of other enzymes. Kinases are one class of enzymes that help to ensure that cellular communication occurs in a timely manner. They signal rapidly by transferring a phosphate group to a target substrate, influencing the activity, expression, and/or conformation of itself or other proteins. This can trigger signaling cascades and influence the fate of a cell. For example, the mitogen-activated protein (MAP) kinases are activated by a MAP2K (MAPKK), which are in turn activated by a MAP3K (MAPKKK) (MacCorkle and Tan, 2005). This cascade can trigger numerous pro-growth or differentiation processes, including exit from G_0 to reenter the cell cycle (Nishida and Gotoh, 1993; Robinson and Cobb, 1997; Chang and Karin, 2001; Yamamoto *et al.*, 2006; Margadant *et al.*, 2013). Although kinase cascades are well recognized to control signaling pathways, their role in controlling mitosis remains poorly defined. The interactions between kinases and their pathways are a major focus of this thesis, especially those involved in cell growth and division. Notably, protein phosphorylation provides reversible control over cycle progression. In mitosis, Aurora B phosphorylation destabilizes kinetochore-microtubule attachments, delaying satisfaction of the mitotic checkpoint (Lampson *et al.*, 2004; Gregan *et al.*, 2011; Lampson and Cheeseman, 2011). This helps to preserve genomic fidelity by allowing for the correction of erroneous attachments prior to anaphase onset. Once proper attachments are made, Aurora B phosphorylation is reduced (in part by protein phosphatase 1), and mitosis continues.

Although phosphorylation controls many aspects of mitosis, it is fully reversible (Potapova *et al.*, 2006). By contrast, other molecular mechanisms, such as ubiquitination-

signaling proteolysis, control the unidirectionality of mitotic progression (Song and Rape, 2008; Wickliffe *et al.*, 2009). During mitosis, the transfer of an ubiquitin group to cyclin B by the ubiquitin ligase anaphase-promoting complex/cyclosome (APC/C) targets cyclin B for proteasomal degradation, enabling anaphase onset (Glotzer *et al.*, 1991; Hershko, 1999; Chang *et al.*, 2003). Conversely, if cyclin B levels are not reduced, the cell cannot transition from metaphase to anaphase, resulting in mitotic arrest. Although degradation is irreversible, the cell has deubiquitinating enzymes (DUBs) to help ensure that proteins aren't degraded too early (Rape *et al.*, 2006; Stegmeier *et al.*, 2007; Song and Rape, 2008). They remove ubiquitin by hydrolyzing the isopeptide bond (Naviglio *et al.*, 1998). DUBs themselves are regulated by protein-protein interactions, adding another layer of regulation (Naviglio *et al.*, 1998; Huang *et al.*, 2006; Stegmeier *et al.*, 2007). Besides targeting a substrate for degradation, the addition of ubiquitin moieties to a substrate can also alter its activity, regulate its cellular localization, or recruit other proteins (Wickliffe *et al.*, 2009). Collectively, cellular enzymes provide essential mechanisms for communication and triggering cell processes; in particular, they enable efficient but regulated information propagation that can progress or halt the cell cycle as necessary.

Kinases

Kinases are a class of proteins that facilitate the transfer of a phosphate group from ATP to a target protein; this can elicit many different effects on the substrate, including: (i) changing enzymatic activity; (ii) inducing protein-protein interactions; (iii) creating a signal for degradation (phospho-degron). Importantly, this modification is reversible (removed by protein phosphatases), allowing for temporary alterations in cell signaling. Modified amino acids include serines, threonines, tyrosines, and histidines. Protein kinases contain an N-

terminal lobe and a C-terminal lobe which are connected by a hinge region. In general, the C-terminal lobe recognizes the sequence up and downstream of the targeted residue and contains the kinase domain (Lowe *et al.*, 1997; Williams and Cole, 2001). The ATP binding pocket in the kinase domain is a hydrophobic region that accommodates the γ-phosphate of ATP (Bayliss *et al.*, 2012). ATP binds in the opening between the lobes in the highly conserved activation segment/loop or T-loop (Johnson *et al.*, 1996; Huse and Kuriyan, 2002; Nolen *et al.*, 2004; Bayliss *et al.*, 2012). The γ-phosphate of ATP is activated by a magnesium ion coordinated by the aspartic acid of the DFG motif (Johnson *et al.*, 1996; Nolen *et al.*, 2004; Bayliss *et al.*, 2012). The DFG motif is highly conserved and is essential for active kinases. Another conserved and essential aspartic acid is in the HRD motif (Johnson *et al.*, 1996). This aspartic acid is conserved among kinases activated by T-loop phosphorylation and is important for catalytic activity because it deprotonates the target residue of the substrate (Knighton *et al.*, 1991). Kinases themselves are regulated by posttranslational modifications and protein-protein interactions. The efficiency and efficacy of these processes are especially important in stages such as mitosis to provide rapid response to events in minutes.

Mitotic Kinase Regulation

Kinases are key players for progressing and restricting the cell cycle and need to be tightly regulated. The kinases featured in this thesis are Plk1, Aurora A, and Cdk1. The conserved polo-like kinase family consists of 5 members (Plk1-4)(Llamazares *et al.*, 1991; Clay *et al.*, 1993; Lake and Jelinek, 1993; Fode *et al.*, 1994; Golsteyn *et al.*, 1994, 1996; Hamanaka *et al.*, 1994; Holtrich *et al.*, 1994; Li *et al.*, 1996; Glover *et al.*, 1998). All contain an N-terminal kinase domain and a characteristic C-terminal polo-box domain (PBDs),

consisting of one or more polo-box repeats (Golsteyn *et al.*, 1996; Lowery *et al.*, 2005). Plk1 is an essential cell cycle and mitotic regulator and is itself regulated by phosphorylation, ubiquitination, and binding to phosphorylated substrates. Plk1's PBD binds to substrates by recognizing a *primed* phosphorylation site on the protein. *Priming* is where a kinase first phosphorylates the target protein, allowing for Plk1 *docking* and subsequent phosphorylation of the substrate (Elia *et al.*, 2003b; Lee *et al.*, 2008). Many Plk1 substrates are *primed* by Cdk1 or Plk1 itself, and Plk1 has a binding preference for substrates with the conserved S-[pS/pT]-P/X motif (Elia *et al.*, 2003a, 2003b; Lee *et al.*, 2008). Binding to these phosphorylated substrates is disrupted by the pincer mutant H538A/K540M (Elia *et al.*, 2003a; Qi *et al.*, 2006; Burkard *et al.*, 2009). Plk1 is believed to be activated by phosphorylation within Plk1's T- or activation-loop at threonine 210 (T210) by Aurora A and possibly Aurora B (Macůrek *et al.*, 2008; Seki *et al.*, 2008; Carmena *et al.*, 2012; Bruinsma *et al.*, 2014; Lasek *et al.*, 2016). In the unphosphorylated state, Plk1 resides in a closed confirmation that involves self-interaction with the (PBD). Interaction with the protein Bora opens Plk1, allowing for phosphorylation by Aurora. Plk1 ubiquitination does not appear to be strictly required as I will demonstrate in Chapter 2, however modification at K492 may regulate Plk1 removal from kinetochores at the metaphase-anaphase transition (Beck *et al.*, 2013). Plk1 expression is cell cycle regulated and is essential for proper mitotic exit and cytokinesis. The C-terminus of Plk1 contains the conserved destruction box RxxL (R337, L340 in Plk1) and degradation is mediated by the APC/C bound to Cdh1 (Lindon and Pines, 2004; Bassermann *et al.*, 2008). Overall, Plk1 is regulated by phosphorylations on itself and on target substrates and through controlled expression. The requirement for multiple levels of regulation is a common feature of crucial biologic pathways, as it is a fail-safe.

The Aurora kinases are another cell cycle regulated kinase family. In mammals, there are three members of the Aurora family: A, B, and, C. Aurora B and C are both members of the chromosomal passenger complex (CPC)(Fu *et al.*, 2007). Aurora A localizes and operates on the mitotic spindle and at the centrosome (Gopalan *et al.*, 1997; Kimura *et al.*, 1997; Schumacher *et al.*, 1998; Berdnik and Knoblich, 2002; Asteriti *et al.*, 2011). Aurora A is activated by autophosphorylation within its T-loop at threonine 288 (T288) that is facilitated by its binding partner TPX2 (Dodson and Bayliss, 2012; Zorba *et al.*, 2014). It's also been shown that TPX2 binding alone is sufficient to increase Aurora A activity and this dephosphorylated form may be important for Aurora A functions at the spindle microtubules (Dodson and Bayliss, 2012; Zorba *et al.*, 2014). Aurora is degraded in a similar fashion to Plk1 in that it has a C-terminal D- box (R378) that targets it for degradation by Cdh1-bound APC/C; however, the D-box is only functional with an intact D-box-activating-domain (DAD) (Honda *et al.*, 2000; Castro *et al.*, 2002a, 2002b; Littlepage and Ruderman, 2002). Regulation of Aurora A expression is essential and overexpression has been attributed to mitotic errors and aneuploidy (Hoar *et al.*, 2007; Nikonova *et al.*, 2013; Asteriti *et al.*, 2014).

In contrast to the polo-like and Aurora kinases, the expression of cyclin-dependent kinases (Cdks) are not cell cycle regulated (Morgan, 1995). Instead, the oscillation of their interaction partners, the cyclins, controls Cdk activities. Cdk-cyclin binding activates the complex and, together, these proteins provide an important source of regulation by moderating cell cycle progression and transcription (Lim and Kaldis, 2013; Malumbres, 2014). There are thought to be 16 (and counting) Cdks in mammals, but Cdk1, especially, has important roles for regulating mitosis (Malumbres, 2014). Cdk1 binds cyclin B and helps regulate centrosome separation, the G2/M transition, and mitotic exit (Murray *et al.*, 1989; Nurse, 1990; Karsenti, 1991; Blangy *et al.*, 1995; Jackman *et al.*, 2003; Gavet and

Pines, 2010). Phosphorylation of Cdk1 threonine 161 (T161) by Cdk activating kinase (CAK) helps to stabilize this interaction and maintain the active conformation (Russo *et al.*, 1996; Larochelle *et al.*, 2007; Deibler and Kirschner, 2010). Cdk1 is also inhibited by phosphorylation at tyrosine 15 (Y15) by Wee1 (and at Y14 by Myt1) (Deibler and Kirschner, 2010; Chow *et al.*, 2011). Importantly, this inhibitory phosphorylation can be reversed by the members of the protein phosphatase family, Cdc25 (Borgne and Meijer, 1996). The balance between Cdk1 activation and inactivation appears to be at least minimally determined by localization (Takizawa and Morgan, 2000). During interphase, Wee1 is localized to the nucleus where it can confine Cdk1 to the inactivated state (Heald *et al.*, 1993); however, as the cell cycle progresses, Cdk1 translocation to the nucleus increases, possibly diluting Wee1 inhibitory signals and allowing for Cdk1 activation (Takizawa and Morgan, 2000). Once the cycle is ready to proceed, active Cdk1, Plk1, and Aurora A stimulate efficient signaling and orchestrate mitosis.

Interplay of Kinase Signaling In and Immediately Prior to Mitosis

The mitotic stage of the cell cycle is responsible for separating the duplicated genetic content but occurs on a comparatively short timeframe, so it's important that signaling occurs quickly and accurately. Kinase phosphorylation provides a solution for this problem and thus plays important roles for signal transmission during mitosis.

Many kinases that are active during mitosis are upregulated beginning in G2 (Katayama *et al.*, 2003; Lindon and Pines, 2004). Prior to mitotic entry, the cell needs to ensure that DNA replication occurred faithfully and that no errors remain; this is the DNA damage checkpoint (Figure 1-1). Some of the key mitotic kinases involved in this checkpoint are Wee1, Cdk1, Plk1, and Aurora A (Smits *et al.*, 2000; Macůrek *et al.*, 2008; van Vugt *et al.*,

2010). Major sources of DNA damage are double-stranded breaks which can be caused by chemicals, radiation, or cases where single-stranded breaks from errors in repair, replication, or mechanical stress become double-stranded. These breaks are detected by the Mre11-Rad50-Nbs1 complex and H2AX is recruited to the site of breaks following phosphorylation by ATM kinase (Paull *et al.*, 2000; Yuan and Chen, 2010). Repair is carried out by non-homologous end-joining (NHEJ) or homologous recombination (HR). Once damage is detected, pATM targets Chk2. Chk2 inactivates Cdc25 phosphatases, maintaining inhibitory phosphorylation of Cdk1-cyclin B by Wee1. Once all the damage is repaired, Cdc25 phosphatases remove the inhibitory phosphorylation, allowing for Cdk1-cyclin B activity. In a parallel and overlapping pathway, cells require active Plk1 to recover from DNA damage and enter mitosis (Macůrek *et al.*, 2008). As mentioned above, Plk1 is phosphorylated by Aurora A and the co-factor, Bora (Seki *et al.*, 2008; Bruinsma *et al.*, 2014). Upon DNA damage, however, activated ATM/ATR phosphorylates Bora, signaling it for degradation (Hyun *et al.*, 2014). This blocks Plk1 activation and arrests cells in G2. Conversely, constitutively active Plk1 can bypass the DNA damage-induced G2 arrest, though this is controversial (Smits *et al.*, 2000; Paschal *et al.*, 2012). It's also been demonstrated that Cdk1 phosphorylates Bora, but in this instance, phosphorylation increases Plk1 activity and promotes mitotic entry (Thomas *et al.*, 2016). Further demonstrating the interconnectedness of this pathway, Plk1 also plays a role in the activation of Cdk1. Active Plk1 phosphorylates Cdc25C, promoting Wee1 degradation (Watanabe *et al.*, 2004; Tsvetkov *et al.*, 2005) and facilitating Cdk1-cyclin B activation (van Vugt *et al.*, 2004). Once the damage in the cell is repaired, Bora is restored, Cdc25 is active, and the cell can enter mitosis. Beginning in G2 and extending into early mitosis, Plk1, Aurora A, and Cdk1 function and cooperate to assist in generating the mitotic spindle apparatus.

Kinases play roles in many aspects of mitosis. Plk1, Aurora A, and Cdk1 have roles in centrosome maturation and establishment of the bipolar spindle which determine whether and how quickly mitosis will progress. All three proteins localize at or near the centrosomes in G2 and early mitosis (Lee *et al.*, 1998; Jackman *et al.*, 2003; De Luca *et al.*, 2006; Joukov *et al.*, 2010; Santamaria *et al.*, 2011). Evidence in *Xenopus* and mammals shows that the centrosomal protein Cep192 recruits Plk1 and Aurora A to the centrosome and works as a scaffold, facilitating activation of each kinase; here, Aurora A dimerizes to autophosphorylate and active Aurora A phosphorylates and activates Plk1 (Joukov *et al.*, 2010, 2014). Centrosome maturation and separation begins in interphase but is essential for mitotic progression as monopolar spindles result in prometaphase arrest. Plk1 inhibition, knockdown, or knockout results in monopolar spindles and was named because of this characteristic phenotype (Sunkel and Glover, 1988; Llamazares *et al.*, 1991; Glover *et al.*, 1995). Without proper spindle formation, the cell will not be able to establish proper kinetochore-microtubule attachments, to satisfy the mitotic (or spindle-assembly) checkpoint. Plk1's importance for establishing the bipolar spindle is firmly established and evidence supports that this is due to errors in centrosome maturation, centrosome migration, and γ-tubulin and pericentrin recruitment (Lane and Nigg, 1996; Nigg *et al.*, 1996; Liu and Erikson, 2002; Casenghi M, Meraldi P, Weinhart U, Duncan PI, Körner R, Nigg, 2003; Sumara *et al.*, 2004; van Vugt *et al.*, 2004; Haren *et al.*, 2009; Johmura *et al.*, 2011; Lee and Rhee, 2011; Smith *et al.*, 2011). Aurora A similarly is proposed to be important for centrosome maturation, although there are some differences seen between species (Glover *et al.*, 1995; Bischoff and Plowman, 1999; Goepfert and Brinkley, 2000; Hannak *et al.*, 2001; Katayama *et al.*, 2001; Berdnik and Knoblich, 2002; Marumoto *et al.*, 2003, 2005). Cdk1, however, appears to have a more minor role in centrosome separation. Eg5 binding to the spindle requires phosphorylation by Cdk1 (Blangy *et al.*, 1995; Sawin and Mitchison, 1995;

Cahu *et al.*, 2008). In spite of this, centrosome separation can occur in the absence of Cdk1, but the process is significantly delayed (Gavet and Pines, 2010; Smith *et al.*, 2011). Plk1, Aurora A, and Cdk1 play significant roles in the establishment of bipolar spindle (by metaphase). As mitosis progresses, these kinases continue to be important as the cell divides its chromosomes.

Early in mitosis and into anaphase, Plk1 and Aurora A are crucial for proper distribution of genetic material. Although cells with low Plk1 and Aurora can establish a bipolar spindle and proceed to anaphase, cells frequently missegregate chromosomes (Hanisch *et al.*, 2006; Asteriti *et al.*, 2011; Lera and Burkard, 2012). Aurora A is necessary to not only achieve a bipolar spindle, but also to maintain it. Aberrant Aurora A expression can cause spindle fragmentation and microtubule hyperstabilization leading to abnormal divisions including multiway divisions (De Luca *et al.*, 2008; Asteriti *et al.*, 2011, 2014). Similarly, reduced active Plk1 leads to abnormal divisions resulting in lagging chromosomes (Lera and Burkard, 2012). This appears to be due to regulation of kinetochore-microtubule attachments where Plk1 stabilizes K-MT attachments (Sumara *et al.*, 2004; O'Connor *et al.*, 2015). Plk1 may itself have roles in the mitotic checkpoint, however this is controversial (Sumara *et al.*, 2004; van Vugt *et al.*, 2004; Lenart *et al.*, 2007; Beck *et al.*, 2013; von Schubert *et al.*, 2015).

Proper anaphase and mitotic exit depends on inactivation and/or degradation of all three kinases discussed here: Plk1, Aurora A, and Cdk1. As mentioned above, Plk1 and Aurora A degradation is dependent on the switch from Cdc20-bound APC/C to Cdh1-bound (Castro *et al.*, 2002a; Littlepage and Ruderman, 2002; Lindon and Pines, 2004; Floyd *et al.*, 2008). Mutation of their respective D-boxes reduces degradation of the protein and overexpression or inhibition of the kinase delays mitotic exit (Castro *et al.*, 2002a; Lindon

and Pines, 2004; Reboutier *et al.*, 2015). However, Plk1 and Aurora A also have essential roles from anaphase to the end of mitosis. Plk1 binding to anaphase furrow and midbody components are essential for furrow ingression and cytokinesis (Petronczki *et al.*, 2007; Wolfe *et al.*, 2009; Lera and Burkard, 2012). Plk1 phosphorylates numerous proteins including Mklp1 and hCyk4 (also known as MgcRacGAP) (Neef *et al.*, 2003; Burkard *et al.*, 2009). Plk1 inhibited cells show reduced recruitment of Ect 2, Rho A, citron kinase, and anillin (Burkard *et al.*, 2007, 2009). Failure to phosphorylate and/or recruit these core components to the equator, results in cytokinesis failure and binucleate cells. Similarly, Aurora A inhibition disrupted the central spindle, causing cytokinesis failure and an increase in binucleate cells (Reboutier *et al.*, 2013). These phenotypes appear to be caused by disgregulation of microtubule dynamics, possibly mediated through a loss of Aurora A phosphorylation of the dynactin component, $p150^{glued}$ (Romé *et al.*, 2010; Reboutier *et al.*, 2013).

Cdk1, however, is not degraded. Instead, inactivation depends on the degradation of its binding partner, cyclin B (Gavet and Pines, 2010). Interestingly, high levels of Cdk1 during the previous interphase are essential for sufficient activation of the APC/C. Without this phosphorylation, cyclin B ubiquitination, and therefore Cdk1 inactivation, does not occur, showing Cdk1 self-regulation (Patra and Dunphy, 1998; Rudner *et al.*, 2000; Lindqvist *et al.*, 2007). Cdk1 activity can also be reduced towards the end of mitosis through the same Wee1 catalyzed inhibitory phosphorylation (Y15) as discussed above (Potapova *et al.*, 2009). Finally, Cdc14 phosphatase dephosphorylates Cdk1 targets, without which cytokinesis does not occur. As an example, the removal of the Cdk1 phosphorylation on PRC1 allows for PRC1 dimerization and midzone localization (Zhu *et al.*, 2006). In the absence of this, proper microtubule bundling and midzone formation is impaired.

This summary of Plk1, Aurora A, and Cdk1 activities makes obvious the interplay between these kinases and the overlap in the processes they regulate. They serve as important regulators of cell cycle progression before and during mitosis (Macůrek *et al.*, 2008; Van Horn *et al.*, 2010; Asteriti *et al.*, 2015) and inhibition or knockout results in cell cycle and mitotic arrest. As mentioned above, Plk1, Aurora A, and Cdk1 have roles in mitotic entry and the recovery from DNA damage, in achieving a bipolar spindle, and at the end of mitosis. So far we know that Cdk1 phosphorylation creates docking sites on Plk1 substrates for Plk1 binding, Plk1 targets Wee1 for degradation, and Cdk1 inhibition prevents mitotic activation of Aurora A, but Aurora A inhibition does not inhibit Cdk1 activation (Van Horn *et al.*, 2010). Additionally, it is known that Plk1 activation requires release of the inhibitory association between the PBD and kinase domain and T-loop phosphorylation. This is mediated through co-factor (Bora) and substrate binding and phosphorylation at residue T210 by Aurora A. What remains unknown is whether the many other phosphorylations and ubiquitinations on Plk1 have important functional roles for Plk1 and how these kinases interact functionally.

Interactions of Kinase Inhibitors in Cancer Therapy

The functional relationships between mitotic kinases suggest a possible role for combination cancer therapy. Heretofore, the role that kinases play in mitosis led to the development of clinical inhibitors as cancer therapeutics. However, the effects of these drugs in the clinic have been modest. The pan-Cdk inhibitor flavopiridol, was the first Cdk inhibitor to enter clinical trials; however low specificity and potency responses have not been sufficient to justify further use as a single agent (Komlodi-Pasztor *et al.*, 2012; Blachly and Byrd, 2013; Lanasa *et al.*, 2015; Murphy and Dickler, 2015). With this, doses need to be

limited due to toxicities such as diarrhea and neutropenia. Combination studies with flavopiridol are in trials and a few studies have looked promising. Flavopiridol in combination with other chemotherapeutic agents such as Taxol or with cytosine arabinoside and mitoxantrone (FLAM) have shown lower toxicities and more favorable patient responses (Colevas *et al.*, 2002; Schwartz *et al.*, 2002; Zhai *et al.*, 2002; Karp *et al.*, 2011; Marzo and Naval, 2013). These results advocate for further analysis of the benefits of flavopiridol treatment in combination.

Also marred by problems with efficacy vs toxicity ratios, trials using the Aurora inhibitor MLN8054 have been terminated due to somnolence (Malumbres and Pérez de Castro, 2014). In part, this was believed to be due to off-target GABA-binding (Dees *et al.*, 2011). In response, Takeda introduced MLN8237, an Aurora inhibitor with much higher potency for Aurora A inhibition (Karthigeyan *et al.*, 2011; Kollareddy *et al.*, 2012; Sells *et al.*, 2015; D'Assoro *et al.*, 2016). Although this inhibitor displays similar GABA-binding to MLN8054, toxicities related to this target were mitigated (Sells *et al.*, 2015). A phase 2 trial showed an objective response to MLN8237 in 18% of breast cancer patients (Melichar *et al.*, 2015); however, in a phase 3 trial, the primary endpoint was not expected to be met and the trial was terminated (NCT01482962) (D'Assoro *et al.*, 2016). With the hopes to actualize MLN8237 use clinically, MLN8237 combination studies have begun (Matulonis *et al.*, 2012; Marzo and Naval, 2013; DuBois *et al.*, 2016; Graff *et al.*, 2016). Patients with small cell lung cancer (SCLC) are being treated in combination with paclitaxel with the hopes to find an effective and safe dose (NCT02038647) (U.S. National Institutes of Health, 2013). Although results have been discouraging overall, the efficacy of MLN8237 has not been fully resolved.

The Plk1 targeting BI2536 is another kinase inhibitor where the benefits of combination therapy have not been fully elucidated. Its use in monotherapy initially looked

promising (Mross *et al.*, 2008; Schöffski, 2009; Sebastian *et al.*, 2010; Frost *et al.*, 2012), but has been terminated. BI2536 demonstrates polypharmacological activity and a short half-life in vivo; therefore, it is being replaced with BI6727, which has shown more favorable results (Rudolph *et al.*, 2009; Schöffski *et al.*, 2010; Mross *et al.*, 2012; Vose *et al.*, 2013). Despite this, BI2536 use in combination encourages further analysis (Hofheinz *et al.*, 2010; Ellis *et al.*, 2013); however, clinicaltrials.gov does not list any active BI2536 trials and published studies using the drug clinically are sparse (Haroon, 1998; U.S. National Institutes of Health, 2013). While, in general, single-agent kinase inhibitors have not performed well, the known functional interactions between kinases and their pathways suggest possible benefits from use in combination. Further exploration *in vitro* may identify valuable interactions to exploit clinically.

Scope of Project

Overall, I have delved into uncovering the ways that mitotic kinases interact.

Gap 1: Posttranslational Regulation of Plk1

Here, I develop a chemical-genetic complementation system for Plk1 and use it to methodically evaluate the functional roles of each of 25 phosphorylation sites and nine ubiquitination sites on this kinase singly and in combination. This reveals that two residues within Plk1's T-loop (T210 and T214) are essential, while all other sites of phosphorylation or ubiquitin modification are individually nonessential; instead, phosphorylation events within the kinase domain operate redundantly to perform its essential mitotic functions (Chapter 2). This demonstrates the existence of redundancy as a source of kinase regulation. The varying levels of Plk1 regulation exemplify a mechanism for moderating

kinase activity, so that signaling cascades are not triggered without proper upstream signals.

Gap 2: Identifying new interactions between kinase inhibitors

Although it's known that Plk1, Aurora A, and Cdk1 have roles regulating each other and similar cell processes, elucidation of the overlap between their respective pathways remains to be fully resolved. Additionally, whether these pathways can be targeted simultaneously to reduce cell growth has not been shown. Clinically, Cdk1, Plk1, and Aurora A inhibitors have not shown an adequate therapeutic window and although combination studies have been proposed, these do not include multiple kinase pathway targeting drugs. I demonstrate that the Aurora inhibitor, MLN8237, cooperates with: the Plk1 inhibitor BI2536 to induce apoptosis, the Cdk inhibitor flavopiridol to delay mitotic entry, and the radiosensitizer IUdR by compounding DNA damage. In all, these drugs combine to reduce cell growth *in vitro* and *in vivo*.

Figure 1-1

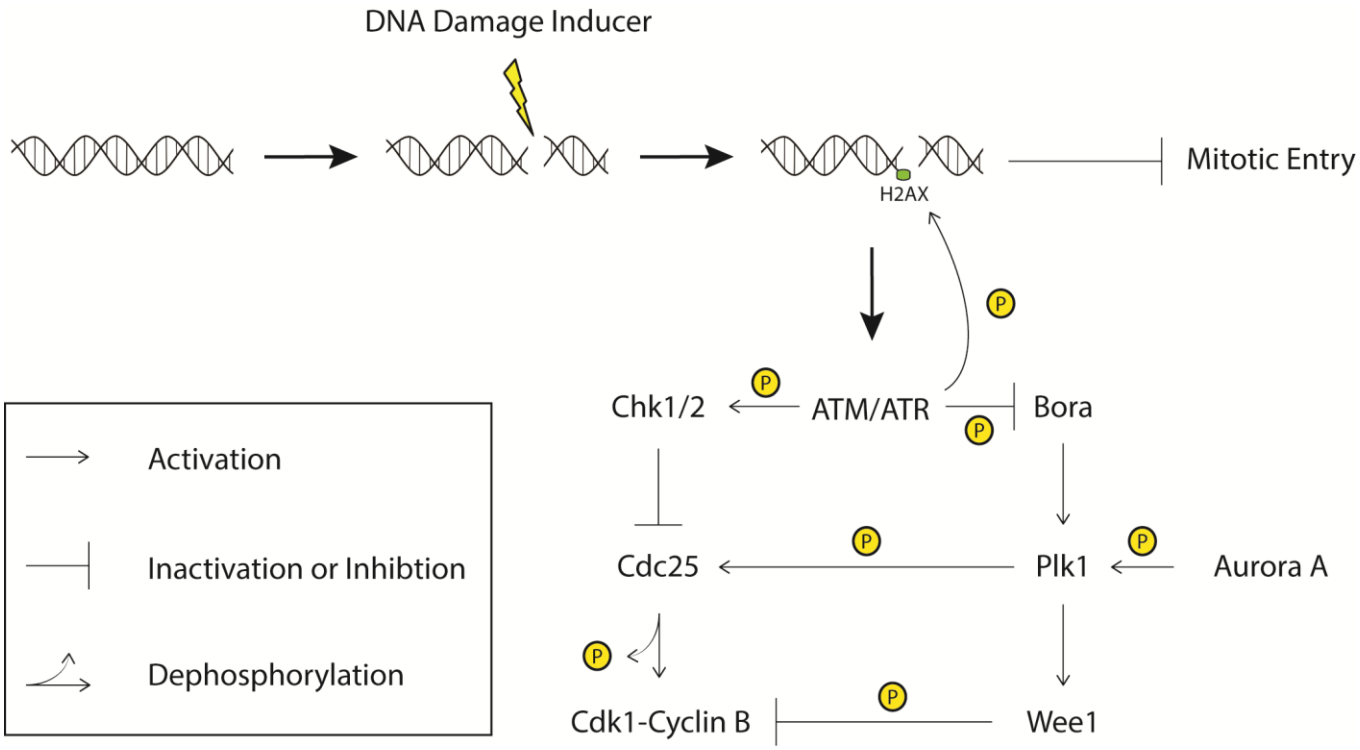
DNA Damage Inducer
H2AX
Mitotic Entry
P
Chk1/2
ATM/ATR
Bora
Activation
Inactivation or Inhibtion
Dephosphorylation
Cdc25
Plk1
Aurora A
Cdk1-Cyclin B
Wee1

Figure 1-1: Kinase signaling regulates the DNA damage checkpoint.

Figure depicts signaling pathways involved in halting cells at the G2-M transition in response to damaged DNA.

Chapter 2: The functional significance of posttranslational modifications on Polo-like kinase 1 revealed by chemical genetic complementation

Work in this chapter was modified from article published in *PLoS One*:

The functional significance of posttranslational modifications on Polo-like kinase 1 revealed by chemical genetic complementation

Lasek AL, McPherson BM, Trueman NG, Burkard ME

PLoS One. 2016 Feb 26;11(2). PMCID: PMC769148

Abstract

Mitosis is coordinated by carefully controlled phosphorylation and ubiquitin-mediated proteolysis. Polo-like kinase 1 (Plk1) plays a central role in regulating mitosis and cytokinesis by phosphorylating target proteins. Yet, Plk1 is itself a target for posttranslational modification by phosphorylation and ubiquitination. We developed a chemical-genetic complementation assay to evaluate the functional significance of 34 posttranslational modifications (PTMs) on human Plk1. To do this, we used human cells that solely express a modified analog-sensitive Plk1 ($Plk1^{AS}$) and complemented with wildtype Plk1. The wildtype Plk1 provides cells with a functional Plk1 allele in the presence of 3-MB-PP1, a bulky ATP-analog inhibitor that specifically inhibits $Plk1^{AS}$. Using this approach, we evaluated the ability of 34 singly non-modifiable Plk1 mutants to complement $Plk1^{AS}$ in the presence of 3-MB-PP1. Mutation of the T-loop activating residue T210 and adjacent T214 are lethal, but surprisingly individual mutation of the remaining 32 posttranslational modification sites did not disrupt the essential functions of Plk1. To evaluate redundancy, we simultaneously mutated all phosphorylation sites in the kinase domain except for T210 and T214 or all sites in the C-terminal polo-box domain (PBD). We discovered that redundant phosphorylation events within the kinase domain are required for accurate chromosome segregation in anaphase but those in the PBD are dispensable. We conclude that PTMs within the T-loop of Plk1 are essential and nonredundant, additional modifications in the kinase domain provide redundant control of Plk1 function, and those in the PBD are dispensable for essential mitotic functions of Plk1. This comprehensive evaluation of Plk1 modifications demonstrates that although phosphorylation and ubiquitination are important for mitotic progression, many individual PTMs detected in human tissue may have redundant, subtle, or dispensable roles in gene function.

Introduction

In mitosis, posttranslational modifications (PTMs) are crucial for regulating protein function and degradation (Walter *et al.*, 2000; Lindon and Pines, 2004; Burkard *et al.*, 2009; Lindqvist *et al.*, 2009; Beck *et al.*, 2013). Mass spectrometry has identified a large set of mitotic posttranslational modifications (Daub *et al.*, 2008; Khoury *et al.*, 2011; Hornbeck *et al.*, 2012; Oppermann *et al.*, 2012), but functional annotation is sparse. Therefore, it is critical to develop efficient techniques to accurately interrogate PTM function. Towards this goal, we have thoroughly evaluated PTMs on polo-like kinase 1 (Plk1), a core regulator of mitosis using chemical genetic complementation.

Plk1 is an ideal target for analysis because it is essential and plays multiple roles in mitotic progression. Knockout of PLK1 in mice results in embryonic lethality and, in human cells, failure of mitotic progression and proliferation (Burkard *et al.*, 2007; Lu *et al.*, 2008). Complete loss of Plk1 function arrests cells in prometaphase, yet it also plays roles in other mitotic stages. Specifically, Plk1 is involved in mitotic entry after DNA damage (Bassermann *et al.*, 2008; Macůrek *et al.*, 2008; van Vugt *et al.*, 2010), centrosome separation (Sumara *et al.*, 2004; van Vugt *et al.*, 2004; Johmura *et al.*, 2011), stabilizing kinetochore-microtubule attachments (Sumara *et al.*, 2004; van Vugt *et al.*, 2004; Elowe *et al.*, 2007), removal of cohesin from sister chromatids (Sumara *et al.*, 2004; Hanisch *et al.*, 2006), and in triggering cytokinesis (Neef *et al.*, 2003, 2007, Burkard *et al.*, 2007, 2009). Thus it is possible that distinct Plk1functions depend on specific PTMs.

Here, we present a comprehensive strategy to evaluate the functional significance of PTMs on Plk1. We first evaluated databases of human Plk1 to identify 34 phosphorylation and ubiquitination modifications (Figure 2-1A) (Gnad *et al.*, 2011; Hornbeck *et al.*, 2012; Kasahara *et al.*, 2013). One crucial site is the activation loop phosphorylation on threonine

210. This site is phosphorylated by Aurora kinases A and/or B and the inability of cells to phosphorylate this residue leads to the Plk1-null phenotype (van Vugt *et al.*, 2004; van de Weerdt *et al.*, 2005; Hanisch *et al.*, 2006; Seki *et al.*, 2008; Carmena *et al.*, 2012; Bruinsma *et al.*, 2014). Modifications at S137 and S326 have also been implicated in regulation of Plk1 functions. Phosphorylation at S137 increases the activity of Plk1 and is reduced in response to DNA damage (Jang *et al.*, 2002; Tsvetkov and Stern, 2005). Phosphorylation of Plk1 S326 promotes progression through mitosis (Tang *et al.*, 2008). Additionally, ubiquitination of K492 may be important for removal of Plk1 at the metaphase-anaphase transition (Beck *et al.*, 2013). However, the function of most posttranslational sites remains obscure.

To evaluate the function of the identified PTMs, We used non-modifiable mutant Plk1 to complement in a chemical genetic system. We employed previously established Plk1^{AS} cells as a chemical genetic tool to probe functions of Plk1 (Burkard *et al.*, 2007). The analog-sensitive system is a versatile technique for studying kinases that provides a method for potent and reversible chemical inhibition with explicit controls for off-target effects (Bishop *et al.*, 2000). In this system, GFP-tagged recombinant Plk1 (C67V/L130G) analog-sensitive (AS) mutant (GFP-Plk1^{AS}; Figure 2-1B) was introduced into human hTERT-immortalized retinal pigment epithelial cells (RPE1) in which both endogenous alleles had been deleted. Plk1^{AS} is fully inactivated by 3-methylbenzyl pyrazolopyrimidine (3-MB-PP1) to reveal the Plk1 inhibition phenotypes including mitotic arrest and immature spindle poles.

Using this complementation assay, Plk1^{AS} cells were stably transduced with a second construct to express Flag-tagged Plk1 that harbors a wildtype kinase domain (Plk1^{WT}) and is thus resistant to 3-MB-PP1, allowing for chemical genetic complementation (Burkard *et al.*, 2012) (Figure 2-1B). When challenged with 3-MB-PP1, the complementing

wildtype Plk1 restores activity, allowing cells to complete normal mitosis (Burkard *et al.*, 2012). We then introduced mutations into the Plk1 rescue construct to determine whether non-modifiable mutants can execute specific functions within mitosis. This system, chemical genetic complementation, allows for rapid temporal inhibition and we demonstrate that it can robustly identify functional PTMs on Plk1.

As we report here, most PTMs on Plk1 have redundant or subtle functions when evaluated singly. Only single PTMs in the kinase activating loop are essential for mitotic progression and long-term proliferation. Additional kinase domain sites operate redundantly. In contrast phosphorylation sites in the PBD are dispensable for essential Plk1 functions as a 16-site mutant restores viability. These data reveal the complexity of PTM-regulation of an essential mitotic protein wherein some PTMs are strictly required, some are redundant, and many are dispensable.

Results

Functional survey of PTMs on Plk1

To evaluate the functional significance of previously identified PTMs, we surveyed 34 mutations which prevent phosphorylation or ubiquitination of Plk1, selected from modification sites identified in proteomic analyses (Gnad *et al.*, 2011; Hornbeck *et al.*, 2012; Kasahara *et al.*, 2013). To do this, we stably expressed constructs each harboring a single non-modifiable mutation. Constructs were generally expressed at levels close to or greater than GFP-Plk1^{AS} (Figure 2-2A). To survey these for function, we challenged each cell line with 10 μM 3-MB-PP1 and evaluated for mitotic arrest (Figure 2-2B,C) and proliferation (Figure 2-2D). These two assays were selected because the mitotic arrest phenotype evaluates the function of Plk1 in assembling a mitotic spindle, whereas long-term

proliferation requires Plk1 to execute its non-spindle mitotic functions. Additionally, hits in the mitotic arrest phenotype using polyclonal cell lines (Figure 2-2B) were re-evaluated in two clonal cell lines (Figure 2-2C and Supplemental Figure 2-1A) to rule out artificial elevation in mitotic index through a sub-population of low-expressing cells.

As expected, mitotic arrest and proliferation defects occur in control (Flag Only), but not in cells rescued by Flag-Plk1^{WT}, which is unaffected by 3-MB-PP1(Figure 2-2B,C,D; leftmost bars or wells) (Burkard *et al.*, 2012). Strikingly, most singly non-modifiable mutants of Plk1 restored mitotic progression and cell viability. A key exception is that bona fide mitotic arrest occurs with Plk1^{T210V}, as noted previously, validating our assay (van Vugt *et al.*, 2004; van de Weerdt *et al.*, 2005; Hanisch *et al.*, 2006; Seki *et al.*, 2008; Carmena *et al.*, 2012). Similarly, cells with Plk1^{T210V} are unable to proliferate over the long term in the presence of 3-MB-PP1 (Figure 2-2D).

In surveys of other mutations, we identified and confirmed defects in Plk1^{T214V}, and to a lesser degree, Plk1^{Y217F}, although the latter mutation was not essential for long-term proliferation (Figure 2-2D). Surprisingly, clonal Plk1^{S137A} is sufficient to rescue mitotic progression and proliferation, despite the known role of phosphorylation of this site in DNA damage and mitotic entry (Jang *et al.*, 2002; Tsvetkov and Stern, 2005; van de Weerdt *et al.*, 2005; Matsumoto *et al.*, 2009). We conclude that while most single Plk1 modifications are non-essential under ordinary conditions, mutations at T210, T214, and to a lesser degree Y217 preclude the ability of Plk1 to execute its essential function for mitotic progression.

It is possible that some residual catalytic activity from GFP-Plk1^{AS} contributed to the rescue phenotypes. To evaluate this possibility, we employed a conditional knockout system to evaluate mutant Plk1 function in cells that do not express any other Plk1 allele. To do

this, constructs were stably introduced into a Cre-sensitive PLK1$^{flox/\Delta}$ RPE1 cell line (Burkard *et al.*, 2007) (Supplemental Figure 2-1B). Next, mitotic index was measured after challenging each with Cre recombinase to delete exon 3 of the floxed PLK1 locus. Plk1^{T210V} and Plk1^{T214V} failed to rescue mitotic progression (Supplemental Figure 2-1C), in contrast to other constructs. Likewise, clonal cell lines showed similar results upon Cre treatment (Supplemental Figure 2-1D,E). Additionally, we subcloned cell lines after introducing Cre to determine if viable clones could be obtained. We recovered monoclonal PLK1$^{\Delta/\Delta}$ cell lines for S137A, K200R, and Y217F (Supplemental Figure 2-1F). We conclude that PTMs of single sites, excepting T210 and T214, are dispensable for viability and mitotic progression in human cells.

Functional evaluation of Plk1T214V

Of the two functional Plk1 sites identified in our survey, T214 is novel. We considered whether function is impaired because of phosphorylation or if its hydroxyl group is important for these functions. To evaluate this, we first tested if T214 phosphorylation is detectable in mitotic cells. Multiple phosphoproteomic analyses have identified T214 phosphorylation (Daub *et al.*, 2008; Dephoure *et al.*, 2008; Oppermann *et al.*, 2012). Although we were unable to generate a phospho-specific antibody, mass spectrometry confirmed T214 phosphorylation on Plk1 immunoprecipitated from mitotic HeLa extracts (Supplemental Figure 2-2). To verify that mutation of T214 does not result in unfolding or prevent ATP binding, we employed differential scanning fluorimetry (DSF) (Simeonov, 2013). Using recombinant Plk1 kinase domain, we examined melting temperatures in the presence and absence of ligand. Both Plk1^{WT} and Plk1^{T214V} had similar melting temperatures, indicating that the mutation does not disrupt Plk1 folding (Figure 2-3A). Moreover, both Plk1^{WT} and Plk1^{T214V} kinase domains are competent to bind ATP, as

evidenced by temperature shifts upon ATP and Mg++ addition. These results are not an artifact of reaction conditions- no shift is detected with GTP and absorbance is absent without SYPRO or Plk1 protein (not shown). Further, Plk1^{T214V} retains some catalytic activity in an in vitro kinase assay with recombinant Plk1 (Figure 2-3B), indicating that T214 mutation does not completely abrogate kinase activity. Taken together, our findings confirm that T214 is phosphorylated and is required for Plk1 function, with no evidence that mutation merely interferes with kinase folding or ATP binding.

Because Plk1 has multiple roles in mitosis, we tested which particular function is impaired by failure to phosphorylate Plk1 at T214. Centrosome separation and bipolar spindle formation are early mitotic activities mediated by Plk1 (Sumara *et al.*, 2004; van Vugt *et al.*, 2004). As expected, Flag-Plk1^{WT} restored bipolar spindle formation whereas cells complemented with control (Flag Only) had a higher percentage of monopolar spindles (Figure 2-3C). Similar to Flag Only, Plk1^{T214V} failed to rescue bipolar spindle formation, demonstrating that the elevated mitotic index in these cells is mediated in part by impaired spindle assembly.

We considered the upstream kinase mediating phosphorylation of Plk1 T214. Plk1 does not autophosphorylate at T214 (Supplemental Figure 2-3A), so we examined the sequence flanking this phosphorylation to identify possible candidates. The +1 proline is conserved across species, and suggests phosphorylation by a proline-directed kinase, such as Cdk1 (Figure 2-4A). Furthermore, Cdk1 is a major mitotic regulator and its yeast homolog, cdc28, phosphorylates S. cerevisiae polo, Cdc5, at the homologous residue (Mortensen *et al.*, 2005). To test if Cdk1 activates human Plk1, we performed an in vitro kinase assay (Figure 2-4B). Cdk1 highly phosphorylated its substrate, Histone H1, but little phosphorylation was detected on purified Plk1 kinase domain, and this was not modulated

by mutation at T214. We conclude that Cdk1 does not directly phosphorylate T214 of human Plk1.

The lack of Cdk1-dependent phosphorylation of T214 in our biochemical assay was surprising given the homology to S. cerevisiae; we therefore confirmed our findings with cell-based assays. Cdk1 activity markedly increases at mitotic onset and rapidly declines at anaphase (Potapova *et al.*, 2009; Gavet and Pines, 2010; Van Horn *et al.*, 2010; Chow *et al.*, 2011). If Cdk1 is required to activate Plk1, then Plk1 function will be impaired during DNA damage-recovery, before Cdk1 is activated (Macůrek *et al.*, 2008; van Vugt *et al.*, 2010) or during mitotic exit, when Cdk1 activity declines (Neef *et al.*, 2003; Burkard *et al.*, 2009; Wolfe *et al.*, 2009). To test the former, we evaluated if Plk1^{T214V} promotes mitotic entry following DNA damage (Macůrek *et al.*, 2008; van Vugt *et al.*, 2010) and for the latter, we tested if Plk1^{T214V} can trigger cytokinesis furrow formation and RhoA localization to the equatorial cortex (Burkard *et al.*, 2009). We found that Plk1^{T214V} fails to function on all accounts (Figure 2-4C,D,E). Combined with our biochemical assay, we conclude that Cdk1 is not the upstream kinase of Plk1 T214. We considered additional proline-directed kinases, ERK1 and ERK2, but did not detect strong phosphorylation from either (Supplemental 2-3B), suggesting that neither are the upstream kinase for T214 phosphorylation. Although the upstream kinase of T214 phosphorylation remains elusive, we conclude that T214 is a crucial residue for mitotic functions of Plk1, although it remains possible that the hydroxyl is required for catalysis independent of its phosphorylation.

Because of T214's proximity to the known Plk1 activation site, T210, we determined if T210 phosphorylation is contingent on intact T214. We found that T210 is phosphorylated in Plk1^{T214V} (Supplemental Figure 2-3C). We conclude that T214 is a crucial residue for Plk1 function in mitosis, but is not upstream of T210 phosphorylation.

Phosphorylations on Plk1 kinase domain have redundant functions

Most individual PTMs surveyed in our complementation assays were not strictly required for viability of human cells. One possible explanation is redundancy of phosphorylation sites, in which phosphorylation at any one of several possible sites is sufficient to restore phosphorylation-dependent function. To evaluate this, we tested if simultaneous mutation of the 23 surveyed phosphorylation sites ($Plk1^{Pan}$) abrogates Plk1 function (the 25 sites initially surveyed, without T210 or T214 mutation) or domain specific mutants (7 sites; $Plk1^{Kin}$, 16 sites; $Plk1^{PBD}$, Figure 2-5A,B). If the phosphorylation sites were redundant, simultaneous mutation of these sites would result in failure to restore essential functions of Plk1. Indeed, simultaneous mutation of all sites in $Plk1^{Pan}$ resulted in elevated mitotic index and interfered with long-term proliferation of human cells as compared to $Plk1^{WT}$ (Figure 2-5C,D), although these constructs localized properly in mitotic cells (Supplemental Figure 2-4A). Surprisingly, $Plk1^{PBD}$ restored both mitotic progression and cell proliferation, indicating that PBD phosphorylation sites are dispensable for the essential functions of Plk1. In contrast, $Plk1^{Kin}$ is unable to restore mitotic progression or cell viability (Figure 2-5C,D), so redundant phosphorylation within the kinase domain is important for Plk1 function.

To characterize the mitotic defect, cells were labeled with fluorescent H2B and imaged by timelapse videomicroscopy (Figure 2-6A). This revealed prolonged mitoses in the kinase domain mutant, characterized by congression defects and lagging chromosomes. In contrast, the $Plk1^{PBD}$ 16-site mutant robustly restored mitosis with minimally changed mitotic duration. To characterize the mitotic defect further, we employed fixed cell analysis with indirect immunofluorescence. The $Plk1^{Kin}$ mutant had increased frequency of prometaphase and metaphase cells, consistent with an early mitotic defect in spindle

attachment (Supplemental Figure 2-4B). However, these constructs were capable of separating centrosomes, an essential component of forming a bipolar mitotic spindle (Supplemental Figure 2-4C).

We next characterized chromosome alignment. In the Plk1^{Kin} and Plk1^{Pan} lines, cells frequently had misaligned chromosomes on the metaphase plate (Figure 2-6B). Additionally, cells that proceeded into anaphase frequently had an increase in anaphase segregation errors (Figure 2-6C). These phenotypes were concordant between Plk1^{Kin} and Plk1^{Pan}, but distinct from Plk1^{PBD}, and consistently demonstrated the importance of redundant phosphorylation in the Plk1 kinase domain. Additionally, these phenotypes are consistent with chromosome-microtubule attachment errors, seen previously with defects in Plk1 kinase activity (Lera and Burkard, 2012). The Plk1^{Kin} has some reduced catalytic activity in an in vitro kinase assay relative to immunoprecipitated WT Plk1 (Supplemental Figure 2-4D), suggesting that impaired catalytic activity may be, in part or wholly, responsible for this phenotype. We conclude that phosphorylation events within the kinase domain operate in a redundant manner, and are required for full Plk1 function.

Discussion

Mass spectrometry has led to the discovery of a large number of PTMs on mitotic proteins (Daub *et al.*, 2008; Khoury *et al.*, 2011; Hornbeck *et al.*, 2012; Oppermann *et al.*, 2012). However, functional assessment of PTMs can be challenging with commonly used techniques. In this study, we extend our chemical genetics system to evaluate the functional significance of 34 PTMs on a single mitotic protein, Plk1. Surprisingly, two sites are strictly and singly essential, there is redundancy among an additional 7 phosphorylation sites within the kinase domain, and 16 phosphorylation sites within the C-terminal polo-box

domain are not required for essential functions of Plk1. This reveals that many observed mitotic PTMs are redundant, non-essential, or dispensable. If this is representative of PTMs on other mitotic proteins, then many observed PTMs will have subtle or dispensable functions.

We have identified T214 as a novel residue essential for Plk1mitotic functions. This is similar to that observed in yeast where the homologous residue is phosphorylated to promote mitotic functions of Cdc5 (Mortensen *et al.*, 2005). This site is required either because it is phosphorylated, or because the hydroxyl is required for catalysis exclusive of its phosphorylation state (Bayliss *et al.*, 2012). We and others have detected T214 phosphorylation in nocodazole treated cells, however it is unclear if it occurs during unperturbed mitosis. Supporting the former idea, phosphorylation on the equivalent residue has been observed in other mitotic kinases, including MPS1 and Aurora A (Bayliss *et al.*, 2012; Hornbeck *et al.*, 2012). However, we have been unable to identify the upstream kinase phosphorylating this site.

Surprisingly, most single phosphorylation sites on Plk1 are not required for its essential functions. However, the identification of redundant phosphorylation sites within the kinase domain has important implications. These redundant sites are essential for chromosome alignment in metaphase and maintenance of proper chromosome segregation during anaphase, which may be attributable to a moderate loss of catalytic activity (Lera and Burkard, 2012). This phenotype may also support a role of Plk1 in the spindle assembly checkpoint (Liu *et al.*, 2012; von Schubert *et al.*, 2015). These mutations do not disrupt all Plk1 function, as rescue of centrosome separation was observed. Taken together, these data demonstrate that proper Plk1 function in mitosis requires specific phosphorylation of T-loop residues and one or more redundant phosphorylations in the

kinase domain, but does not require PBD phosphorylation for its ordinary functions.

Among the mutations, functional rescue with Plk1^{S137A} was most surprising. Previous studies have demonstrated that S137 can be phosphorylated in mitosis (Tsvetkov and Stern, 2005; van de Weerdt *et al.*, 2005), although levels of phosphorylation are low in HeLa cells (Jang *et al.*, 2002). Phospho-mimetic S137D increases Plk1 kinase activity and alters mitosis (Jang *et al.*, 2002; van de Weerdt *et al.*, 2005). In U2OS cells, knockdown of endogenous Plk1 and replacement with Plk1^{S137A} results in metaphase arrest, suggesting that phosphorylation of this residue is important for metaphase-anaphase transition (van de Weerdt *et al.*, 2005). These are difficult to reconcile wholly with our observations here. However, the phosphomimetic findings do not indicate that S137 phosphorylation is necessary and S137A mutation does not reduce Plk1 activity (Jang *et al.*, 2002). Moreover, we do not exclude the possibility that S137 phosphorylation plays a critical role in the context of DNA damage. Similarly, we did not confirm a crucial role for K492. It has been suggested that ubiquitination of this residue is important for removal of Plk1 from the kinetochores (Beck *et al.*, 2013). In HeLa cells, knockdown of endogenous Plk1 and replacement with Plk1^{K492R} results in mitotic delay and an increase in apoptosis. The low penetrance of this phenotype may explain why we did not observe proliferation defects with K492R mutation. Alternatively there could be differences due to alternative models and methods used previously to deplete/replace endogenous Plk1. Some differences could be attributed to cell lines, since p53 null cells like Hela are more susceptible to Plk1 inhibition (Sur *et al.*, 2009). Our data suggest that S137 phosphorylation or K492 ubiquitination of Plk1 play important roles only for non-essential functions of Plk1.

There are some limitations of our observations. First, our assays are designed to observe Plk1 functions that are essential occur in differentiated human epithelial cells in

mitosis. For example, our assays would not identify the effects of Plk1 phosphorylation of Orc2, which is not strictly required for S-phase (Song *et al.*, 2011). Second, it is formally possible that the wildtype PBD of the Plk1^{AS} allele could complement in trans- with the second Plk1 allele. However, we find this unlikely as previous studies have shown the importance of a cis-acting PBD to localize Plk1 kinase activity (Elia *et al.*, 2003b; Hanisch *et al.*, 2006; Lera and Burkard, 2012), and we found concordant results using knockout for many mutants. Third, the polyclonal pools used for screening have varying expression levels. Although overexpression could cause mitotic defects, we derived subclones for mutants with strong mitotic defects making it unlikely that the defects were due to expression.

In conclusion, chemical genetics complementation can reveal the role of PTMs on Plk1. This system could be extended to other non-catalytic mitotic proteins using auxin-inducible degradation which is rapid and reversible (Nishimura *et al.*, 2009). Many other techniques, however, have limitations and the data can be difficult to interpret. RNA-interference based depletions may not sufficiently deplete endogenous protein and re-expressed non-modifiable mutants can be expressed heterogeneously by transient transfection. Residual levels of endogenous protein may impair phenotypic assessments—for example, 10% residual Plk1 is sufficient to complete mitosis, whereas knockout or >90% chemical inhibition reveals the null phenotype (Liu *et al.*, 2006; Burkard *et al.*, 2007; Lera and Burkard, 2012). Genetic techniques can edit the genomic copy, but complex conditional systems are required for essential proteins. Moreover, these techniques lack the temporal resolution necessary to assess functions within the timescale of human mitosis of approximately one hour. Chemical genetic complementation, demonstrated here, provides allele specific, highly penetrant inhibition with the time advantage of a small molecule

inhibitor to allow comprehensive analysis of PTM function. This can be applied to study function of other mitotic protein kinases.

Materials and Methods

Cell culture and synchronization

HeLa and hTERT-RPE1 (ATCC, Manassas, VA) cells were grown at 37°C in 5%CO2 in 1:1 mixture of DMEM and Ham's F-12 medium supplemented with 2.5mM L-glutamine (hTERT-RPE1) or DMEM supplemented with 4 mM L-glutamine, 4500 mg/liter glucose (HeLa). Both were further supplemented with 10% fetal bovine serum and 100 units/ml penicillin-streptomycin.

Stable cell lines were created by retroviral infection. Recombinant viral particles were generated by cotransfecting Flag-tagged constructs in pQCXIN plasmid (Clontech) with vesicular stomatitis virus glycoprotein envelope plasmids into gag-pol expressing 293T Phoenix packaging cells using Fugene HD (Promega E2311). Target cells were treated with viral-containing media in the presence of polybrene. Cells expressing rescue construct were selected for using 0.4μg/ml G418. Cell lines for chemical genetic complementation were created from the EGFP-Plk1^{as} cell line used by Burkard et al. (Burkard *et al.*, 2007). For experiments, cell lines selected by this method were used except when subcloned as indicated. For Cre-dependent knockout, constructs were created from flox/Δ cell line (Burkard *et al.*, 2007). Clones were obtained by limiting dilution and selected using 0.4μg/ml G418.

All transient transfections were performed with HeLa cells and FuGENE HD transfection reagent with mitotic synchronization as noted. For anaphase synchronizations, cells were treated with monastrol for 8 hours, released for 40 minutes, treated for 20 minutes with 3-MB-PP1 +/- blebbistatin, and then fixed with 4% paraformaldehyde or 10% trichloroacetic acid. For Cre-dependent knockout of PLK1$^{flox/\Delta}$, cells were treated with Ad-Cre (Baylor University Vector Development Laboratory) at a multiplicity of infection of

5x104 plaque-forming units per cell.

Chemicals

Chemicals used in this study include 10μM 3-MB-PP1 (Toronto Research Chemicals), 5mM caffeine, 100μM monastrol (Tocris), 0.2μg/ml nocodazole (EMD Biosciences), 5mM thymidine (EMD Biosciences), 0.2μg/ml doxorubicin (MP Biomedicals), 50μM blebbistatin.

Antibodies and Cell Stains

Antibodies used in this study include anti-phospho-210 PLK1 (BD 558400), anti-γ-tubulin (Thermo MA1-20248, clone GTU-88), anti-α-tubulin (MAB1864 Millipore), anti-anillin (polyclonal rabbit, Kim and Burkard, unpublished), anti-Plk1 (F-8, Santa Cruz Biotechnology sc-17783), anti-β-actin (AC-15, ab6276), anti-flag (M2) HRP (Sigma A8592), anti-RhoA (SC418 Santa Cruz), anti-pericentrin (ab44448 Abcam), anti-ACA (HCT0100 Immunovision), and anti-mouse HRP (Jackson Immunoresearch Laboratories Inc. #115-035-003). Immunoprecipitation of flag constructs was performed using anti-flag M2 affinity gel (Sigma A2220). For immunofluorescence, Alexa-flour antibodies were used (Invitrogen). Mitotic index was determined through Hoechst 33258 staining and microscopy. Crystal violet stain is composed of crystal violet (Sigma C-0775) with buffered formalin (Sigma HT-50-1-128).

Recombinant Proteins

His-tagged constructs were cloned into pET-28a vector and kinase dead version has K82R mutation. Proteins were purified using Rosetta DE3 cells and extracted with Ni-NTA His-Bind Resin (Novagen, 70666). GST-tagged construct were cloned into pGEX-6P-1 vector.

Proteins were purified using BL21 DE3 cells and extracted with Glutathione Sepharose 4B (GE Healthcare, 17-0756-01). Truncated protein included amino acids 1-352. Active Cdk1-Cyclin B (Invitrogen, PV3292), ERK1 (Promega, V1951), and ERK2 (Promega, V1961) were purchased as well as substrates Histone H1 (ab89813) and α-casein (Sigma C8032).

Immunofluorescence, Microscopy, and Immunoblotting

For western blotting, cells were washed with PBS, incubated for 20 minutes on ice in lysis buffer (50mM HEPES, pH 7.5, 100 mM NaCl, 0.5% Nonidet P-40, 10% glycerol, 10mM sodium pyrophosphate, 5mM β-glycerol phosphate, 50mM NaF, 0.3mM Na3VO4,1mM phenylmethylsulfonyl fluoride (PMSF), 1X protease inhibitor mixture (Thermo Scientific), and 1mM dithiothreitol (DTT)), and centrifuged at 4°C. Equal amounts of protein were separated on SDS-PAGE, immunoblotted, and detected by chemiluminescence on film (Denville Scientific). Antibody incubations were performed in TBST + 4% milk or TBST + 5% BSA for phosphospecific antibodies.

For immunofluorescence (IF) cells were plated on coverslips. Antibody incubations were performed in PBS + 0.1% Triton X-100 with 3% BSA. Centrosome separation was determined following fixation with 100% ice cold methanol. Furrow formation was determined following fixation with 4% paraformaldehyde. RhoA accumulation at the equatorial cortex was determined following fixation with 10% trichloroacetic acid.

Image acquisition and analysis was performed on a Nikon Eclipse Ti inverted microscope with a CoolSNAP HQ2 charge-coupled device camera (Photometrics). Nikon Elements was used to process images which were transferred to Adobe Photoshop and Illustrator for final figures.

Kinase Assays

All kinase assay reactions were incubated at 30°C for 30 minutes and resolved by SDS-PAGE. γ-32P incorporation was visualized by Typhoon TRIO imager (GE Healthcare). For Cyclin-dependent kinase 1, 100ng Cdk1-Cyclin B was incubated in buffer (50mM Tris-HCl, pH 7.5, 10mM MgCl2, 0.1mM NaF, 10μM Na3VO4) with 1mM DTT 1μM cold ATP, 5μCi [γ-32P] ATP, and 2μg substrate. For Plk1 autophosphorylation kinase assays, 100ng GST-Plk1 AA1-352 was incubated with concentration-matched indicated His-Plk1 substrate (His-tagged kinase dead Plk1kinase domain with or without T214V mutation), buffer (20mM Tris, pH 7.4, 10mM MgCl2, 50mM KCl), 100mM DTT, 1μM cold ATP, and 5μCi [γ-32P] ATP. For recombinant Plk1 kinase assays, His-tagged kinase domain of Plk1 with or without T214V mutation and α-casein were incubated with buffer (20mM Tris, pH 7.4, 10mM MgCl2, 50mM KCl), 100mM DTT, 1μM cold ATP, and 5μCi [γ-32P] ATP. For ERK kinase assays, ERK1 and ERK2 (Signal Chem, M29-10Uand M28-10G) were incubated in 1X Signal Chem buffer (K01-09) with 1mM DTT, 1μM cold ATP, 5μCi [γ-32P] ATP, and concentration-matched substrates.

Kinase activity of flag-tagged Plk1 was determined from stable cell lines. Flag constructs were immunoprecipitated with M2-agarose slurry and incubated in buffer (20mM Tris, pH 7.4, 10mM MgCl2, 50mM KCl) with 1mM DTT 1μM cold ATP, 5μCi [γ-32P] ATP, and 5μg α-casein.

Mass Spectrometry

HeLa cells were transiently transfected with Flag-Plk1 and treated with nocodazole for 17 hours. Flag-Plk1 was immunoprecipitated with M2-agarose slurry and resolved by SDS-PAGE. Coomassie R-250 stained gel pieces were de-stained, dried, and rehydrated

with 20µl of trypsin solution with 0.01% ProteaseMAX surfactant [10ng/µl trypsin (Trypsin Gold from PROMEGA Corp.) in 25mM NH4HCO3/0.01% w/v of ProteaseMAX (Promega Corp.)] The digestion was conducted for 3hrs at 42°C, peptides generated from digestion were transferred to a new Protein LoBind tube (~50µl volume) and digestion was terminated by acidification with 2.5% TFA [Trifluoroacetic Acid] to 0.3% final (7µl added). Supernatant was collected for spectrometry.

Peptides were analyzed by nanoLC-MS/MS using the Agilent 1100 nanoflow system (Agilent, Palo Alto, CA) connected to a hybrid linear ion trap-orbitrap mass spectrometer (LTQ-Orbitrap, Thermo Fisher Scientific, Bremen, Germany) equipped with a nanoelectrospray ion source. Chromatography of peptides prior to mass spectral analysis was accomplished using C18 reverse phase HPLC trap column (Zorbax 300SB-C18, 5µM, 5x0.3mm, Agilent) and capillary emitter column (in-house packed with MAGIC C18, 3 µM, 150x0.075mm, Michrom Bioresources, Inc.) onto which 8µl of extracted peptides were loaded. As peptides eluted, MS scans were acquired in the Orbitrap with a resolution of 100,000 and up to 5 most intense peptides per scan were fragmented and detected in the ion trap over the 300 to 2000 m/z; redundancy was limited by dynamic exclusion. Raw MS/MS data were converted to mgf file format using Trans Proteomic Pipeline (Seattle Proteome Center, Seattle, WA). Resulting mgf files were used to search against human Plk1 sequence. All of the predicted phosphopeptides were manually investigated to confirm proper phosphoresidue assignment.

Differential Scanning Fluorimetry (DSF)

Recombinant Plk1 protein (5µg) was mixed with DSF buffer (400mM Hepes, 600mM NaCl, pH 7.5), 15X SYPRO, DMSO, and 5mM DTT. As indicated ATP (MP Biomedicals), GTP

(Amersham Pharmacia Biotech Inc), and/or MgCl2 are added to the above mix and are run in 96 well plate in a RT-qPCR machine (Roche LightCycler® 480 Instrument II) with the following protocol: Step 1: Temperature is increased 2°C per second to 25°C. Hold at 25°C for six seconds. Step 2: Temperature is increased 0.11°C per second to 95°C, acquiring five fluoresce measurements per degree; hold 95°C for 30 seconds.

Genomic DNA

Genomic DNA was purified using Wizard SV Genomic DNA Purification System (Promega, A2360). Touchdown PCR was used to visualize the floxed locus using primers: AGGAAAGCCCTGACTGAGCC and TGCTTTTTACACAACTTTTGGGTTAC. Products were run on agarose gel and detected by ethidium bromide staining.

Figure 2-1

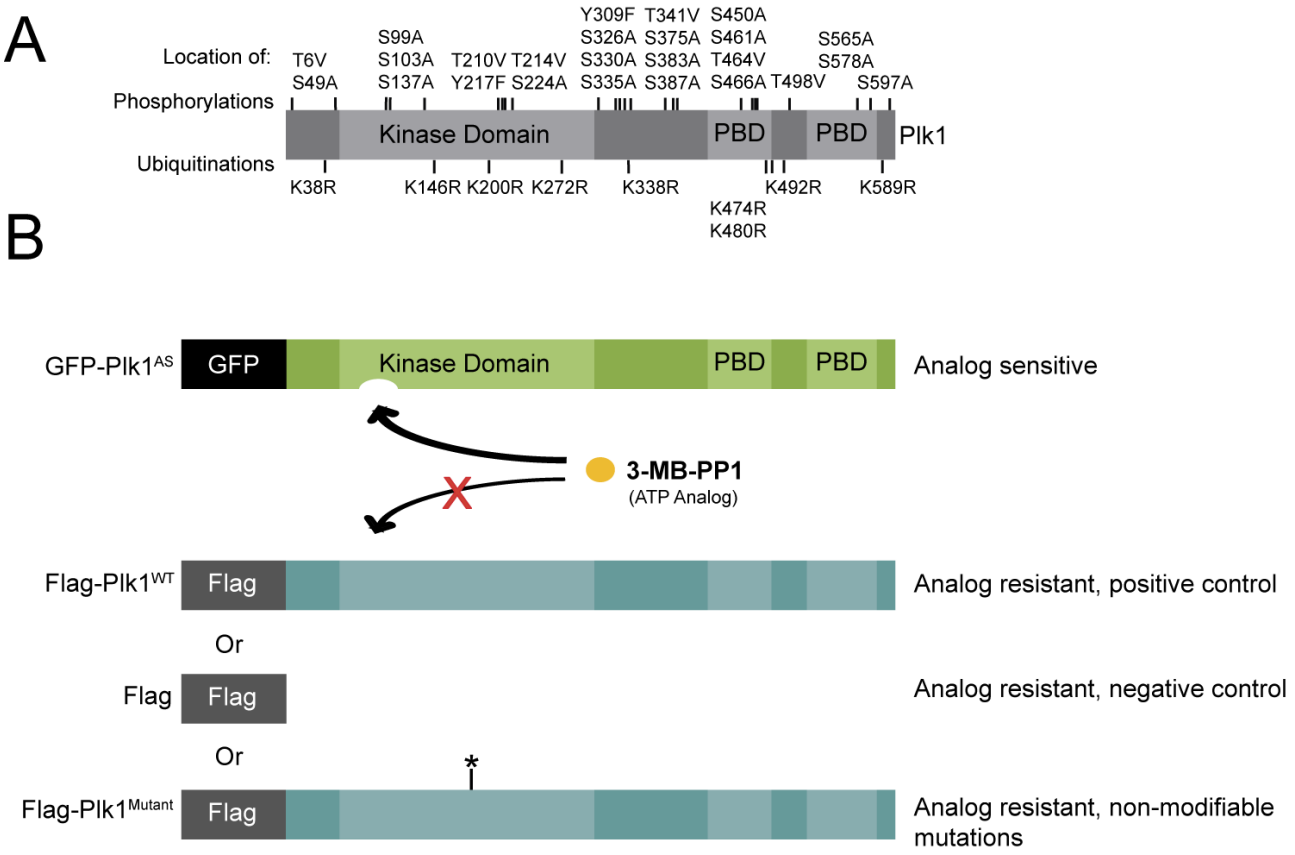
A
Location of:
Phosphorylations
Ubiquitinations
T6V
S49A
S99A
S103A
S137A
T210V T214V
Y217F S224A
Y309F T341V S450A
S326A S375A S461A
S330A S383A T464V
S335A S387A S466A T498V
S565A
S578A
S597A
Kinase Domain
PBD
PBD
Plk1
K38R
K146R K200R K272R
K338R
K474R
K480R
K492R
K589R
B
GFP-Plk1AS
GFP
Kinase Domain
PBD
PBD
Analog sensitive
3-MB-PP1
(ATP Analog)
Flag-Plk1WT
Flag
Analog resistant, positive control
Or
Flag
Flag
Analog resistant, negative control
Or
Flag-Plk1Mutant
Flag
*
Analog resistant, non-modifiable mutations

Figure 2-1: Using chemical genetics to assess the functional significance of Plk1 posttranslational modification sites.

(A) Distribution of identified phosphorylation and ubiquitination sites on Plk1 by domain. (B) Analog sensitive Plk1 ($Plk1^{AS}$) is complemented with flag-tagged (analog resistant) rescue constructs. Flag-Plk1 is mutated ($Plk1^{Mutant}$) to render it non-modifiable.

Figure 2-2

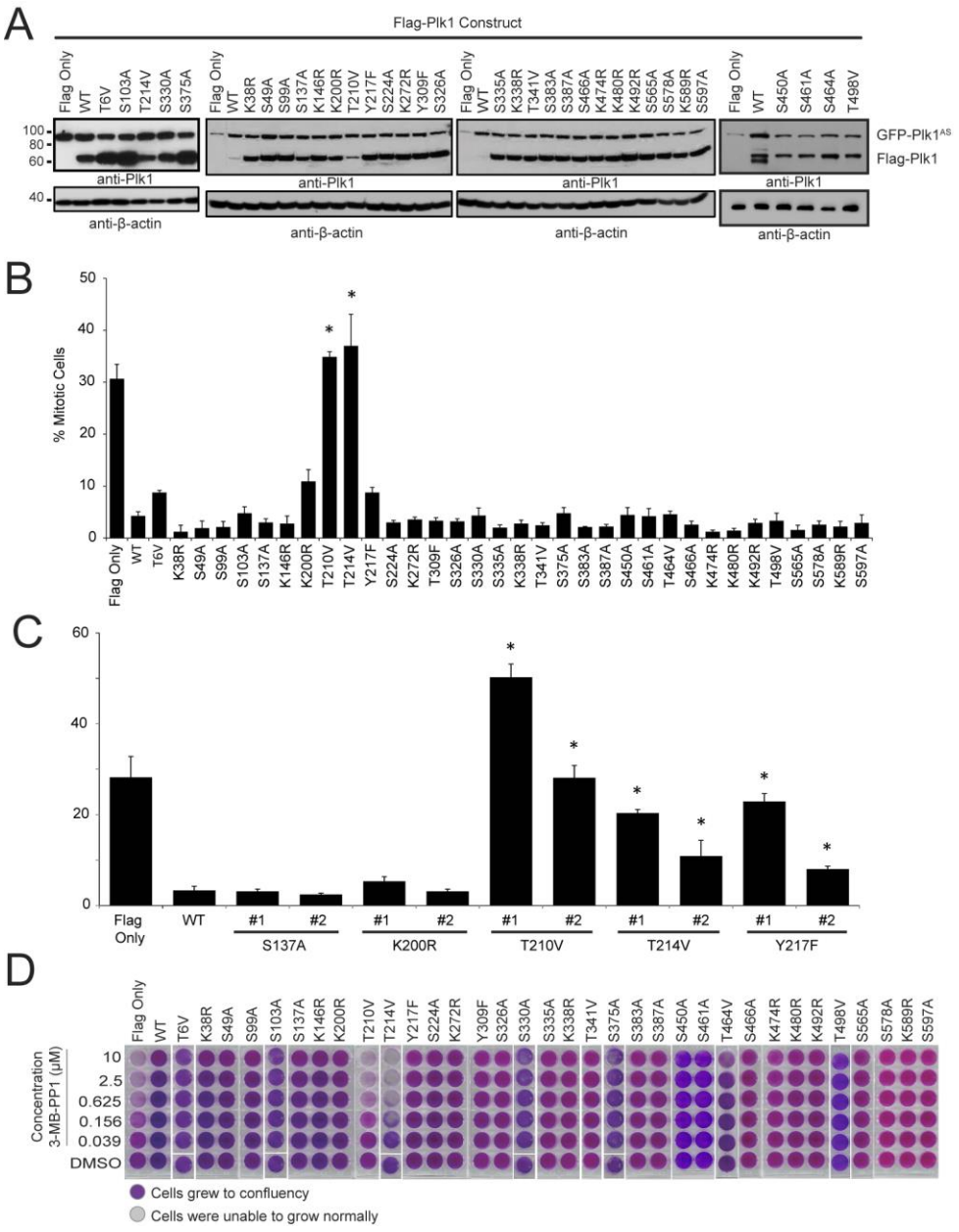
A
Flag-Plk1 Construct
Flag Only
WT
T6V
S103A
T214V
S330A
S375A
K38R
S49A
S99A
S137A
K146R
K200R
T210V
Y217F
S224A
K272R
Y309F
S326A
S335A
K338R
T341V
S383A
S387A
S466A
K474R
K480R
K492R
S565A
S578A
K589R
S597A
S450A
S461A
S464A
T498V
100
80
60
40
anti-Plk1
anti-β-actin
GFP-Plk1AS
Flag-Plk1
B
% Mitotic Cells
50
40
30
20
10
0
C
60
40
20
0
Flag Only
WT
#1
#2
S137A
K200R
T210V
T214V
Y217F
D
Concentration 3-MB-PP1 (μM)
10
2.5
0.625
0.156
0.039
DMSO
Cells grew to confluency
Cells were unable to grow normally

Figure 2-2: Plk1 T214V disrupts progression of mitosis and cell proliferation.

(A) Western blots showing the expression of analog sensitive Plk1 (GFP-Plk1^{AS}) and Flag-tagged Plk1 (Flag-Plk1) constructs with and without different S/T mutations in RPE cell lines. Cells were synchronized in mitosis with nocodazole prior to collection. Blot probed with anti-Plk1 (upper) and anti-β-actin (lower) antibodies. (B) Mitotic index of AS cell lines in (A) treated with 10μM 3-MB-PP1 for 16 hours. 900 cells were scored as mitotic or non-mitotic through Hoechst 33258 staining. n≥3, *p<0.05 compared to WT (GFP-Plk1^{AS}/Flag-Plk1^{WT}). (C) Mitotic index of Flag only and monoclonal AS cell lines in (Supplemental Figure 2-1A) treated with 10μM 3-MB-PP1 for 16 hours. 900 cells were scored as mitotic or non-mitotic through Hoechst 33258 staining. n≥3, *p<0.05 compared to WT Clone (GFP-Plk1^{AS}/Flag-Plk1^{WT}). (D) 6000 cells were plated in complete medium and treated with concentrations of 3-MB-PP1 as indicated, and allowed to grow until control (DMSO) wells were confluent (six days). Cell density is qualitatively detected by crystal violet staining.

Figure 2-3

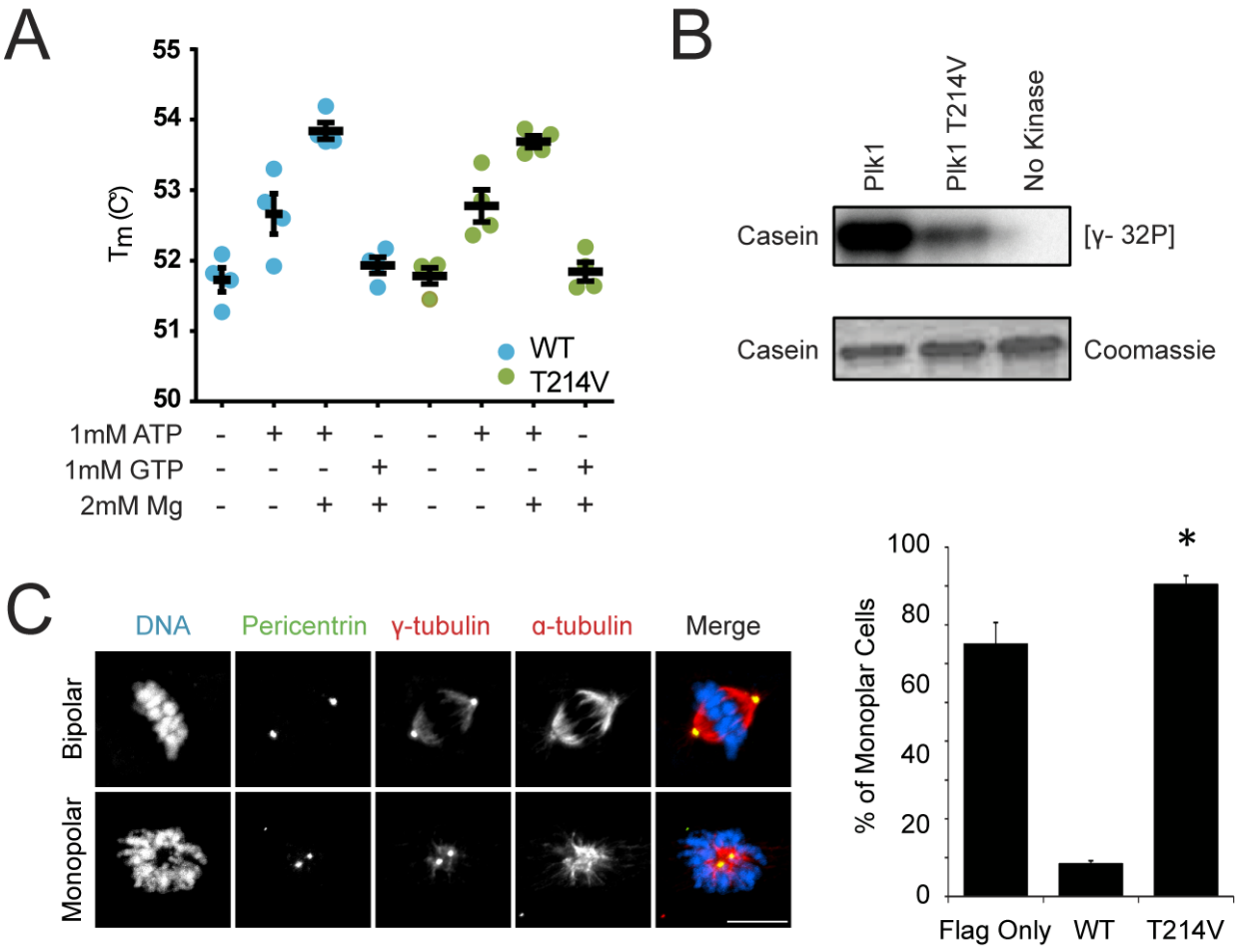
A
55
54
53
52
51
50
Tm (C)
WT
T214V
1mM ATP - + + - - + + -
1mM GTP - - - + - - - +
2mM Mg - - + + - - + +
B
Plk1
Plk1 T214V
No Kinase
Casein
[γ- 32P]
Casein
Coomassie
C
DNA
Pericentrin
γ-tubulin
α-tubulin
Merge
Bipolar
Monopolar
% of Monoplar Cells
100
80
60
40
20
0
*
Flag Only
WT
T214V

Figure 2-3: Plk1 T214V does not rescue Plk1 functions.

(A) Plk1 T214V is not unfolded and can bind ATP. Recombinant His-tagged Plk1 kinase domains with and without T214V mutation were assessed for proper protein folding using Differential Scanning Fluorimetry. Equivalent conditions except where indicated. n=3 (B) Recombinant His-tagged kinase domain of Plk1 with or without T214V mutation and α-casein were incubated with [γ-32P], resolved by SDS-PAGE, and visualized by autoradiography. (C) Cells shown were treated with 3-MB-PP1 for 6 hours, fixed, and stained with DAPI and for pericentrin, γ-tubulin and α-tubulin. n=3, 300 or more cells were counted for each cell line. *$p<0.05$ compared to incidence of monopolar spindles in GFP-$Plk1^{AS}$/Flag-$Plk1^{WT}$ cells. Scale bar, 10μm.

Figure 2-4

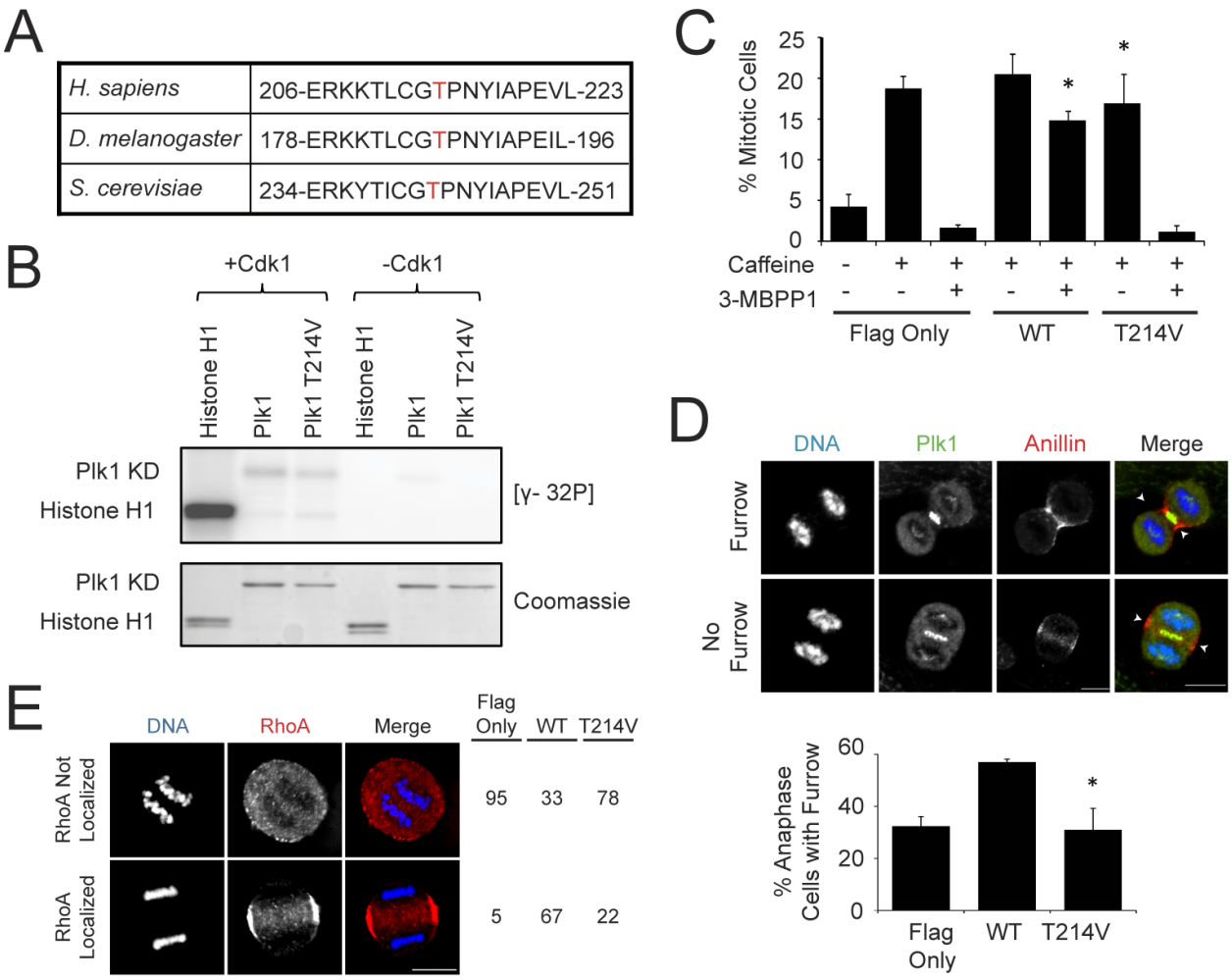
A
H. sapiens
206-ERKKTLCGTPNYIAPEVL-223
D. melanogaster
178-ERKKTLCGTPNYIAPEIL-196
S. cerevisiae
234-ERKYTICGTPNYIAPEVL-251
B
+Cdk1
-Cdk1
Histone H1
Plk1
Plk1 T214V
Plk1 KD
Histone H1
[γ- 32P]
Coomassie
C
% Mitotic Cells
Caffeine
3-MBPP1
Flag Only
WT
T214V
D
DNA
Plk1
Anillin
Merge
Furrow
No Furrow
% Anaphase Cells with Furrow
E
DNA
RhoA
Merge
Flag Only
WT
T214V
RhoA Not Localized
RhoA Localized
95
33
78
5
67
22

Figure 2-4: Plk1 T214 is not phosphorylated by Cdk1.

(A) Sequence alignment of polo kinases with T214 or equivalent in red. (B) Recombinant Cdk1 and indicated substrates (His-tagged Plk1 kinase domains with or without T214V mutation or Histone H1) were incubated with [γ-32P], resolved by SDS-PAGE, and visualized by autoradiography. (C) Cell lines were synchronized with 5mM thymidine for 24 hours, released into complete media, treated with 0.2μg/ml doxorubicin for one hour, treated as indicated for 9 hours, stained with Hoechst, and scored as mitotic or non-mitotic. n=3, 300 cells each, *p<0.05 compared to GFP-Plk1^{AS}/Flag-Plk1^{T214V} cells treated with 5mM caffeine and 3-MB-PP1. (D) Cell lines were treated with 100μM monastrol for 8 hours, released for 40min, treated with 3-MB-PP1 for 20 min, fixed, and stained for Plk1, and Anillin and with DAPI. n=3, >300 anaphase cells were quantified as having a furrow or not. *p<0.05 compared to incidence for furrow formation in GFP-Plk1^{AS}/Flag-Plk1^{WT} cells. Scale bar, 10μm. Arrows indicate site of cleavage furrow. (E) Plk1 activity is required to localize RhoA to the equatorial cortex. Cells were synchronized with monastrol, released for 40 min, and then treated for 20 min with blebbistatin and 3-MB-PP1. Cells were scored for equatorial RhoA staining. n=1, 100 cells per cell line were scored for RhoA localization.

Figure 2-5

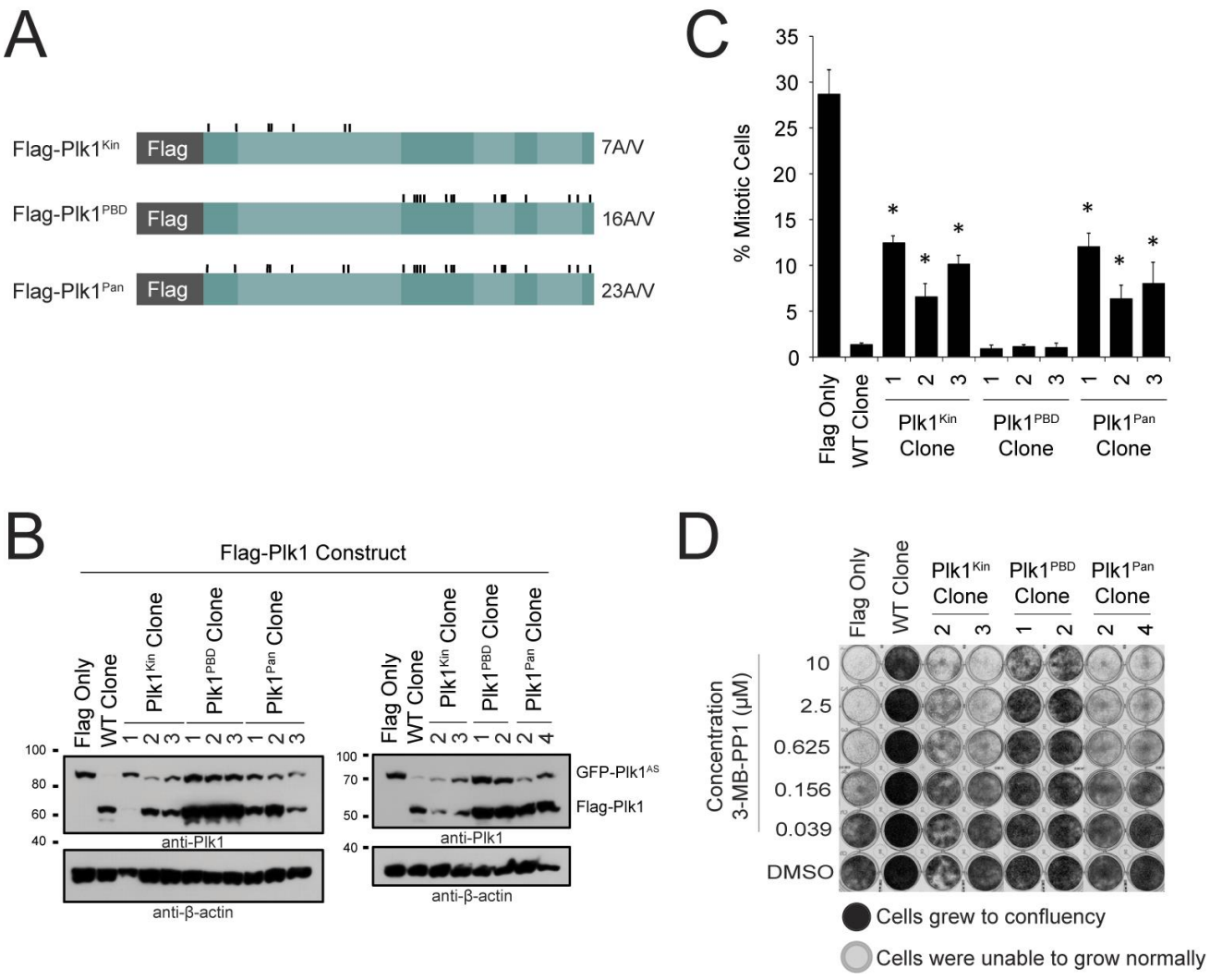
A
Flag-Plk1Kin
Flag
7A/V
Flag-Plk1PBD
Flag
16A/V
Flag-Plk1Pan
Flag
23A/V
C
% Mitotic Cells
35
30
25
20
15
10
5
0
Flag Only
WT Clone
Plk1Kin Clone
Plk1PBD Clone
Plk1Pan Clone
B
Flag-Plk1 Construct
Flag Only
WT Clone
Plk1Kin Clone
Plk1PBD Clone
Plk1Pan Clone
100
80
60
40
anti-Plk1
anti-β-actin
70
50
GFP-Plk1AS
Flag-Plk1
D
Concentration 3-MB-PP1 (μM)
10
2.5
0.625
0.156
0.039
DMSO
Cells grew to confluency
Cells were unable to grow normally

Figure 2-5: Plk1^{PBD} rescues mitotic progression and cell proliferation.

(A) Plk1AS is complemented with one of the indicated flag-tagged (analog resistant) rescue constructs. Flag-Plk1 is mutated at 23 phosphorylation sites (Plk1^{Pan}, excluding T210 and T214) that were able to rescue in previous experiments. These 23 phosphorylation groups were then divided into two groups, based on domain. Plk1^{Kin} has 7 mutations in the kinase domain, while Plk1^{PBD} has 16 in the PBD region of the protein. (B) Western blot to show expression in indicated monoclonal cell lines probed with anti-Plk1 (upper) and anti-β-actin (lower) antibodies. (C) Mitotic index of AS cell lines from (B) treated with 3-MB-PP1 for 16 hours. 900 cells were scored as mitotic or non-mitotic through Hoechst staining. n≥3, *$p<0.05$ compared to WT Clone (GFP-Plk1^{AS}/Flag-Plk1^{WT}). (D) 6000 cells were plated in complete medium and treated with concentrations of 3-MB-PP1 as indicated, and allowed to grow until control wells were confluent (eight days). Cell density is qualitatively detected by crystal violet staining.

Figure 2-6

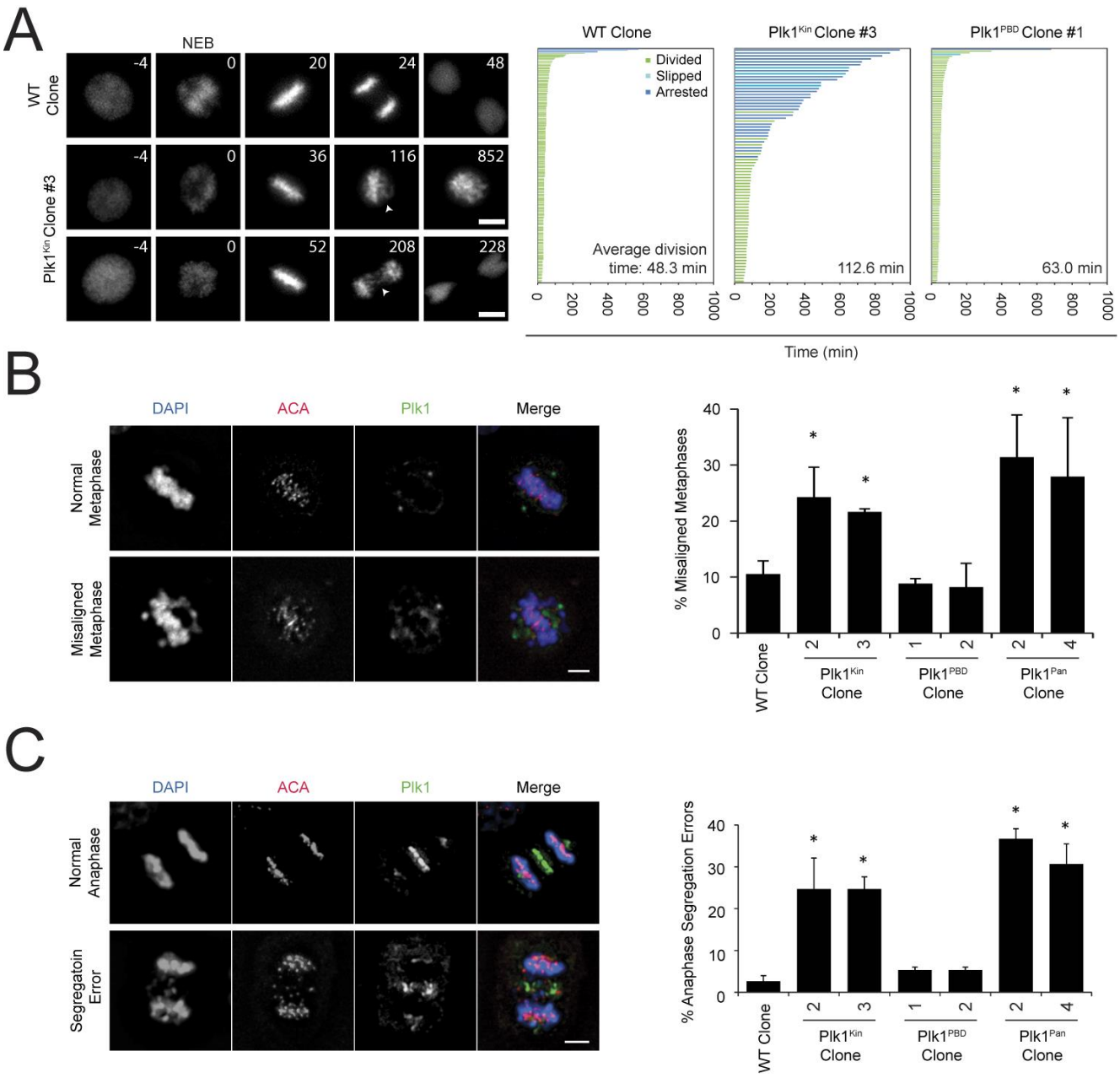
A
NEB
WT Clone
Plk1Kin Clone #3
-4
0
20
24
48
36
116
852
52
208
228
WT Clone
Plk1Kin Clone #3
Plk1PBD Clone #1
Divided
Slipped
Arrested
Average division time: 48.3 min
112.6 min
63.0 min
0
200
400
600
800
1000
Time (min)
B
DAPI
ACA
Plk1
Merge
Normal Metaphase
Misaligned Metaphase
% Misaligned Metaphases
WT Clone
Plk1Kin Clone
Plk1PBD Clone
Plk1Pan Clone
C
Normal Anaphase
Segregatoin Error
% Anaphase Segregation Errors

Figure 2-6: Plk1^{Kin} is unable to rescue chromosome alignment or chromosome segregation.

(A) Cells were infected with H2B-FusionRed lentivirus for 48 hours, treated with 3-MB-PP1, and placed on microscope in chamber containing 5% CO2 at 37°C. Images were taken every 4min with a 20X objective for 16+ hours. Duration of mitosis was quantified from mitotic entry to when daughter cells sat down. Still frames from time lapse showing representative cell fates for WT and Plk1^{Kin} clones. Times indicate minutes from nuclear envelope breakdown (NEB). Arrows indicate examples of misaligned (middle row) and lagging chromosomes (bottom row). Scale bar, 5μm. Graph indicates individual cell fate and time in mitosis (≥ 79 cells in each condition). Average division time in lower right hand corner only includes cells that divided. Arrested (blue bars) indicates cells that did not divide during the movie. In this case, the data was censored and time in mitosis was quantified from mitotic entry to the end of the movie. Cells that began mitosis with <120min to the end of the movie and did not divide or left the screen were discarded. (B) Cells were treated with 3-MB-PP1 for 6 hours, fixed, and stained for Plk1 and ACA and with DAPI. n=3, 63 or more metaphase cells were counted for each cell line for each replicate. *p<0.05 compared to incidence misaligned metaphases in WT Clone. Scale bar, 5μm. (C) Cells shown were treated with 3-MB-PP1 for 6 hours, fixed, and stained for DAPI, Antibody Against Centromere (ACA), and Plk1. n=3, 60 or more anaphase cells were counted for each cell line for each replicate. *p<0.05 compared to incidence of anaphase segregation errors in WT Clone. Scale bar, 5μm.

Supplemental Figure 2-1

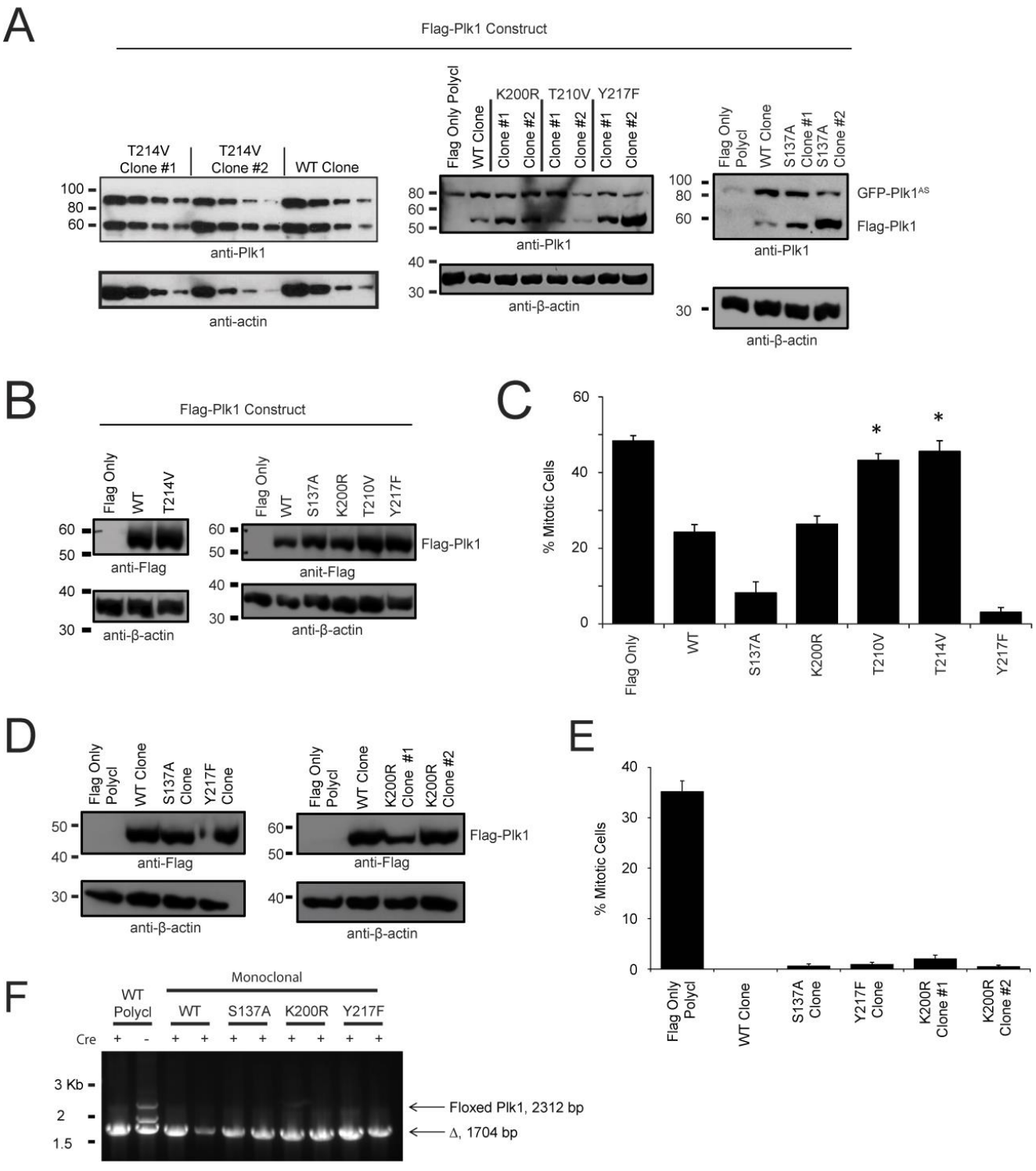

Supplemental Figure 2-1: Probing the importance of Plk1 PTMs.

(A) Western blots showing the expression in monoclonal analog sensitive Plk1 (GFP-Plk1^{AS}) and flag-tagged Plk1 (Flag-Plk1) constructs with and without different S/T mutations in RPE cells. Blot probed with anti-Plk1 (upper) and anti-β-actin (lower) antibodies. (B) Western blot showing expression levels in indicated Cre-sensitive cell lines. Blots probed with anti-flag HRP (upper) and anti-β-actin (lower) antibodies. (C) Mitotic index of cells treated with Ad-Cre for ~48 hours. 900 cells were scored as mitotic or non-mitotic through Hoechst staining. n≥3, *p<0.05 compared to Plk1^{flox}/WT cell line. (D) Western blot showing expression levels in indicated monoclonal Cre-sensitive cell lines. Blots probed with anti-flag HRP (upper) and anti-β-actin (lower) antibodies. (E) Mitotic index of cells treated with Ad-Cre for ~48 hours. 900 cells were scored as mitotic or non-mitotic through Hoechst staining. n≥3. (F) Genomic DNA was isolated from Cre-sensitive cell lines were treated with Ad-Cre for ~48 hours and then subcloned into 96-well plates. PCR was run using primers flanking either side of the floxed locus. Upper band indicates PCR fragment containing floxed-Plk1. Lower band indicates Plk1 locus excision.

Supplemental Figure 2-2

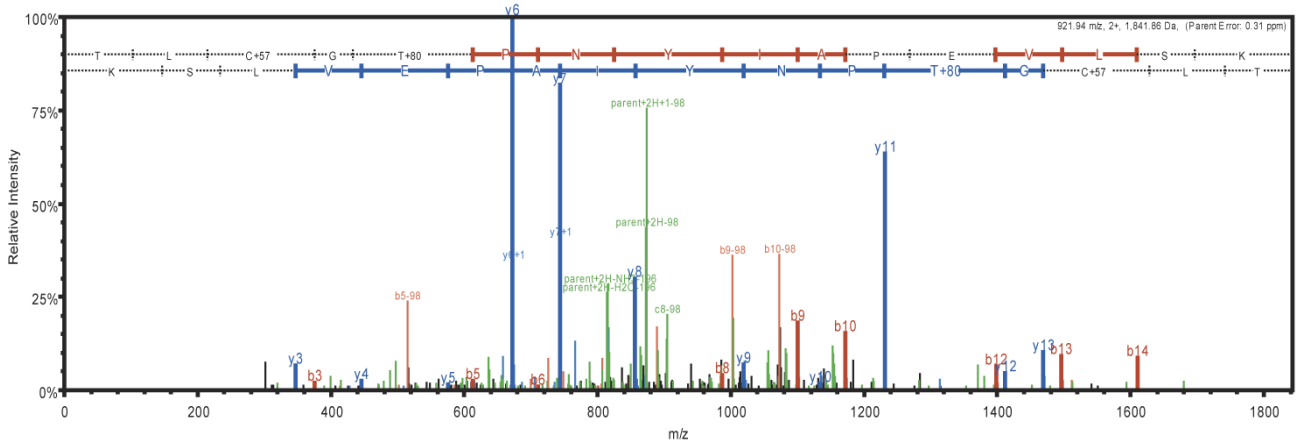

B	B Ions	B+2H	B-NH3	B-H2O	AA	Y Ions	Y+2H	Y-NH3	Y-H2O
1	102.1			84.0	T	1,842.9	921.9	1,825.8	1,824.9
2	215.1			197.1	L	1,741.8	871.4	1,724.8	1,723.8
3	375.2			357.2	C+59	1,628.7	814.9	1,611.7	1,610.7
4	432.2			414.2	G	1,468.7	734.9	1,451.7	1,450.7
5	613.2			595.2	T+80	1,411.7	706.3	1,394.7	1,393.7
6	710.3	355.6		692.2	P	1,230.7	615.8	1,213.6	1,212.7
7	824.3	412.7	807.3	806.3	N	1,133.6	567.3	1,106.6	1,115.6
8	987.4	494.2	970.3	969.4	Y	1,019.6	510.3	1,002.6	1,001.6
9	1,100.4	550.7	1,083.4	1,082.4	I	856.5	428.8	839.5	838.5
10	1,171.5	586.2	1,154.5	1,153.5	A	743.4	372.2	726.4	725.4
11	1,268.5	634.8	1,251.5	1,250.5	P	672.4	336.7	655.4	654.4
12	1,397.6	699.3	1,380.6	1,379.6	E	575.3		558.3	557.3
13	1,496.6	748.8	1,479.6	1,478.6	V	446.3		429.3	428.3
14	1,609.7	805.4	1,592.7	1,591.7	L	347.2		330.2	329.2
15	1,696.8	848.9	1,679.7	1,678.8	S	234.1		217.1	216.1
16	1,842.9	921.9	1,825.8	1,824.9	K	147.1		130.1	

Supplemental Figure 2-2: Mass spectrometry confirms phosphorylation of Plk1 T214.

Flag-Plk1 was transfected into HeLa cells, which were synchronized in mitosis for collection. After immunoprecipitation, samples were processed as indicated in methods. MS/MS spectra of peptides corresponding to the T214 tryptic fragment are shown with b-ions in red and y-ions in blue. The table shows the expected m/z for ions observed.

Supplemental Figure 2-3

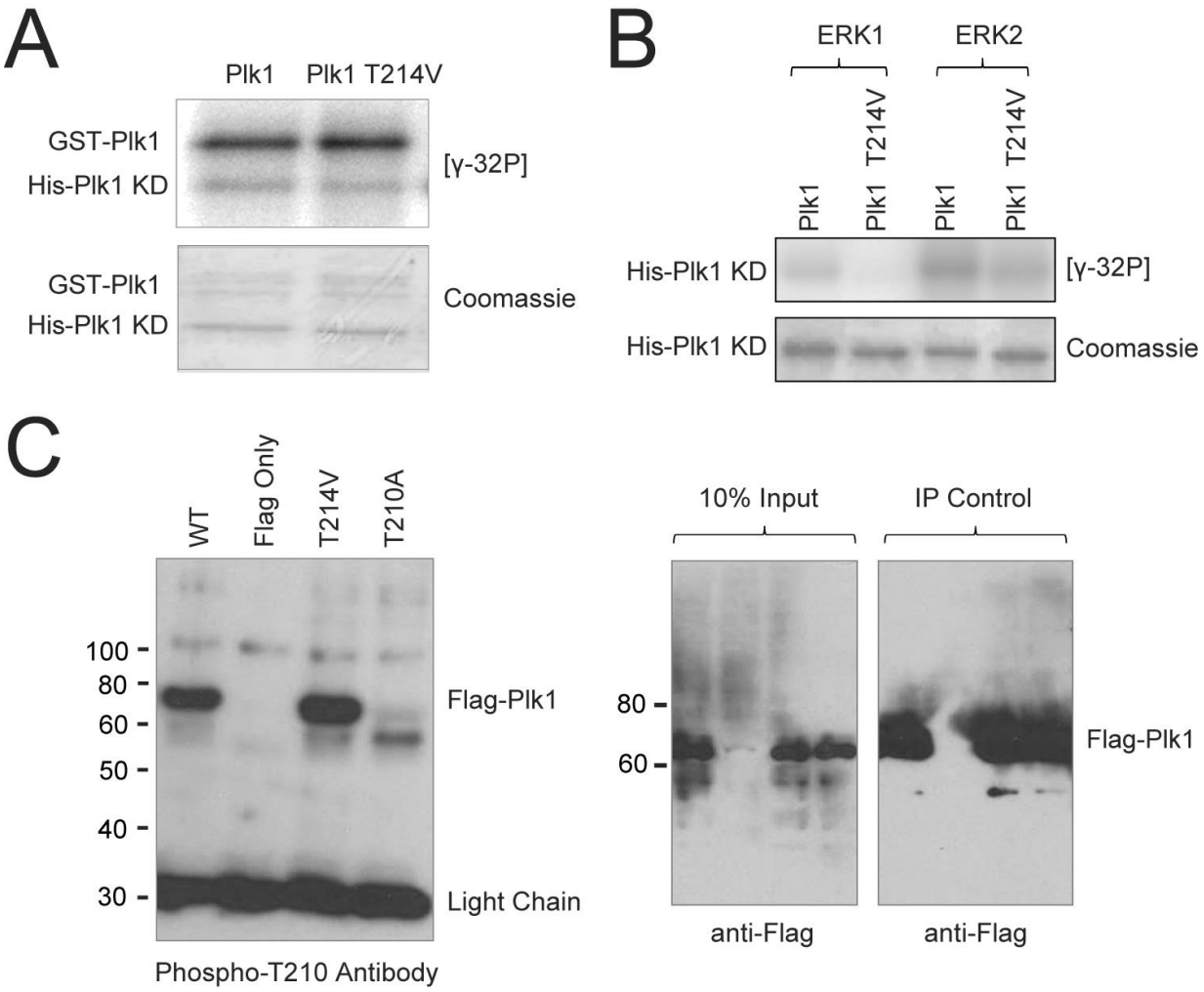

Supplemental Figure 2-3: Plk1 is not autophosphorylated or phosphorylated by ERK1/2 or Aurora A/B.

(A) GST-Plk1 and kinase dead (KD) His-Plk1 kinase domains, with and without T214V mutation, were incubated with [γ-32P], resolved by SDS-PAGE, and visualized by autoradiography. (B) ERK1 or ERK2 and His-Plk1^{KD} kinase domain, with and without T214V mutation, were incubated with [γ-32P], resolved by SDS-PAGE, and visualized by autoradiography. (C) HeLa cells were transiently transfected with flag-tagged constructs and arrested with nocodazole for 5.5 hours. Cell extracts were incubated with anti-flag agarose beads. Pulldown samples were resolved by SDS-PAGE and blotted with anti-phospho-T210 antibody. At right, western blot showing input and immunoprecipitation (IP) controls. Blots probed with anti-flag antibody.

Supplemental Figure 2-4

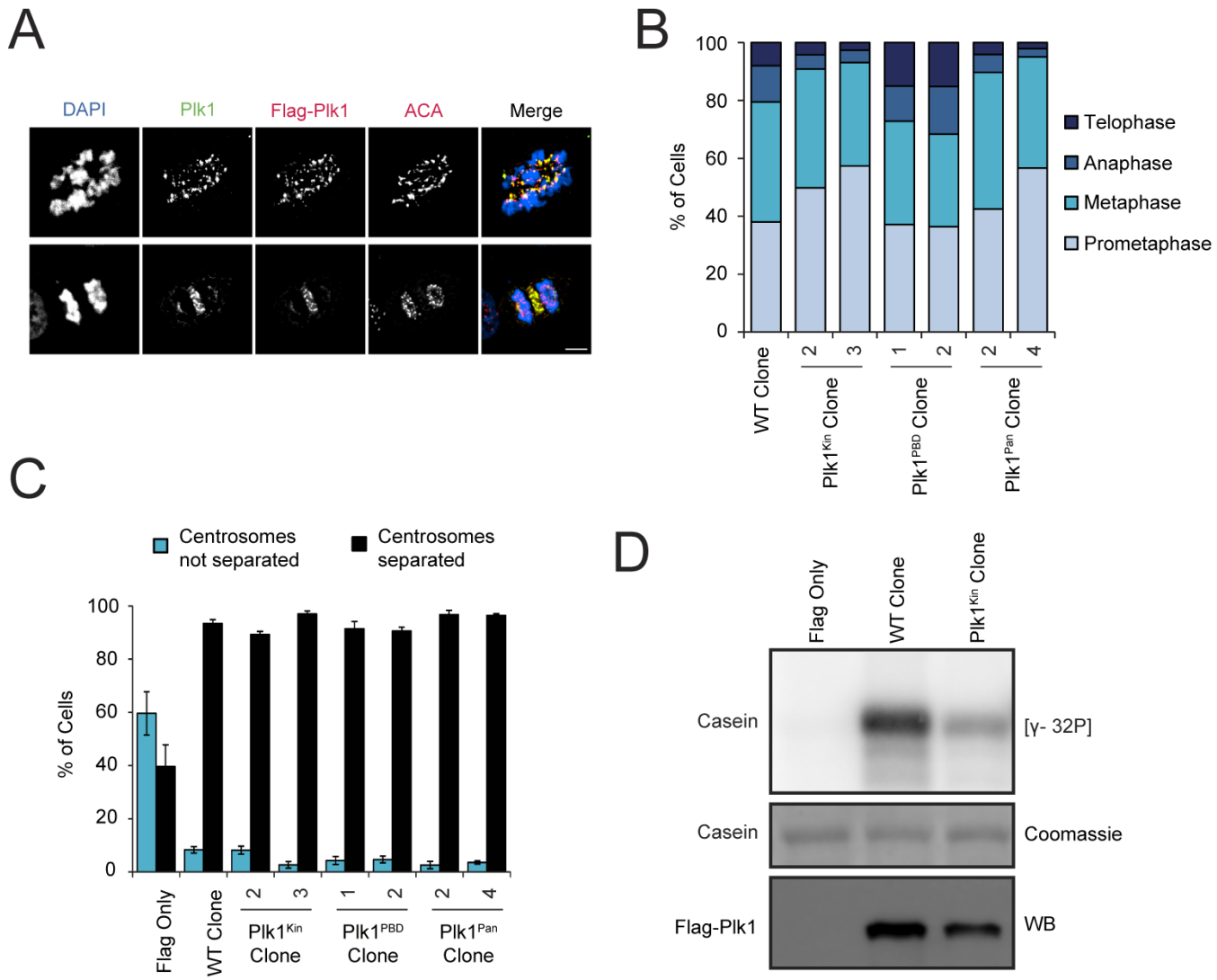

Supplemental Figure 2-4: Plk1^{Kin} rescues some Plk1 functions

(A) Plk1^{Pan} localizes properly in early and late mitosis. Cells were stained for total Plk1, Flag, and ACA and with DAPI. (B) Cells were treated with 3-MB-PP1 for 6 hours, fixed, and stained for DAPI, ACA, and Plk1. n=3, 200 or more mitotic cells were counted for each cell line for each replicate. (C) Cells were treated with 3-MB-PP1 for 6 hours, fixed, and stained for DAPI and γ-tubulin. n=3, 60 or more cells were counted for each cell line for each replicate. *$p<0.05$ compared to incidence of not separated centrosomes in WT Clone. (D) Stable cell lines with indicated flag-tagged constructs were arrested with 0.2μg/ml nocodazole. Cell extracts were incubated with anti-flag agarose beads. Pulldown samples were incubated with [γ-32P] and α-casein, resolved by SDS-PAGE, stained with coomassie, and visualized by autoradiography. Western blot showing immunoprecipitation control probed with anti-flag antibody.

Acknowledgements

We thank William M. Bement, Beth A. A. Weaver, Robert F. Lera, and Ryan A. Denu for critical review of this manuscript.

Chapter 3: Distinct mechanisms of action for the Aurora A inhibitor MLN8237 in combination with inhibitors of Cdk or Plk1 and with the radiosensitizer IUdR

Work in this chapter is in preparation for submission:

Novel combinations of MLN8237, an Aurora A kinase inhibitor, in triple-negative breast cancer

Amber Lasek, Murtuza Rampurwala, Alka Choudhary, and Mark E Burkard.

Abstract

Triple-negative breast cancer (TNBC) is a highly proliferative tumor with overall poor prognosis due to an aggressive and early pattern of metastasis and a relative lack of therapeutic targets. Chemotherapy remains the cornerstone of treatment but has relatively high toxicity and is often ineffective. Recently, MLN8237, an inhibitor of Aurora A, has shown modest efficacy in treating breast cancer. We hypothesized that combining antimitotics and cell cycle agents could enhance effectiveness, decrease resistance, and reduce toxicities. Here, we focused on combinations between cell cycle targeting agents given TNBC is often highly proliferative. We assembled a library of antiproliferative agents with unique mechanisms and targets that have subtly different effects on cancer cell proliferation. We performed a screen testing 105 unique two-drug combinations in MDA-MB-231 TNBC cells. We validated hits through Chou Talalay Combination Index (CI) and mechanistic analyses. We discovered an enhanced antiproliferative response between MLN8237 (Alisertib) and two kinase inhibitors (BI 2536 and flavopiridol) and one radiosensitizer (IPdR). Each combination cooperated in distinct pathways revealing novel mechanisms of action and the potential to enhance the effectiveness of clinically utilized drugs: MLN8237 in combination with flavopiridol arrested cells in G2 due to delayed or inhibited mitotic entry; MLN8237 with BI2536 led to a G2 arrest-associated induction of apoptosis; MLN8237 increased DNA damage when coupled with IUdR treatment. Surprisingly, none of these combinations obviously augmented errors during mitosis which are anticipated with Aurora A inhibition. This screen not only offers a strategy for combinatorial therapeutics, but also provides new insights into their biologic targets and the complex dynamics of cell cycle regulation. These findings suggest that Aurora A inhibition is privileged for cancer therapy as it coordinates with multiple other agents and with distinct mechanisms.

Introduction

One of eight U.S. women is diagnosed with breast cancer during her lifetime (National Cancer Institute, 2009). Triple-negative breast cancer (TNBC) is a highly proliferative breast cancer type that lacks estrogen (ER), progesterone receptors (PR), and human epidermal growth factor 2 (HER2) and constitutes ~15% of breast cancers (Hudis and Gianni, 2011; Boyle, 2012). Chemotherapy is the mainstay of medical treatment for TNBC, but outcomes are poor compared with other breast cancer subtypes (Kassam *et al.*, 2009; Gelmon *et al.*, 2012). This is due to innate aggressive biological characteristics and a relative dearth of effective therapeutics. An attractive therapeutic approach is to reduce or exploit the high proliferative rate commonly associated with TNBC. Amongst available chemotherapeutic options, antimitotic agents like taxanes (paclitaxel, nab-paclitaxel and docetaxel) are among the most effective, albeit with disappointing single agent activity (response rates of ~25% and short overall survival) (Winer *et al.*, 2004; Harris *et al.*, 2006). New effective therapeutics are critically required.

A key to improving treatments may be the identification of drug combinations which enhance effectiveness, decrease resistance, and reduce toxicities. Given that antimitotics have performed comparatively well, using these agents in combination may prove to provide a valid strategy. Here, we investigated the potential utility of antimitotics and agents that target specific aspects of proliferation. MLN8237 is a selective inhibitor of Aurora A kinase; Aurora A localizes to centrosomes where it enforces spindle bipolarity by managing centrosome organization and microtubule assembly. If this is misregulated, spindle defects lead to monopolar, multipolar, or fragmented spindles, often leading to aneuploidy (Fu *et al.*, 2007; Hoar *et al.*, 2007; Asteriti *et al.*, 2011, 2014). Aurora A is amplified or overexpressed in human cancer and contributes to genomic instability and

invasiveness (Tanaka *et al.*, 1999; Miyoshi *et al.*, 2001; Katayama *et al.*, 2003). The TNBC basal subtype, notably, is characterized by an increased proliferative index and is enriched for cell cycle components, including Aurora A (Nadler *et al.*, 2008; Yamamoto *et al.*, 2009; Lehmann *et al.*, 2011). In a recently completed multicenter phase II clinical trial, MLN8237 demonstrated promising activity in breast cancer patients treated with multiple prior lines of therapy (80% of patients with ≥ 4 lines) with an objective response rate of 18% (Melichar *et al.*, 2015).

We evaluated the effect of combining the Aurora A inhibitor MLN8237 with a number of new drugs with unique intracellular mechanisms and targets that have subtly different effects on cell division. These include checkpoints activators (microtubule poisons and inhibitors for polo-like kinase 1 (Plk1), cyclin dependent kinases (Cdks), and centromere protein E (CENP-E)) as well as checkpoint inactivators (inhibitors for monopolar spindle 1 kinase (MPS1) and Aurora B kinase). Further, agents with non-mitotic primary targets can also alter mitotic function through abnormal chromosome replication and/or damage to DNA (PARP inhibitor and ropidoxuridine (5-iodo 2-deoxypyrimidinone 2'-deoxyribose, IPdR).

We have identified novel distinct combinations of MLN8237with flavopiridol, a Cdk inhibitor (Senderowicz, 1999; Sedlacek, 2001), BI2536, a selective Plk1 inhibitor (Steegmaier *et al.*, 2007; Degenhardt and Lampkin, 2010), and IPdR, a radio-sensitizing agent (Kinsella *et al.*, 1994, 2008; Saif *et al.*, 2007; Kummar *et al.*, 2013) using *in vitro* and *in vivo* models of TNBC. This establishes that it may be possible to potentiate the response to MLN8237 in TNBC. Collectively, the enhanced effects seen in these combinations demonstrate that Aurora A targeting MLN8237 is privileged in its ability to collaborate with other drugs through diverse pathways and mechanisms.

Results

Drug Screen

We assembled a drug library, and constructed dose-response curves (DRC) for each chemical using fluorescent analysis of proliferation in MDA-MB-231, a TNBC cell line (Table 3-1). A concentration leading to 20% loss in cell viability (EC_{20}) was computed for each agent. EC_{20} was selected because of the steep slope of the DRC just above this concentration. We subsequently performed the screen with 15 different chemicals for 105 unique two-chemical combinations (Figure 3-1). Our screen discovered some promising combinations of MLN8237. Interestingly, MLN8237 furthered the antiproliferative effect of the radiosensitizer IPdR, the Plk1 inhibitor BI2536, and the Cdk inhibitor flavopiridol.

We analyzed whether these combinations followed Chou Talalay's definition of synergy using Combination Index (CI) analysis and constant combination ratio experimental design after determining the EC_{50}'s for each drug in multiple cell lines (Chou and Talalay, 1984; Chou, 2010; Chou *et al.*, 2010; Zhang *et al.*, 2016) (Example shown in Supplemental Figure 3-1). In this assay, a CI of < 1 indicates synergism, CI = 1 indicates additivity and a $CI > 1$ indicates antagonism. IUdR (5-iodo-2'-deoxyuridine), rather than IPdR, was used at this point forward since it is the metabolite of the pro-drug IPdR and is believed to be the active molecule (Kinsella *et al.*, 1994). Moreover, the effective concentration of IUdR (EC_{20} ~10 μM) is significantly lower, suggestive that the higher effective concentration for IPdR (EC_{20} ~750 μM) is merely due to poor metabolism into active IUdR in a cell line system. Low to moderate synergy was observed in some of the combinations: B+M in MDA-MB-468 cells and F+M in MCF10A, Cal51, and MDA-MB-231 cells (Supplemental Figure 3-2); nevertheless, understanding the mechanisms and

pathways that MLN8237 utilizes to enhance the antiproliferative response will help to identify biologic targets and unravel the complex dynamics of cell cycle regulation.

MLN8237 combinations do not increase mitotic errors

MLN8237 inhibits Aurora A and elicits mono and multipolar mitotic spindles and arrest (Asteriti *et al.*, 2011, 2014; Zhou *et al.*, 2013). To assess the mechanism for synergy in these drug combinations, we first assessed mitotic arrest after exposure to single drugs or combinations (Figure 3-2). Although each combination treatment includes at least one mitotic kinase inhibitor, there was no statistically significant increase in the mitotic indices at the indicated timepoints. This was especially surprising for the B+M combination since both inhibit mitotic kinases that, when used at high concentrations, cause a mitotic arrest. We conclude that none of these combinations generate a mitotic arrest, but we further explored particular mitotic phenotypes since all of the combinations include at least one drug that is known to affect mitosis.

Aurora A inhibition is known to result in monopolar and multipolar spindles (Asteriti *et al.*, 2011, 2014) (Supplemental Figure 3-3A). To evaluate spindle structure, we probed for α- and γ-tubulin after exposure to drug treatments. However, there was no significant effect of the combination treatments on spindle structure, as judged by a lack of a difference between drug combinations and MLN8237 alone (Figure 3-3A,B). Since MLN8237 and Aurora A inhibition is also known to cause chromosome congression and segregation problems (Hoar *et al.*, 2007), we quantified the incidence of misaligned chromosomes in metaphase (Figure 3-4A) and segregation errors during anaphase, including lagging chromosomes and chromosome bridges (Figure 3-4B and Supplemental Figure 3-3B). We also added conditions with a reduced dose of MLN since the MLN alone

treatment was sufficient to cause about 80% of mitoses to be defective and could mask enhanced effects when used in combination. However, no increase was seen in the combination conditions, at any concentration of MLN. Thus we conclude that the drug combinations are not enhancing Aurora A inhibition effects through mitotic defects associated with spindle structure or chromosome separation.

Despite the lack of synergy in mitotic phenotypes, it is possible that subtle defects occur. To assess this, we performed timelapse imaging of cells expressing fluorescently labeled histone H2B (H2B-mcherry) (Supplemental Figure 3-4A,B). Nevertheless, no differences were detected in the time from nuclear envelope breakdown to anaphase onset. Although there appeared to be an increased incidence of cells that failed to complete mitosis or cytokinesis (Supplemental Figure 3-4C), fixed analysis did not support a significant increase in multinucleated cells (Supplemental Figure 3-5). We conclude that MLN8237 does not cooperate with IUdR, BI2536, or flavopiridol to affect mitotic phenotypes.

MLN8237 synergizes to arrest cells in G2 with Flavopiridol and BI2536, but not with IUdR

To broadly survey the cell-cycle defects elicited by these combinations, we employed flow cytometry. Following four days of treatment, cell populations were subjected to cell cycle analysis with PI staining or cells were probed with an antibody against pS10-Histone H3 (pH3). Here, we uncovered a difference between the drug combinations. While the G2/M fraction in the I+M combination was similar to MLN alone, B+M and F+M had an increased presence of G2/M cells (Figure 3-5A). When scrutinized with the pH3 data, we discovered that this increase was due to an increased G2 population, without an increase in the mitotic population (Figure 3-5B). Importantly, the pH3 data

closely matched mitotic assessment performed as in 2A (Supplemental Figure 3-6). We conclude that B+M and F+M combinations operate similarly by delaying cells in G2, but distinctly from IUdR.

Flavopiridol, MLN8237 combination reduces mitotic entry

Because of the increase in G2, we next focused on the B+M and F+M combinations to evaluate their respective mechanisms of action. We anticipated a delay in mitotic entry for these combinations as inhibition of Aurora A, Plk1, and Cdk1, all can delay mitotic entry (Seki *et al.*, 2008; Lindqvist *et al.*, 2009; Lobjois *et al.*, 2009; Gavet and Pines, 2010; Van Horn *et al.*, 2010; Aspinall *et al.*, 2015; Asteriti *et al.*, 2015; Lee *et al.*, 2015). To do this, we used timelapse microscopy to look for defects. For these experiments, cells were synchronized with aphidicolin for 24 hours, released for 4 hours before indicated drug treatment, and subjected to image acquisition to determine whether and how quickly cells entered mitosis (Figure 3-6) (Aspinall *et al.*, 2015). Only cells present in the field of view at the beginning of the movie were included in analysis. Intriguingly the F+M combination showed a slight increase in cells that never entered mitosis, although there was only a small difference in time to mitosis for those that did enter. Additionally, for those that were able to enter, fewer were able to reach a second mitosis in the duration of the movie as compared to the other treatment conditions. This mitotic entry delay would result in an accumulation of G2 cells, as seen in the flow experiments above and distinguishes the mechanism of action of the F+M combination. There was also a slight reduction of cells that entered a second mitosis for the B+M combination, which also supports an interphase delay in this condition. It was surprising, however, that a more dramatic phenotype wasn't seen

given Plk1's known roles at the G2/M transition. We conclude that concurrent Aurora A and Cdk inhibition is able to reduce proliferation through a decrease in mitotic entry.

Early apoptotic events are seen in MLN8237, BI2536 combination

Aurora A inhibition has been shown to cause apoptosis, while its overexpression reduces it (Wang *et al.*, 2006; Scharer *et al.*, 2008; Li *et al.*, 2010; Ding *et al.*, 2015); therefore, it's plausible that MLN8237 could collaborate with one of the other drugs to trigger apoptosis. Similarly, reduced Plk1 or Plk1 activity and flavopiridol treatment induces apoptosis (Bible and Kaufmann, 1996; König *et al.*, 1997; Parker *et al.*, 1998; Lei and Erikson, 2008; Maire *et al.*, 2013; Matthess *et al.*, 2014). Although an increased incidence of dead cells were not observed in timelapse analysis following 4 days of treatment, Annexin V staining revealed evidence of early apoptosis in the B+M combination (Annexin V+ and 7-AAD-, Figure 3-7 and Supplemental Figure 3-7). Phosphatidylserine exposure, detected by Annexin V, is considered to be an early and widespread event in apoptosis and can occur prior to the customary morphological changes associated with apoptosis (Martin *et al.*, 1995; Wlodkowic *et al.*, 2011). Interestingly, the population as a whole is shifted right; we hypothesize that this indicates that the "healthy" cells may also be in the early stages of apoptosis, where plasma membrane alterations are beginning. This may be caused by unresolved roles of Aurora A or Plk1 in apoptotic induction or through off-target effects. These results suggest that simultaneous treatment with MLN8237 and BI2536 causes cells to enter the apoptotic process through mechanisms associated with G2 arrest instead of the classically defined induction attributed to mitotic arrest.

MLN8237 and IUdR combination enhances DNA damage

Finally, we focused on the MLN, IUdR combination. As mentioned above, IPdR is an orally bioavailable pro-drug of the radiosensitizer IUdR (Saif *et al.*, 2007; Kinsella *et al.*, 2008; Kummar *et al.*, 2013). IUdR is a dThd (thymidine) analog which is sequentially phosphorylated to 5-iodo-dUTP (deoxyuridine triphosphate) and is incorporated into DNA. This DNA incorporation is the proposed mechanism of action for IUdR and through an increased sensitivity to radiation exposure and the effects of steric hindrance, causes DNA damage (Sundell-Berman and Johanson, 1992; Wang and Iliakis, 1992; Seo *et al.*, 2006; Gurkan *et al.*, 2007). Importantly, we were able to detect IUdR and DNA colocalization *in vitro* (Figure 3-8A). Analogously, Aurora A has been implicated in the DNA damage response (Wang *et al.*, 2014). To see if the I+M combination caused an increase in DNA damage over IUdR alone, we probed for pS139-Histone H2AX (γH2AX) positive cells by flow cytometry. I+M had an increased percentage of γH2AX positive cells (Figure 3-8B) that was not seen in the BI/Flavo and MLN combinations (Supplemental Figure 3-8A). A higher concentration of IUdR (20μM, I20) also caused an increase in DNA damage, consistent with earlier data (Sedelnikova *et al.*, 2002), and strengthening this proposed mechanism of action. Using quantitative immunofluorescence there was no difference seen in overall γH2AX signal, however (Supplemental Figure 3-8B), demonstrating the importance of employing the correct assay. Additionally, no difference was seen in overall p53 or phospho-p53 signal (Supplemental Figure 8C,D). We proceeded with validating the IUdR and MLN combination in animal models of TNBC (Figure 3-8C). Three mice per group were treated for 14 days: control (red); IPdR (green; 750 mg/kg/day by gavage); MLN8237 (blue; 30 mg/kg/day by gavage); and IPdR + MLN8237 at same doses (black). This revealed that IPdR alone does not have direct anticancer effects and MLN8237 had modest effects. However, the combination of these two markedly reduced tumor growth, demonstrating that IPdR potentiates

MLN8237 activity. Although there wasn't a statistically significant difference (combination vs. MLN8237 arm, p = 0.2606), this may be in part due to small sample size. Importantly, we did not observe differences in mouse behavior or toxicity across arms in this study, possibly due to the MLN8237 dose being relatively modest. These results support the clinical validation of this drug combination.

Discussion

We have identified novel combinations of Aurora A inhibition. MLN8237 is a selective inhibitor of Aurora A kinase which has numerous roles both prior to and within mitosis (Macůrek *et al.*, 2008; Seki *et al.*, 2008; Sourisseau *et al.*, 2010; Cervigni *et al.*, 2011; Katayama *et al.*, 2013; Mahankali *et al.*, 2014; Sun *et al.*, 2014; Wang *et al.*, 2014). This provides multiple potential avenues to target the heterogeneity within and between tumors. It also provides numerous targetable pathways to utilize in the clinic and helps to unravel the complex network of protein interactions within the cell. This study provides mechanistic insight into interactions between MLN8237 and other therapeutics with differing mechanisms of action. Aurora A inhibition appears to be uniquely suited for combination therapies. MLN8237 potentiated the effects of the Cdk inhibitor flavopiridol to impede mitotic entry, the Plk1 inhibitor to induce apoptosis, the radiosentizer IUdR to increase DNA damage. This study not only represents a key therapeutic advancement for the treatment of proliferative TNBC, providing new targets to investigate clinically, but also provides a strategy to assess the interaction of cellular pathways.

To our knowledge, this is the first evidence that MLN8237 can potentiate the effects of flavopiridol, BI2536, or ropidoxuridine. It is surprising that the Aurora A and Cdk inhibitors collaborate at mitotic entry given that both kinases appear to function in the

same pathway (Lindqvist *et al.*, 2009), however it is possible that both drugs reduce the activation of Plk1 through reducing T-loop phosphorylation or Bora-associated Plk1 activation, respectively (Macůrek *et al.*, 2008; Seki *et al.*, 2008; Bruinsma *et al.*, 2014; Thomas *et al.*, 2016). The discovery that MLN8237 and BI2536 combine to push cells towards apoptosis is also novel. Plk1 inhibition or knockdown has been shown to induce apoptosis through Fas mediated death receptor signaling (Matthess *et al.*, 2014). Plk1 phosphorylates procaspase-8, contributing to an anti-apoptotic signal within the extrinsic pathway; however, reduced Plk1 leads to increased caspase-8 cleavage and apoptosis. Numerous kinases have been shown to phosphorylate procaspase-8, depending on cell type (Alvarado-Kristensson *et al.*, 2004; Cursi *et al.*, 2006; Matthess *et al.*, 2010; Peng *et al.*, 2011) and it's conceivable that Aurora A could also partake in this pathway, especially given the known role of Aurora A in apoptosis (Wang *et al.*, 2006; Scharer *et al.*, 2008; Li *et al.*, 2010; Ding *et al.*, 2015). It's also possible that these drugs alter the cells redox status through unknown direct or off-target means. Indeed, MLN8237 treatment has also been shown to induce the production of reactive oxygen species (Niu *et al.*, 2015).

Moreover, this is the first time reduced proliferation was observed with IPdR in combination with any anti-mitotic agents. As seen in our initial screen, this is the first discovery of cytotoxic effect of IPdR without requiring hepatic metabolism to IUdR. We propose that in cell-lines, there may be limited metabolism of IPdR by aldehyde oxidase to IUdR mediating biological effects. Further, in our screen validation and mechanistic studies, we have provided evidence that the underlying biologically active metabolite of IPdR is IUdR. Although useful for cell culture studies, IUdR has a short half-life ($t_{1/2}$) making it a cumbersome drug to use *in vivo* (Kinsella *et al.*, 1994, 1998). Additionally, IPdR has an improved therapeutic index compared with IUdR (Kinsella *et al.*, 1998; Kummar *et al.*, 2013). It is a promising radiosensitizer and a phase 1 dose escalation study of IPdR in

combination with radiotherapy in advanced gastrointestinal malignancies is expected to open in the next few months (National Cancer Institute (NCI)). Importantly our in vivo, xenograft mouse model study demonstrates the translatability of this drug combination.

Although our study identified novel combinations of MLN8237, there are some limitations. Using Chou- Chou Talalay's definition of synergy, our combinations demonstrated low synergy. Despite this, the ability to reduce doses clinically could potentiate patient responses when compared to single agent treatment. Additionally, we did not observe selectivity for cancer cell lines over the breast epithelial cell line, MCF10A; however, MCF10A cells are highly proliferative with a doubling time of about 16 hours (American Type Culture Collection, 2012); therefore, they may not serve as an accurate control to demonstrate selectivity for transformed, proliferative tumor cells. Further, although we saw encouraging effects with MLN8237 and IPdR *in vivo* mouse models, it's possible the other combinations will not translate, but further investigation is required.

In addition to exploring the translatability of the MLN8237 combinations explored here, additional analysis should probe the combination of other therapeutic agents. In particular, given the relative efficacy of taxanes clinically, a more thorough examination of the validity of these agents in combination is imperative. With agents such as Taxol, toxicities are often dose-limiting; combinatorial strategies could provide the means to moderate these effects. In general, combining clinical or investigative agents may elucidate new effective therapies and provides hope for the future of cancer treatment.

Materials and Methods

Cell-culture

MDA-MB-231, MDA-MB-468, and MCF10A cell lines were obtained from American Type Culture Collection (ATCC, Manassas VA). CAL-51 cell lines were obtained from Beth Weaver, UW Madison. MCF10A cells were cultured in Dulbecco's Modification of Eagle's Medium (DMEM) F12 (HyClone, Utah USA) plus 5% (vol/vol) horse serum, 20 ng/mL EGF, 0.5 mL/mL hydrocortisone, 100 ng/mL cholera toxin, and 10 µg/mL insulin. All other cell lines were cultured in DMEM – high glucose (HyClone, Utah USA) supplemented with 10% (vol/vol) fetal bovine serum (FBS). All media contained 100 U/mL Penicillin-Streptomycin and cells were incubated at 37º C in a humidified atmosphere containing 5% CO_2.

Chemicals

Chemicals used throughout this study include Ropidoxuridine (IPdR, National Cancer Institute (NCI), used at 750µM), IUdR (5-iodo-2'-deoxyuridine, Sigma-Aldrich, used at 5µM unless otherwise stated), BI2536 (ThermoFisher, used at 3.125nM), Flavopiridol (Selleck, used at 50nM), and MLN8237 (Alisertib, Millennium Pharmaceuticals, Selleck, used at 25nM unless otherwise stated). For xenograft experiments, bulk MLN8237 was obtained from Adooq Biosciences. Other chemicals for the screen included paclitaxel, monastrol and reversine (ThermoFisher, Waltham MA), vinflunine, ispinesib, ZM447439, AZ3146 and ABT888 (Selleck Chemicals), vincristine (NCI), 0.2µg/ml nocodazole (Sigma-Aldrich), and GSK923295 (ChemScene, Monmouth NJ) 50µM blebbistatin (EMD Millipore), 0.2µg/ml doxorubicin (MP Biomedicals), and 0.2µM Staurosporine (Enzo Life Sciences).

Antibodies and Cell Stains

Antibodies used in this study include anti-γ-tubulin (MA1-20248, clone GTU-88Thermo), anti-α-tubulin (MAB1864 Millipore), anti-Plk1 (F-8, sc-17783 Santa Cruz Biotechnology), anti-pericentrin (ab44448 Abcam), anti-ACA/CREST (HCT0100 Immunovision), anti-pH3-S10 (9701S Cell Signaling), anti-pH2AX-S139 (05-636 Millipore), and anti-IdU (SAB3701448 Sigma). For immunofluorescence and flow cytometry, Alexa-fluor secondary antibodies were used (Invitrogen). Mitotic index was determined through Hoechst 33258 staining and microscopy.

Synergy Screen

The synergy screen was performed for 105 unique two-chemical combinations. Prior to the screen, dose-response curves for each chemical was constructed using fluorescent analysis of proliferation. Cells were plated in 96-well plates at initial counts of 5000 cells/100 µl/well. After overnight incubation, cells were treated with DMSO vehicle control or chemical at serially diluted concentrations. 96 h post treatment, SYBR green (Lonza) was diluted 1:600 in 1X phosphate-buffered saline (PBS) and 20 µl were added to make final volume 140 µl. After an overnight incubation, fluorescence was read using the BioTek Synergy 4 plate reader. Assays were prepared in triplicate with average values recorded. A concentration leading to 20% loss in cell viability (EC_{20}) was computed for each chemical agent. Analysis of proliferation was performed as above with MDA-MB-231 cells treated with DMSO control, individual chemical at EC_{20} or in pairs with each chemical at ½ EC_{20}.

Combination Index (CI) Analysis

To test for synergy in the drug combinations, combination Index (CI) analysis was performed using the Chou Talalay principle using the constant combination ratio design. In

this assay, treatment concentrations were centered around the EC_{50} calculated for each cell line: IUdR (MDA-MB-231: 312.5-5000μM; MDA-MB-468: 78.125-1250μM; Cal51: 25-400μM; MCf10A: 25-400μM), MLN8237 (MDA-MB-231: 75-1200μM; MDA-MB-468: 12.5-200μM; Cal51: 12.5-200μM; MCf10A: 50-800μM), BI2536 (MDA-MB-231: 5-80μM; MDA-MB-468: 0.625-10μM; Cal51: 5-80μM; MCf10A: 5-80μM), and flavopiridol (MDA-MB-231: 312.5-5000μM; MDA-MB-468: 78.125-1250μM; Cal51: 25-400μM; MCf10A: 25-400μM) and were used singly and in combination. Cells were plated in 96-well plates at initial counts of 5000 cells per well and were treated for 4 days. The effect size was measured using colormetric analysis of proliferation (Vita-Orange. Biotool.com; B34302) and CI analysis was performed using the Compusyn® software. Three independent replicates were performed unless otherwise indicated. Dose-response curves were created in Prism using data collected from VitaOrange analysis. CI scores above 10 were excluded and believed to the result of amplified noise in the experiment.

Immunofluorescence (IF) and Microscopy

For IF cells were plated on coverslips and antibodies were incubated in PBS + 0.1% Triton X-100 with 3% BSA. Spindle structure was determined following fixation with 100% ice cold methanol. IUdR incorporation was determined following fixation with 4% PFA, DNA denaturing with 2N HCl, and neutralization with sodium borate. Other phenotypes were determined following fixation with 4% paraformaldehyde.

Nikon Eclipse Ti inverted microscope with a CoolSNAP HQ2 charge-coupled device camera (Photometrics) was used to acquire images. Nikon Elements software was used to process and analyze images. Final figures were formatted in Adobe Photoshop and Illustrator.

All timelapse movies were performed using H2B-RFP labeled MDA-MB-231 cells. For mitotic entry experiments, cells were seeded in 6-well plates to be at about 60% confluency when treated with aphidicolin. 24 hours later, cells were released into complete media for 4 hours, then treated with indicated drugs for one hour before movie was started. Images were collected every 5 minutes for 48 hours. Cellular phenotypes were only recorded for those that were present at the beginning of the movie. For other timelapse movies, cells were plated to reach about 60% confluency when movie was started, following indicated treatment times and conditions. Images were collected every 4 minutes for 24 hours.

Mitotic Index

MDA-MB-231 cells were seeded in a 12-well plate to reach 60-80% confluency on day of collection. Adherent and non-adherent cells were collected at 24 hour, 48 hour, 72 hour, and 96 hour time points post-treatment and stained with Hoeschst 33258. 300 cells were counted for each condition categorizing cells as mitotic vs. non-mitotic.

Flow cytometry

All flow cytometry experiments were analyzed on a BD FACScalibur flow cytometer (BD Biosciences). Any experiments where control treatments (nocodazole, doxorubicin, staurosporine) did not produce the anticipated effects were omitted.

For apoptosis assays, cells were treated with indicated drugs for 4 days. 60 nmol/L staurosporine was used overnight. Apoptosis was evaluated by an Annexin V-PE/7-AAD apoptosis detection kit (Ebiosciences). For analysis, the percent early apoptotic cells positive cells were Annexin V+ and7-AAD- (lower right quadrant).

DNA content was determined by fixing cells in ethanol and staining with propidium iodide (PI, MP Biomedicals).

Xenograft assays

$5x10^6$ MDA-MB-231 cells in PBS were inoculated into the mammary pads of 6-week-old female athymic nude mice (Jackson laboratories, ME). When average tumor size reached 50 to 80 mm^3, 3 mice per group were treated for 14 days: control; ropidoxuridine (750 mg/kg/day by gavage); MLN8237 (30 mg/kg/day by gavage); and ropidoxuridine + MLN8237 at same doses. Tumors were measured every 3 days by calipers during treatment and mice were sacrificed at 14 days. Mice were monitored daily for toxicity while on treatment.

Statistical Analysis

Dose-response curves and EC_{20} calculations for the initial screen were performed using BioDataFit 1.02 (Chang Bioscience) using an exponential decay model. Replicate experiments were performed, and standard errors are reported as indicated below. Combination indices (CI) and Isobolograms were constructed using the CompuSyn® software and prisim. For animal studies, a sample size of 3 mice per group afforded a power of 80%, to detect a tumor volume change of 40% more by the drug combination than each drug individually, with two-sided significance level of 0.05 and expected variation of 30% amongst tumor sizes in individual cohorts. Differences in the mean tumor value between cohorts were analyzed using a paired t test.

Table 3-1

TABLE 1: DRUG LIBRARY		
No	Agent	Mechanism of Action
Activates Spindle Assembly Checkpoint (SAC)		
1	Taxol	Microtubule stabilizer
2	Vinflunine	Microtubule depolymerizer
3	Vincristine	Microtubule depolymerizer
4	Nocodazole	Microtubule depolymerizer
5	Ispinesib	Kif11 (Eg5) inhibitor
6	Monastrol	Kif11 (Eg5) inhibitor
7	GSK 923295	Centromere protein E (CENP-E) inhibitor
8	BI 2536	Polo-like kinase 1 (Plk1) inhibitor
9	MLN 8237	Aurora A selective kinase inhibitor
Inactivates Spindle Assembly Checkpoint (SAC)		
10	ZM 447439	Aurora B kinase inhibitor
11	Reversine	Monopolar spindle 1 (MPS1) kinase inhibitor
12	AZ 3146	Monopolar spindle 1 (MPS1) kinase inhibitor
Other mechanisms		
13	Ropidoxuridine	Radiosensitizer
14	Flavopiridol	CDK inhibitor
15	ABT 888	PARP inhibitor

Adapted from Murtuza Rampurwala

Table 3-1: Drug library

Drugs included in the drug combination screen.

Figure 3-1

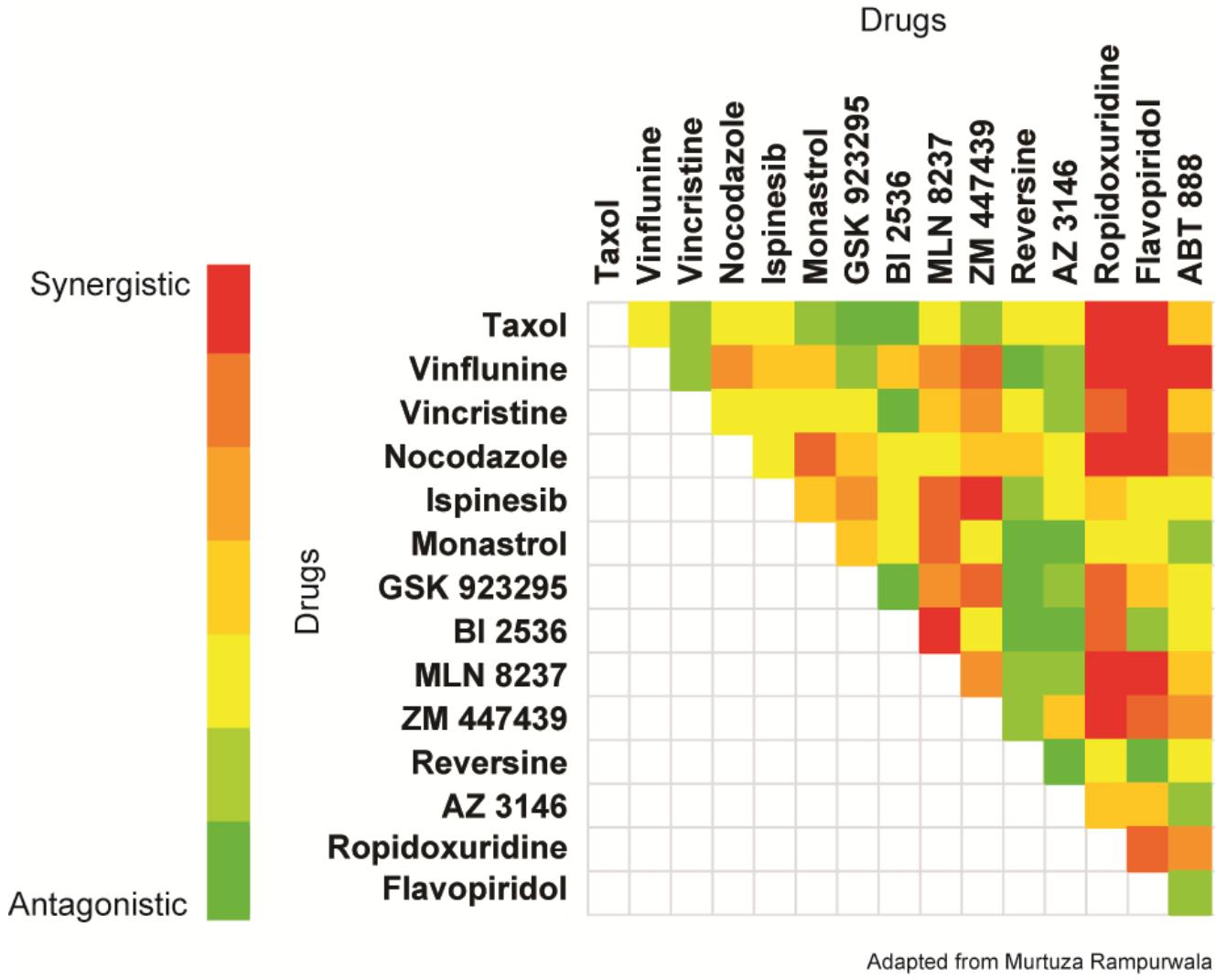
Drugs
Taxol
Vinflunine
Vincristine
Nocodazole
Ispinesib
Monastrol
GSK 923295
BI 2536
MLN 8237
ZM 447439
Reversine
AZ 3146
Ropidoxuridine
Flavopiridol
ABT 888
Synergistic
Antagonistic
Drugs
Taxol
Vinflunine
Vincristine
Nocodazole
Ispinesib
Monastrol
GSK 923295
BI 2536
MLN 8237
ZM 447439
Reversine
AZ 3146
Ropidoxuridine
Flavopiridol
Adapted from Murtuza Rampurwala

Figure 3-1: Drug screen identifies possible synergistic combinations.

Drug combinations are color coded for the level of synergy observed, with red being the most synergistic and green being the least.

Figure 3-2

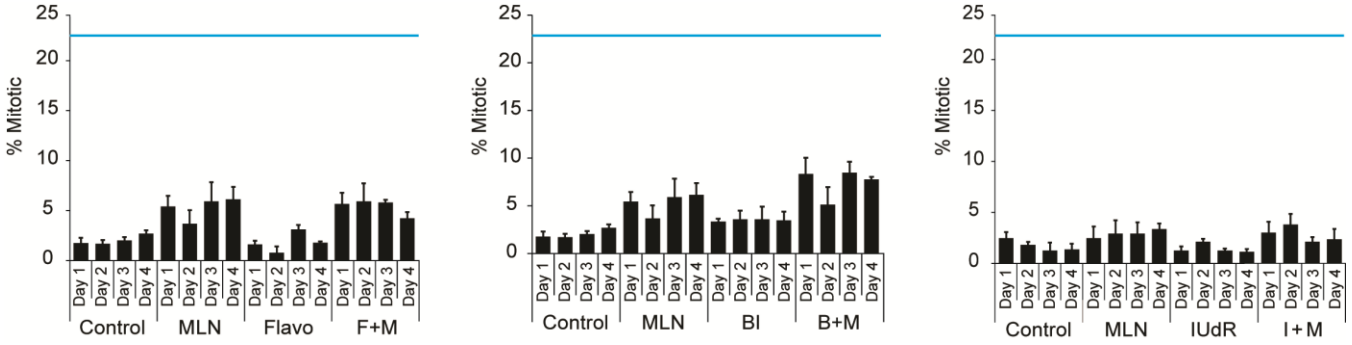
% Mitotic
25
20
15
10
5
0
Day 1
Day 2
Day 3
Day 4
Control
MLN
Flavo
F+M
% Mitotic
Control
MLN
BI
B+M
% Mitotic
Control
MLN
IUdR
I+M

Figure 3-2: BI2536, flavopiridol, and IUdR do not enhance mitotic cell accumulation observed with MLN8237 treatment.

Mitotic index of cells treated with indicated drugs for 4 days. Nocodazole treatment indicated by blue line. 900 cells were scored as mitotic or non-mitotic through Hoechst 33258 staining. n≥3. Error bars indicate SEM. No MLN combinations compared to single drug treatments were statistically significant.

Figure 3-3

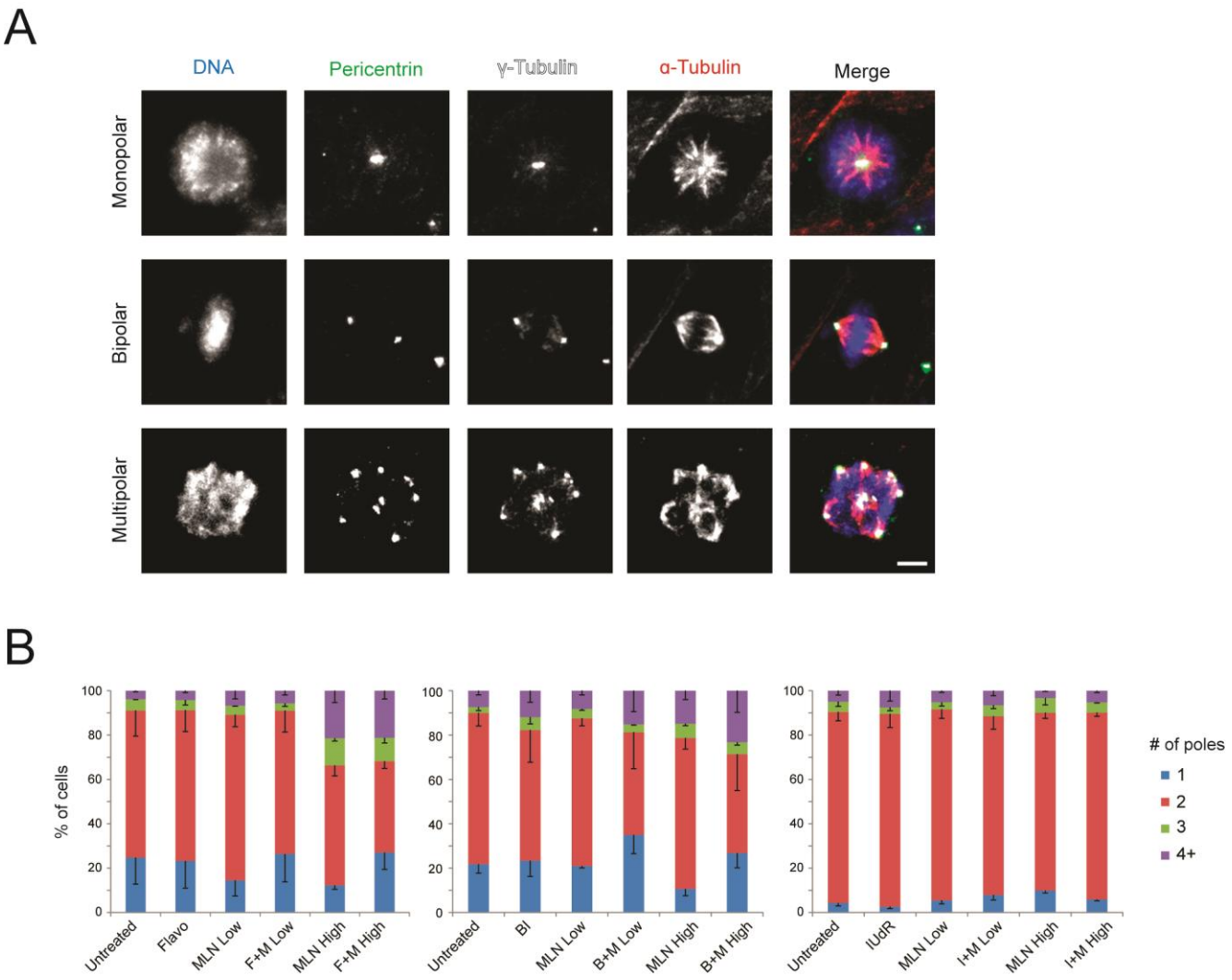
A
DNA
Pericentrin
γ-Tubulin
α-Tubulin
Merge
Monopolar
Bipolar
Multipolar
B
% of cells
100
80
60
40
20
0
Untreated
Flavo
MLN Low
F+M Low
MLN High
F+M High
Untreated
BI
MLN Low
B+M Low
MLN High
B+M High
Untreated
IUdR
MLN Low
I+M Low
MLN High
I+M High
# of poles
1
2
3
4+

Figure 3-3: BI2536, flavopiridol, and IUdR do not alter spindle structure with MLN8237 treatment.

(A,B) Cells were treated as indicated for 4 days, fixed, and stained with DAPI and for pericentrin, γ-tubulin and α-tubulin to characterize spindle structure. n=3, 300 or more cells were counted for each condition. Error bars indicate SEM. No MLN combinations compared to single drug treatments were statistically significant. Scale bar, 10μm.

Figure 3-4

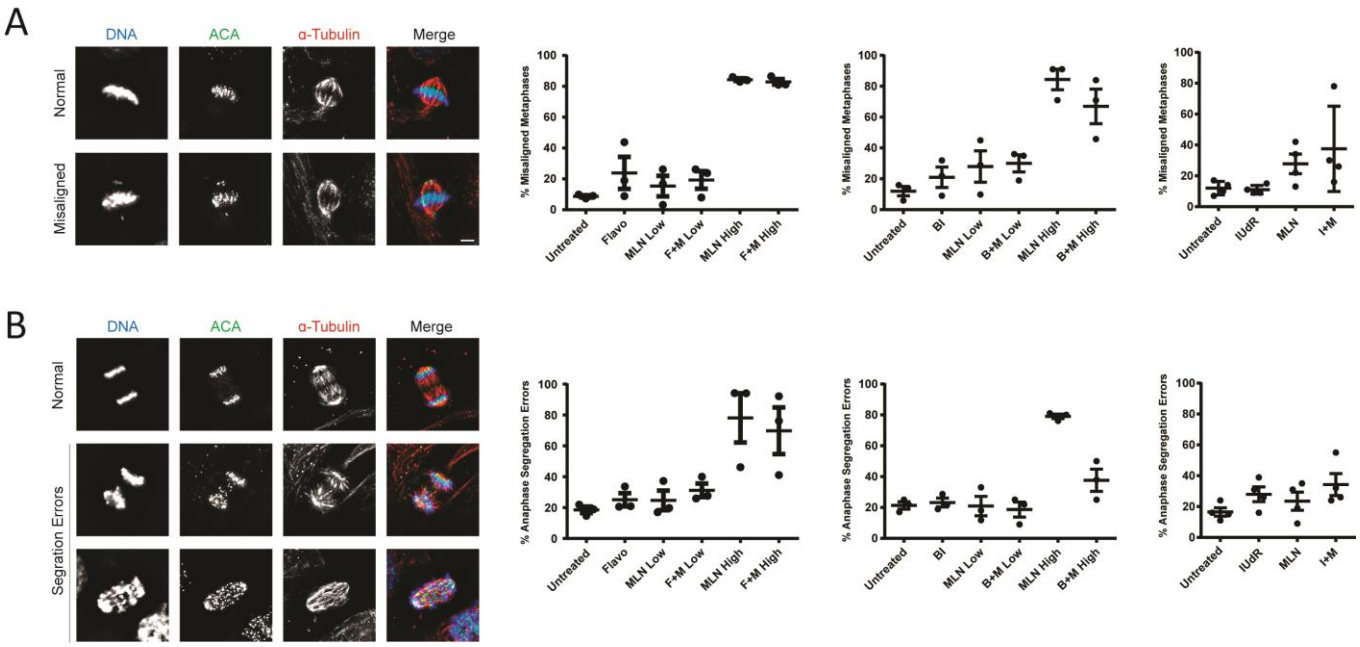
A
DNA
ACA
α-Tubulin
Merge
Normal
Misaligned
% Misaligned Metaphases
Untreated
Flavo
MLN Low
F+M Low
MLN High
F+M High
BI
B+M Low
B+M High
IUdR
MLN
I+M
B
Segration Errors
% Anaphase Segregation Errors

Figure 3-4: BI2536, flavopiridol, and IUdR do not enhance mitotic errors observed with MLN8237 treatment.

(A,B) Cells were treated as indicated for 4 days, fixed, and stained with DAPI and probed for ACA and α-tubulin to determine whether metaphase cells are characterized by misaligned chromosomes or whether anaphase/telophase cells had segregation errors. Here, MLN High cells were treated with 25nM MLN8237 (same concentration used throughout this chapter). MLN Low cells were treated with 5nM MLN8237. n=3, 300 or more cells were counted for each condition. Error bars indicate SEM. No MLN combinations (for analogous MLN concentrations) compared to single drug treatments were statistically significant. Scale bar, 10μm.

Figure 3-5

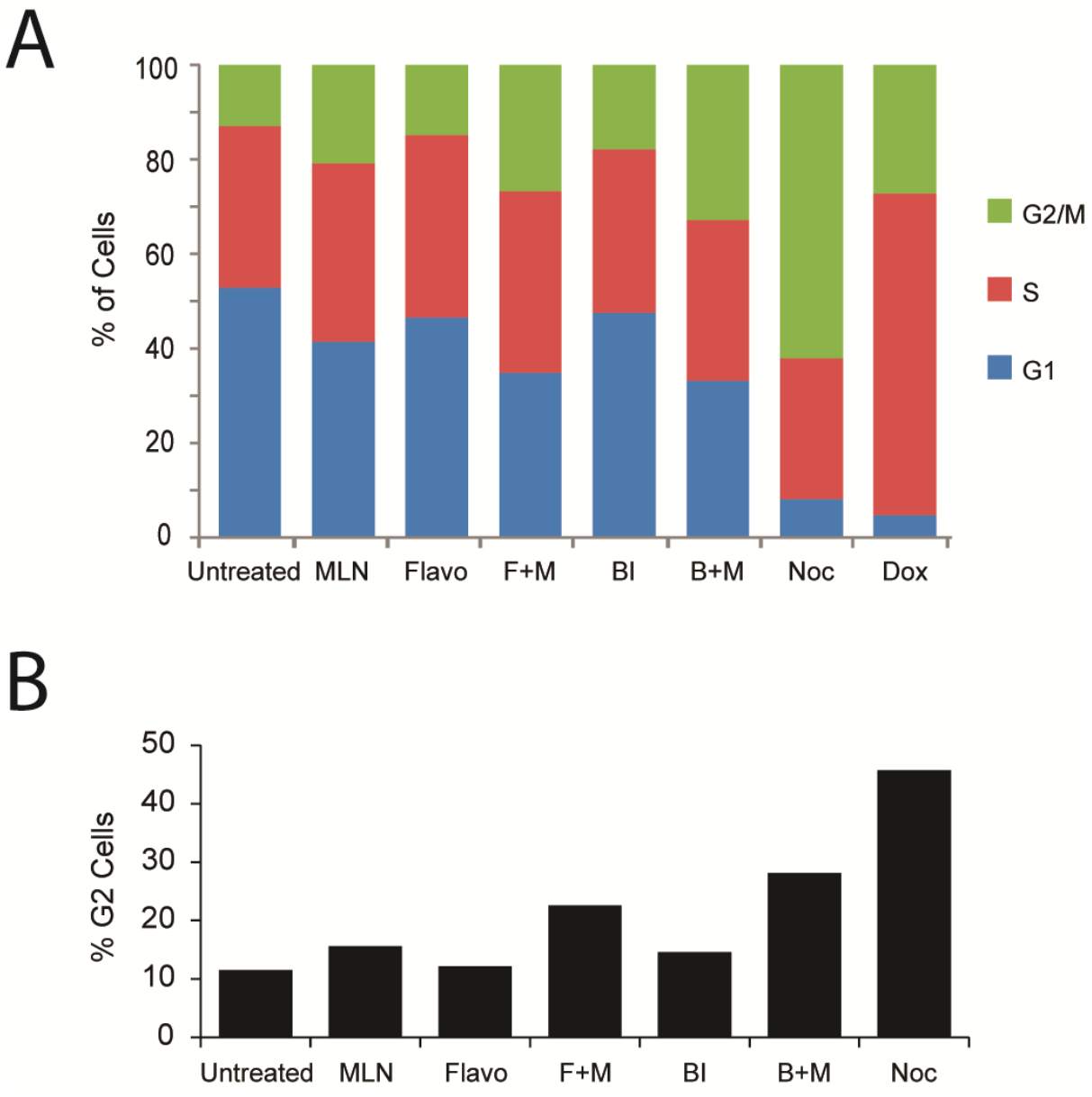
A
100
80
60
40
20
0
% of Cells
G2/M
S
G1
Untreated
MLN
Flavo
F+M
BI
B+M
Noc
Dox
B
50
40
30
20
10
0
% G2 Cells
Untreated
MLN
Flavo
F+M
BI
B+M
Noc

Figure 3-5: MLN8237 co-treament with BI2536 and flavopiridol results in G2 accumulation

(A) Cells were treated as indicated for 4 days. Nocodalzole (Noc) and doxorubicin (Dox) treatments were for 16 hours. All cells were collected, fixed with ethanol, and stained with PI. Stage distribution was determined following data collection on BD FACScalibur flow cytometer and cell cycle analysis. n=2. (B) Cells were treated and collected as in (A), however cells were fixed with 4%PFA, methanol and stained with pH3 antibody to determine the proportion of mitotic cells. % G2 cells were determined by subtracting %pH3 positive cells from the G2/M population in (A). n=2.

Figure 3-6

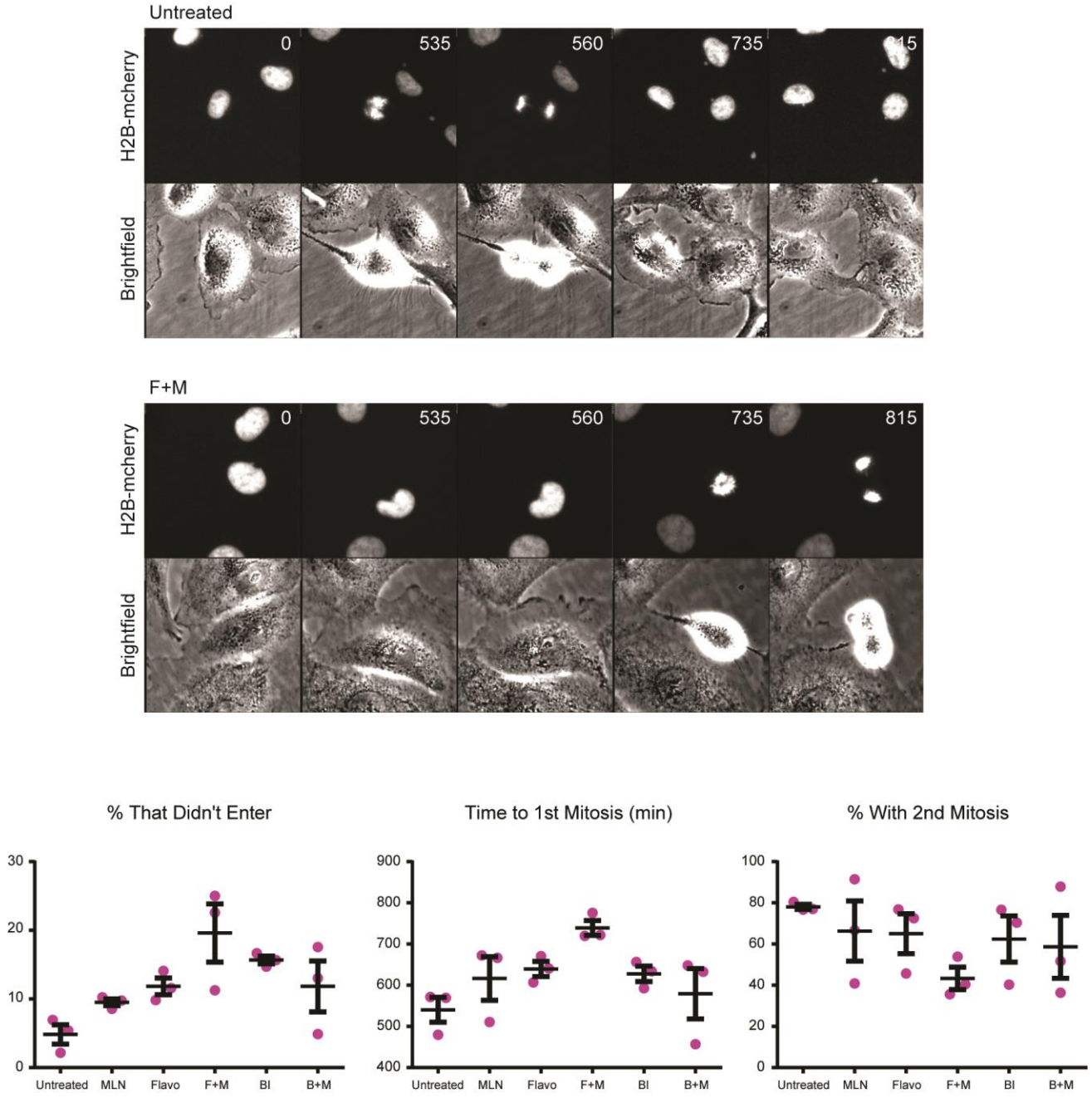
Untreated
H2B-mcherry
Brightfield
0
535
560
735
815
F+M
H2B-mcherry
Brightfield
0
535
560
735
815
% That Didn't Enter
30
20
10
0
Untreated
MLN
Flavo
F+M
BI
B+M
Time to 1st Mitosis (min)
900
800
700
600
500
400
Untreated
MLN
Flavo
F+M
BI
B+M
% With 2nd Mitosis
100
80
60
40
20
0
Untreated
MLN
Flavo
F+M
BI
B+M

Figure 3-6: Flavopiridol and MLN8237 co-treatment delays and reduces mitotic entry.

Cells were treated with aphidicolin for 24 hours, released into complete media for 4 hours, and treated with indicated drug for one hour. Cells were then imaged every 5 minutes for 48 hours. Three fields of view for each condition. n=3. Error bars indicate SEM. Only cells present in the first field were analyzed. Montage shows representative time to 1st mitosis for Untreated and F+M treated cells that divided. Time in minutes indicated in upper right hand corner. *% That Didn't Enter* indicates that during the time of the movie, the cell never entered mitosis. *Time to 1st Mitosis* (min) indicates how long, from the beginning of the movie, it took each cell to enter its first mitosis. % with 2nd Mitosis indicates, of the cells that entered mitosis one time, the number of cells that entered a second mitosis. Although a trend is observed, none of the MLN combinations compared to single treatments were statistically significant.

Figure 3-7

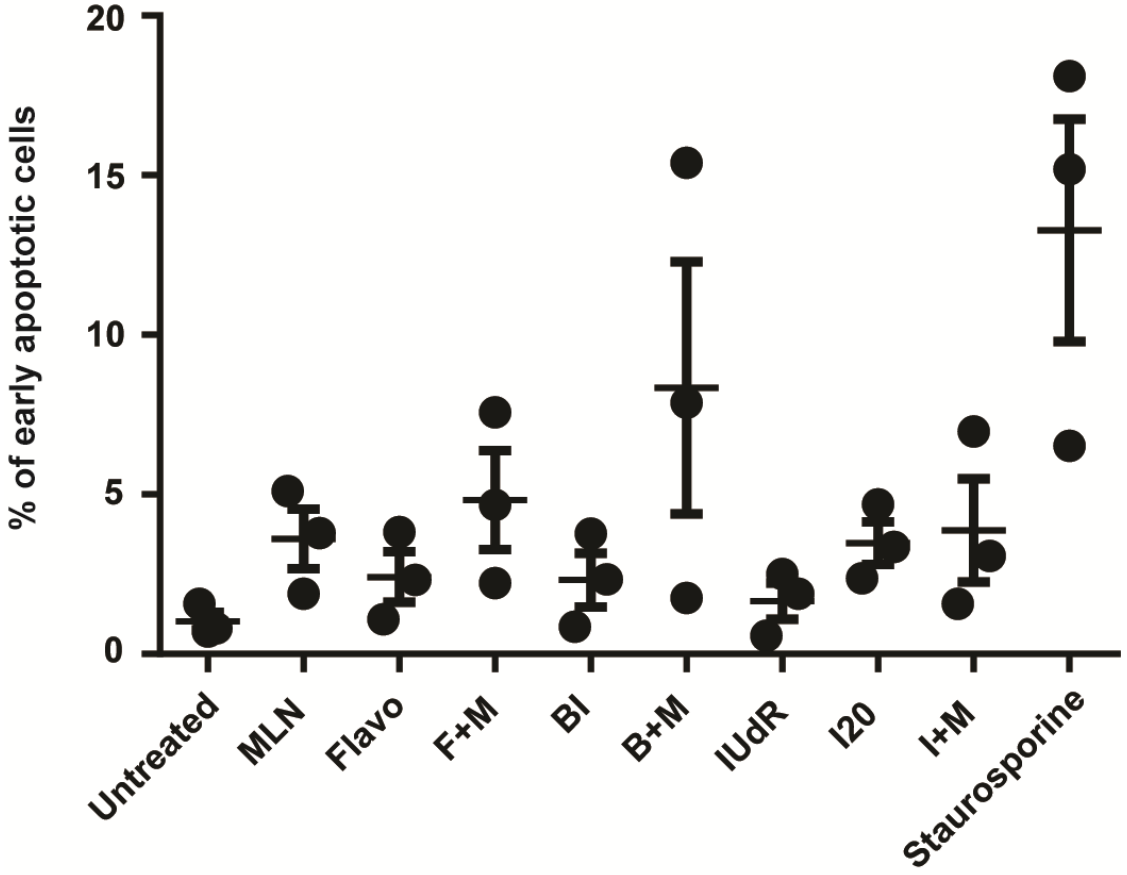
% of early apoptotic cells
20
15
10
5
0
Untreated
MLN
Flavo
F+M
BI
B+M
IUdR
I20
I+M
Staurosporine

Figure 3-7: BI2536 and MLN8237 combination increases the incidence of apoptotic cells.

Cells were treated as indicated for 4 days. Staurosporine treatments were for 16 hours. All cells were collected and stained with Annexin V and 7-AAD to determine the proportion of apoptotic cells. % apoptotic cells indicates % of cells that were in early apoptosis: Annexin V positive and7-AAD negative. N=3. Error bars indicate SEM. Although a trend is observed, none of the MLN combinations compared to single treatments were statistically significant.

Figure 3-8

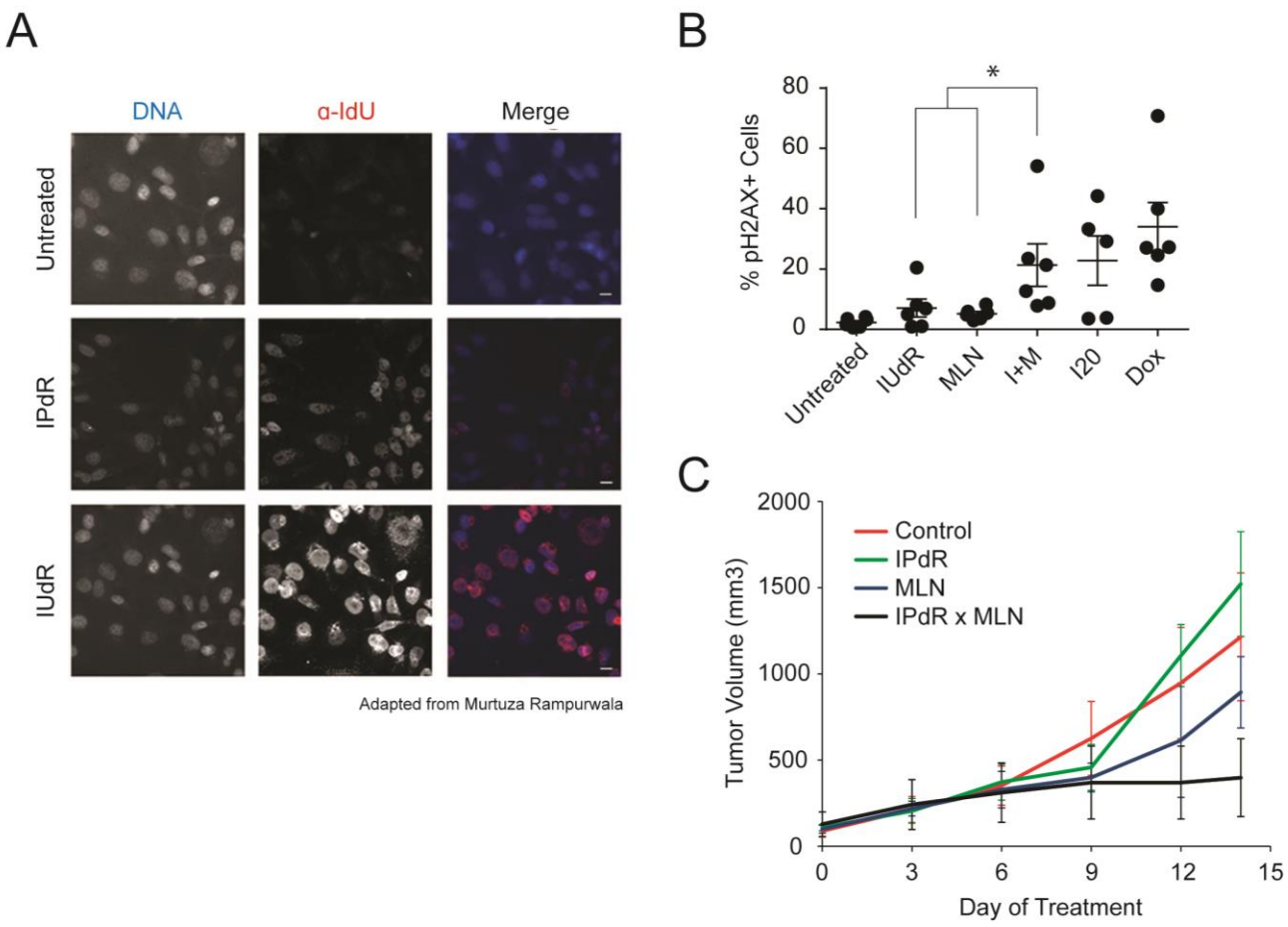
A
DNA
α-IdU
Merge
Untreated
IPdR
IUdR
Adapted from Murtuza Rampurwala
B
% pH2AX+ Cells
80
60
40
20
0
*
Untreated
IUdR
MLN
I+M
I20
Dox
C
Tumor Volume (mm3)
2000
1500
1000
500
0
Control
IPdR
MLN
IPdR x MLN
0
3
6
9
12
15
Day of Treatment

Figure 3-8: MLN8237 with IUdR increases DNA damage in vitro and reduces tumor volume in vivo.

(A) Cells were treated as indicated for 48 hours, fixed, and stained with α-IdU antibody. (B) Cells were treated as indicated for 4 days. Doxorubicin (Dox) treatments were for 16 hours. All cells were collected, fixed with 4%PFA, methanol and stained with γH2AX antibody to determine the proportion of cells with DNA damage. n≥5. (C) Quantification of tumor volumes from MDA-MB-231 xenograft mice treated with indicated drugs. Three tumors for each treatment condition. Although a trend is observed, there was no statistical significance (I+M vs MLN8237 p = 0.2606 by t-test).

Supplemental Figure 3-1

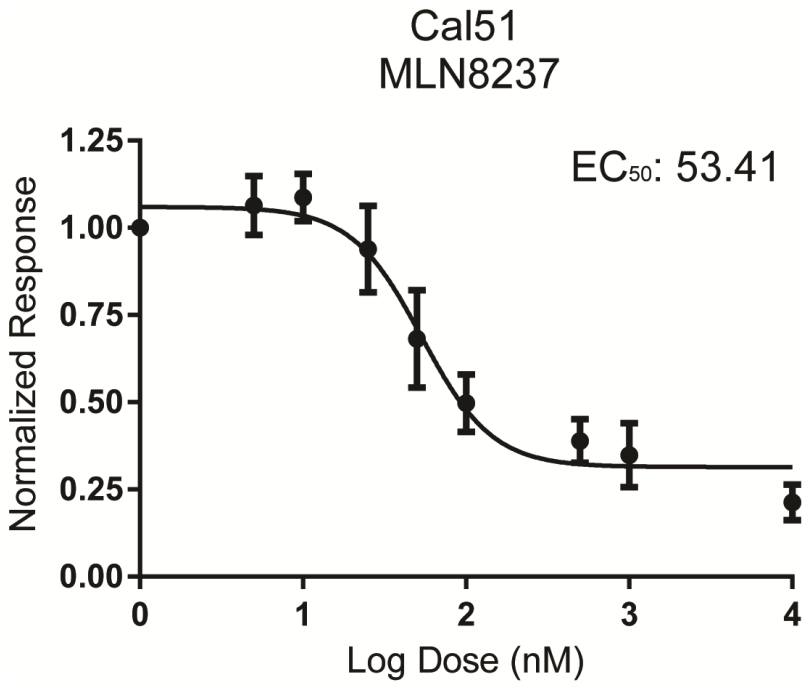

Supplemental Figure 3-1: Representative dose response curve used to determine EC_{50}.

Supplemental Figure 3-2

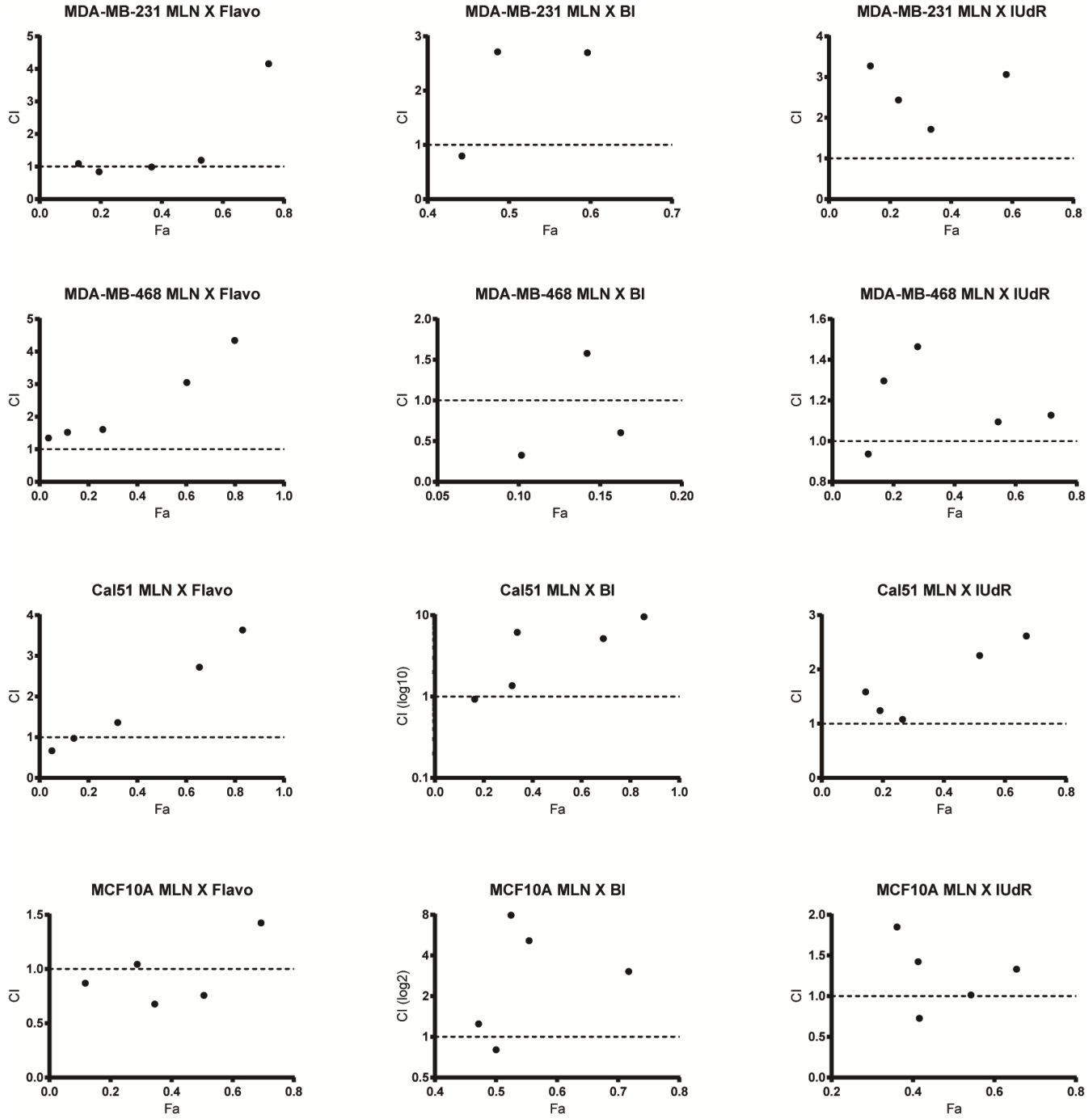

Supplemental Figure 3-2: CI-Fa plots for MLN8237 combinations in MDA-MB-231, MDA-MB-468, Cal51, and MFC10A cell lines.

Plots showing combination index (CI) versus effect (fa) for indicated cell lines and drug combinations. n=3.

Supplemental Figure 3-3

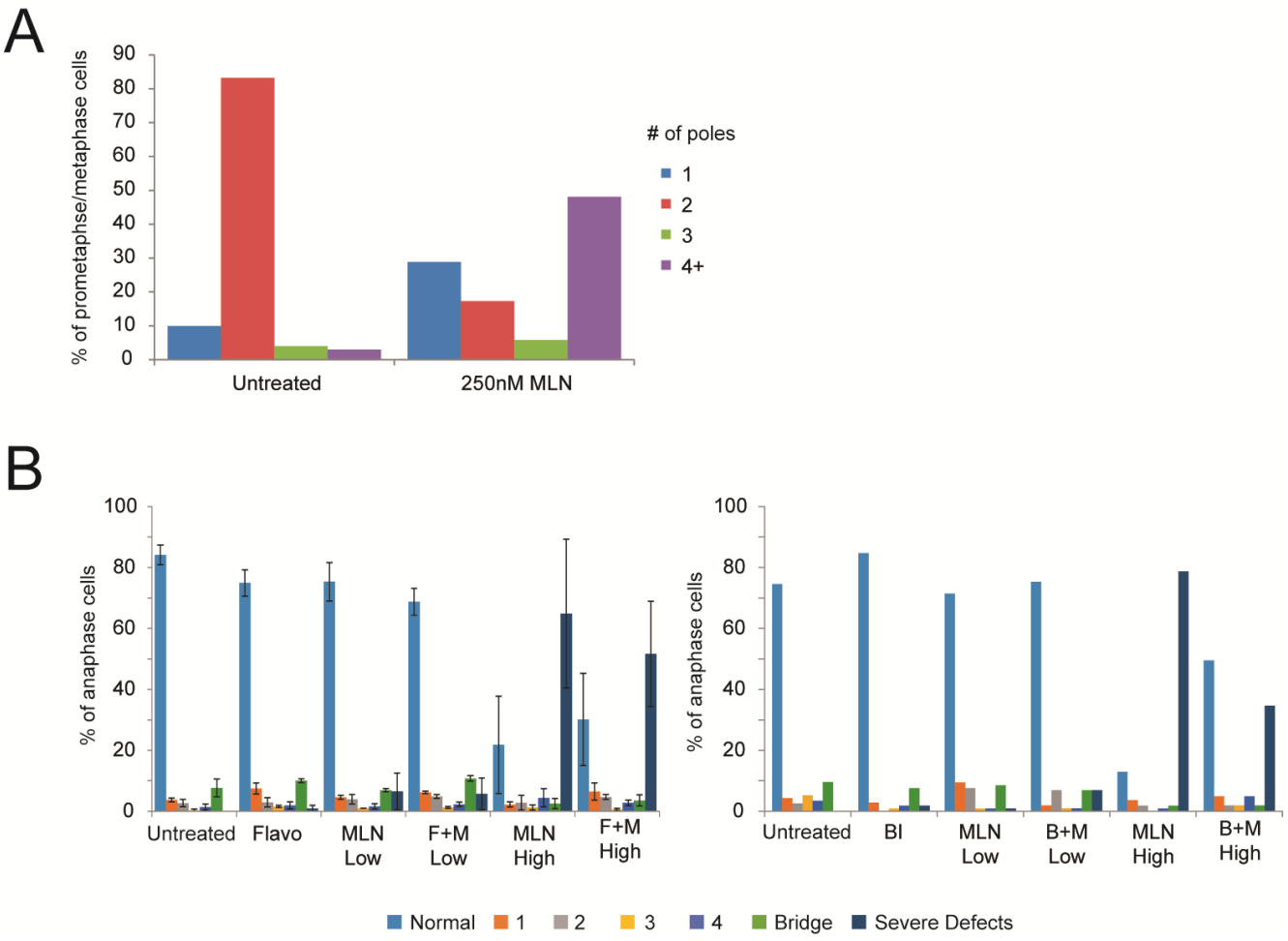

Supplemental Figure 3-3: BI2536 and flavopiridol do not alter the type of mitotic errors observed with MLN8237 treatment.

(A) Cells were treated as indicated for 16 hours. Spindle pole structure was determined as in Figure 3-2B. n=1. (B) Anaphase segregation errors from Figure 3-2D were qualified based on number of lagging chromosomes or type or error. n=1 for conditions in BI2536 graph, n=3 for conditions in flavopiridol graph. No statistical significance. Error bars indicate SEM.

Supplemental Figure 3-4

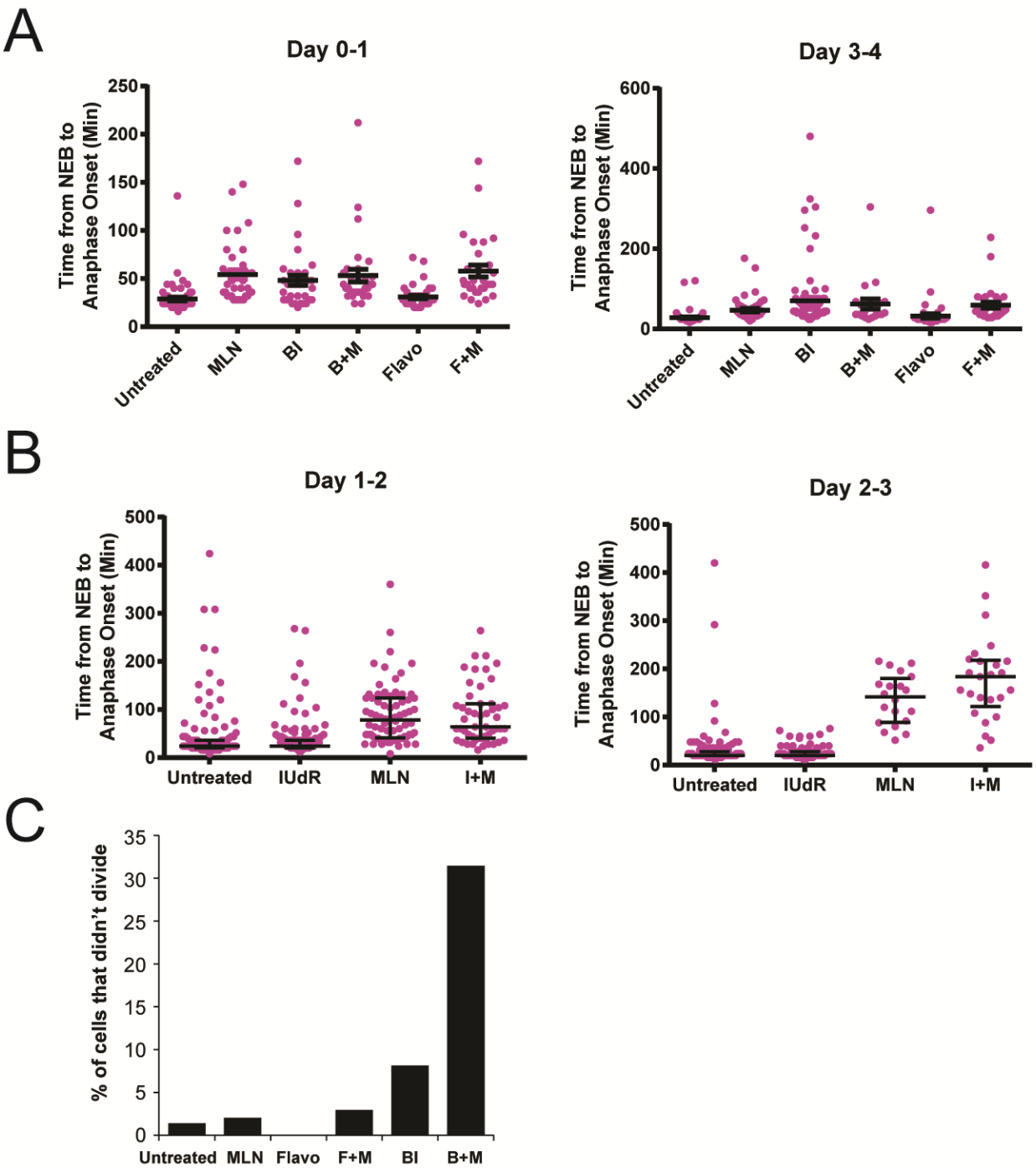

Supplemental Figure 3-4: BI2536, flavopiridol, and IUdR do not increase time in mitosis.

(A,B) Cells with mcherry labeled H2B were treated for indicated time (Day) and imaged every 4 minutes for 24 hours. Each point represents time from nuclear envelop breakdown (NEB) to anaphase onset for an individual cell. n=1. Time for at least 20 cells were counted and are displayed in the above charts. Error bars indicated SEM. (C) % of cells that entered mitosis but did not divide from Day 3-4 movie from (B). n=1.

Supplemental Figure 3-5

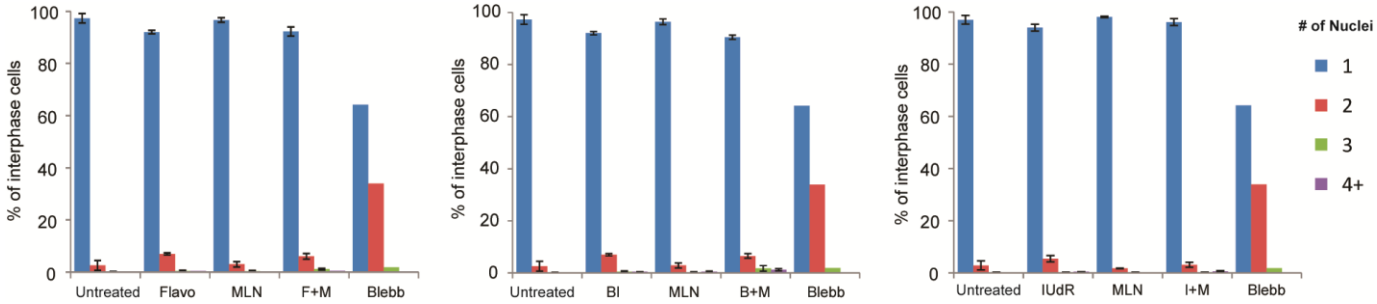

Supplemental Figure 3-5: BI2536, flavopiridol, and IUdR do not increase multinucleate cells with MLN8237 treatment.

Cells were treated for 4 days as indicated, fixed, and stained with DAPI and phalloidin. Number of nuclei was quantified for least 600 cells for each treatment condition. n=3. Error bars indicate SEM. No statistical significance.

Supplemental Figure 3-6

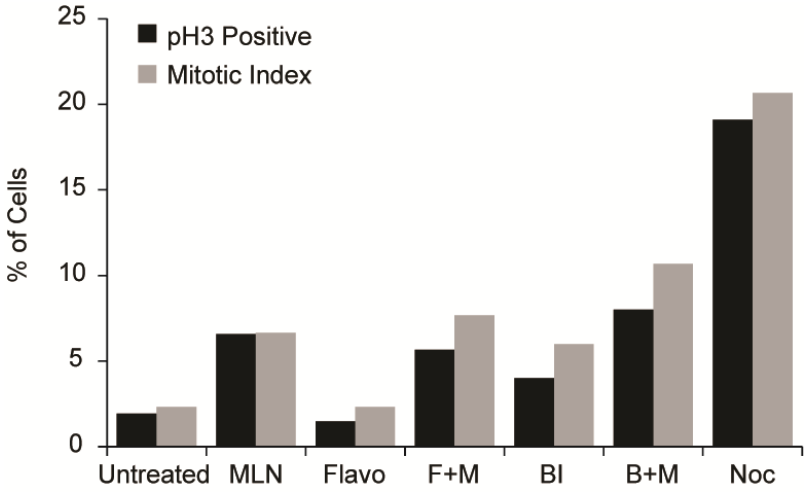

Supplemental Figure 3-6: Methods for quantifying % mitotic cells were equivalent.

Cells were treated as indicated for 4 days. pH3 positive cells were quantified as in Figure 3-3B. Mitotic Index cells were quantified as in Figure 3-2A. n=1.

Supplemental Figure 3-7

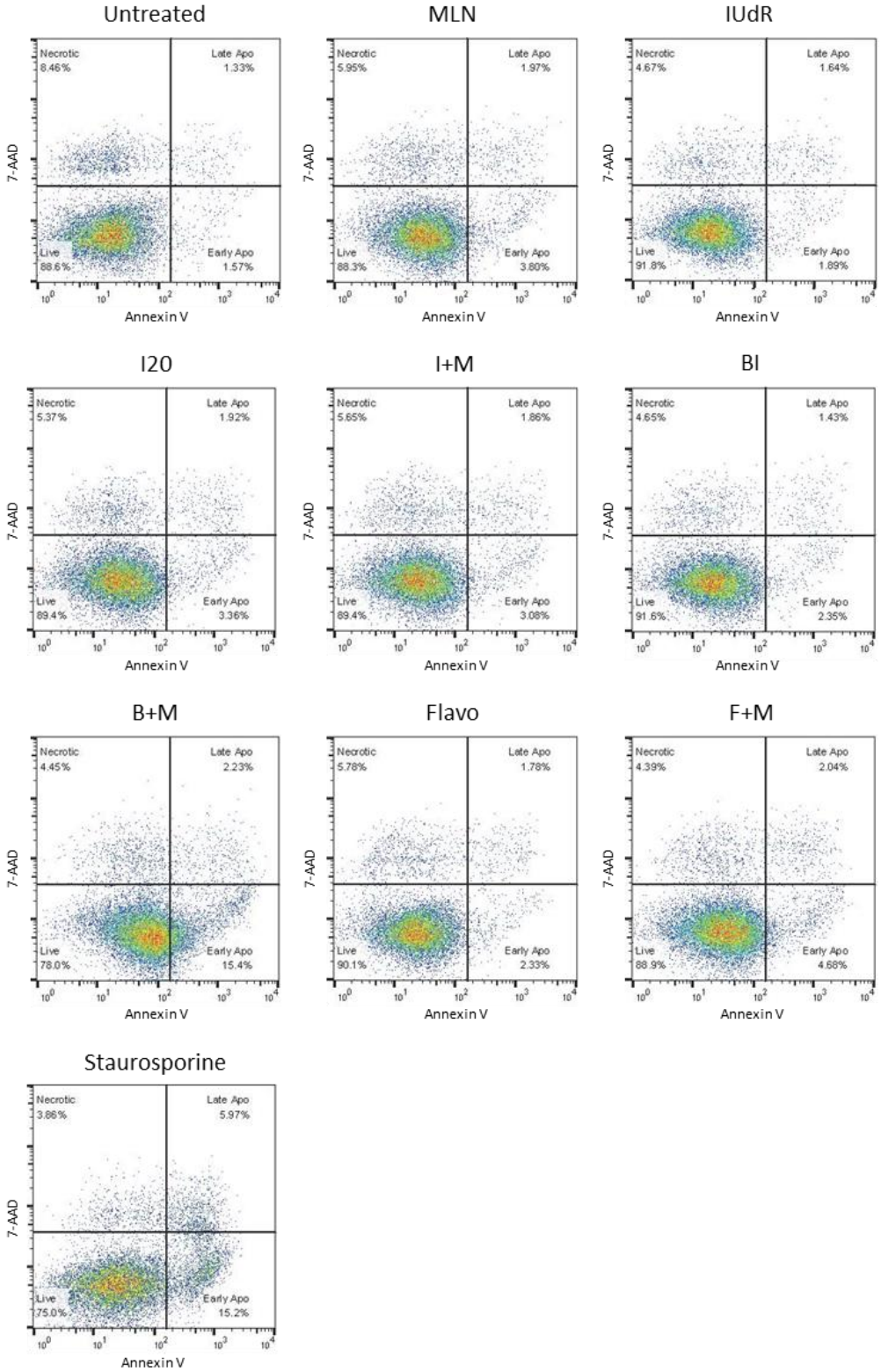

Supplemental Figure 3-7: BI2536 and MLN8237 combination increases the incidence of apoptotic cells.

Example of flow data showing incidence of apoptosis in varying treatment conditions. Cells were treated for 4 days and stained with Annexin V and 7-AAD.

Supplemental Figure 3-8

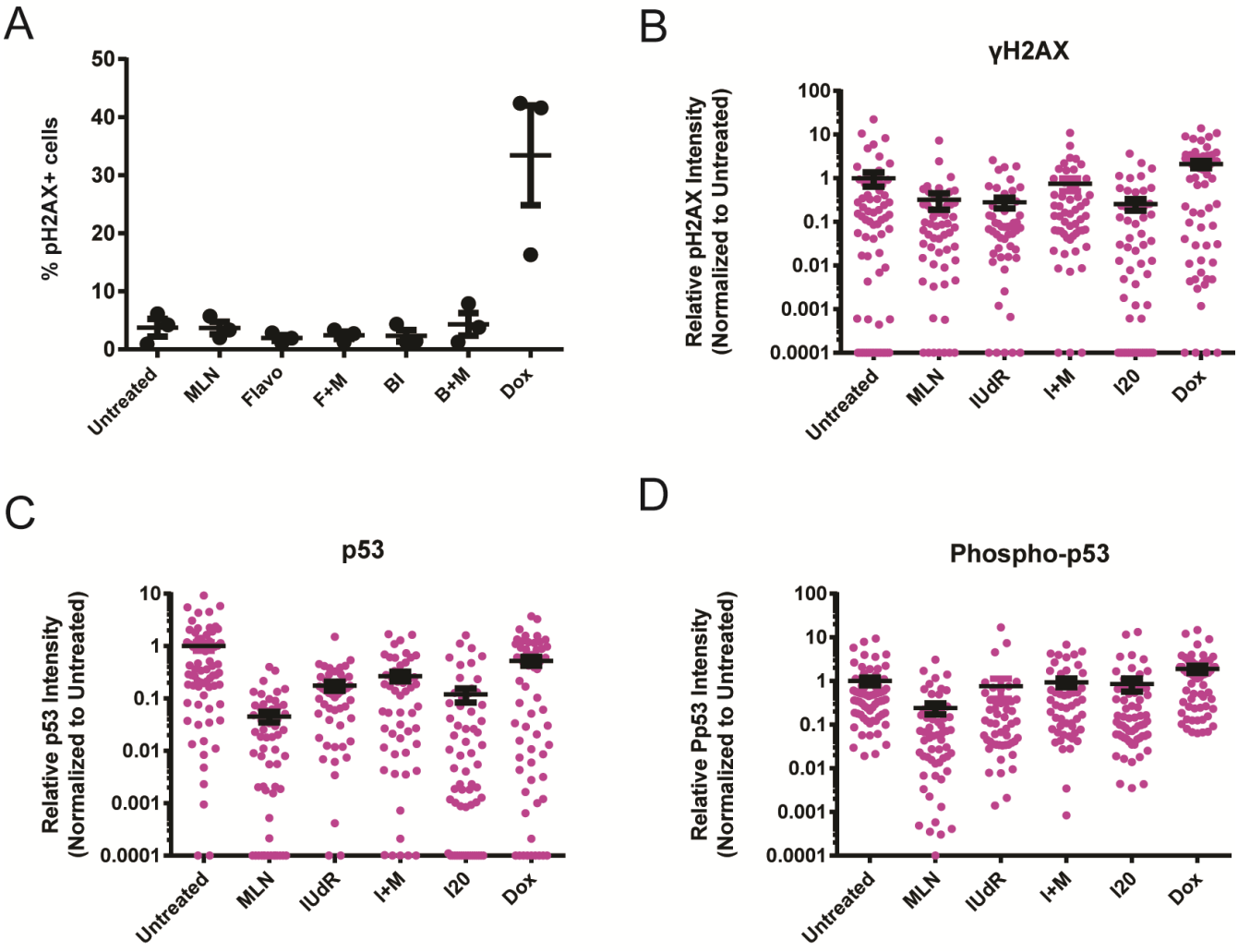

Supplemental Figure 3-8: MLN8237 does not increase DNA damage in combination with BI2536 or flavopiridol.

(A) Cells were treated, fixed, and stained as in Figure 3-6B. n=3. (B,C,D) Cells were treated as indicated for 4 days. Doxorubicin treatments were for 16 hours. Cells were fixed with 4% PFA, probed for indicated antibodies, and stained with DAPI. Cells in each graph were imaged on the same day. n=1. Error bars indicate SEM.

Chapter 4: Perspectives

Amber L. Lasek

Protein kinases provide efficient and controlled machinery for the propagation of signals. Through ATP catalysis and phosphate transfer, a kinase can quickly alter the activity and/or conformation of another protein or itself to influence a particular action in a cell. They can signal to progress the cell cycle or to halt it due to the presence of errors such as DNA damage. Together, this thesis has provided further insight into the complex nature of this signaling. It has further elucidated the nature of phosphoregulation of kinases and the interconnectedness of involved pathways.

Regulation of Plk1 by posttranslational modifications

Work in Chapter 2 revealed that regulation of the mitotic kinase Plk1 is not confined to a single modification within the kinase domain. Although it was previously known that phosphorylation of residue T210 was crucial, the significance of other residues, such as S137, is somewhat controversial (Jang *et al.*, 2002; van de Weerdt *et al.*, 2005). In my analysis, mutation of this residue to an alanine did not delay mitotic progression (Figure 2-2 and Supplemental Figure 2-1); however, my experiments would only expose essential residues. Further analysis needs to be done to determine whether these modifications are involved at more minor levels or for a particular condition in the cell, such as when subjected to a stressor (i.e. cold). These discrepancies are in part due to advancements in the tools used to study these modifications. As discussed in Chapter 2, the Plk1^{AS} system is superior to many of the methods used previously; looking forward, however, as advancements continue to be made, further analysis of the precise role that posttranslational modifications play in the cell will continue to evolve. For example, the advent of CRISPR technology has significantly improved methods to investigate protein function and regulation. In my AS system, both endogenous loci are deleted, and GFP-Plk1^{AS} and Flag-Plk1^{Mut} were inserted randomly into the genome under control of the CMV

promoter; in contrast, using CRISPR, the AS mutation can be made in one of the endogenous loci to better mimic innate conditions. The other locus should remain WT or have the posttranslational modification mutation created. This way, genes can be controlled by endogenous regulators such as promoters and transcription factors.

Major findings for Chapter 2 developed from elucidation of the role that phosphorylation and ubiquitination sites play for the activity and functionality of kinases; although my experiments focused on Plk1, this insight likely translates to other kinases and other proteins. To start, I identified the essential nature of the phosphorylation site, T214. Although T214 is proposed to be important for forming a hydrogen bond with the HRD motif's aspartic acid (discussed in Chapter 2) (Bayliss *et al.*, 2012), numerous studies have identified its phosphorylated state (Mortensen *et al.*, 2005; Daub *et al.*, 2008; Dephoure *et al.*, 2008; Oppermann *et al.*, 2012), including my own analysis (Figure 2-2). Further work is needed to distinguish whether the phosphorylation or the hydroxyl controls Plk1 function. Perhaps phosphorylated Plk1^{T214} is crucial for restraining Plk1 activity or it causes a minor change in conformation, increasing its activity above a required threshold (Liu *et al.*, 2006; Burkard *et al.*, 2007; Lera and Burkard, 2012). Current models show a hypothesized hydrogen bond between T214 and D176 (Elling *et al.*, 2008; Bayliss *et al.*, 2012) (Figure 4-1), however, one crucial piece of evidence to settle this matter would be resolution of Plk1's crystal structure with T214 in its phosphorylated state. A comparison of the phosphorylated and unphosphorylated structures would identify how Plk1 is able to accommodate a bulky phosphate group at T214 and how this would alter the positioning of other catalytic residues important for Plk1 activity and functions. This is likely to apply to other kinases as well; the T-loop of kinases is highly conserved and many contain a threonine at the site equivalent to T214 including the mitotic kinases Aurora A and Aurora B (Table 4-1).

In addition to exposing the functional role of individual phosphorylation sites, my work mutating phosphorylated residues grouped by domain, revealed that phosphorylations within the PBD are not required (Figure 2-5 and 2-6). Surprisingly, mutation of 16 sites concurrently within this region did not inhibit cell cycling or other investigated Plk1 functions. It would have been expected that mutation of this many residues simultaneously would severely disrupt the kinase through protein folding or protein-protein interactions. Others have shown that the PBD is essential for some functions of Plk1. The truncated form of Plk1 lacking the PBD, is able to perform various roles of Plk1, although Plk1 localization and anaphase are disrupted (Elia *et al.*, 2003b; Hanisch *et al.*, 2006; Lera and Burkard, 2012); however, this was not seen in my experiments with the mutated PBD (Figure 2-5 and 2-6 and Supplemental Figure 2-4). This discrepancy may be because, in my constructs, the PBD and the phospho-substrate binding pincer residues, His-538 and Lys-540, are still present. What remains of the PBD in the $Plk1^{PBD}$ cell lines is sufficient to perform the essential functions of Plk1. Further analysis should test whether $Plk1^{PBD}$ expressed at endogenous levels would similarly rescue assayed functions and whether the non-essential nature of posttranslational modifications in the C-terminus of Plk1 is conserved among other polo-boxes in the polo-like kinase family. It will also be interesting to investigate whether phosphorylation sites in the binding domains of other kinases, such as C1 domains, are similarly nonessential.

Mutation of the N-terminal kinase domain was also revealing. Although only 7 residues were mutated, the $Plk1^{Kin}$ cell lines were unable to rescue cell cycle progression, metaphase congression, and proper chromosome segregation in anaphase (Figure 2-5B,C). When compared to $Plk1^{WT}$, immunoprecipitated $Plk1^{Kin}$ has reduced kinase activity (Supplemental Figure 2-4D). Interestingly, this cell line did not have errors in centrosome separation, demonstrating that there is enough activity for less sensitive phenotypes

(Supplemental Figure 2-4C). This data supports redundancy of these phosphorylated residues at the N-terminus. Future work should analyze the effect of mutating these residues in differing combinations, differing by number of altered residues and the combinations. I hypothesize that these residues contribute to a titering of Plk1 activity, and combinations of fewer mutations will have a reduction of Plk1 activity that is between that of $Plk1^{WT}$ and $Plk1^{Kin}$. It will also be important to see if this redundancy is conserved in other kinase domains.

Targeting kinase-mediated networks to reduce cell proliferation

Following investigation on how individual protein kinases are regulated, work in Chapter 3 expanded upon our knowledge of the signaling networks facilitated by kinases. Kinase signaling cascades transmit information in the cell and form large networks; as a result, an alteration in one kinase pathway can influence signaling in others. Further, targeting two converging pathways simultaneously can expose functions at their juncture that may be otherwise obscured by dominant phenotypes. Utilizing this strategy, my work revealed that combining Aurora A inhibition with IUdR treatment and Cdk and Plk1 inhibition reduces proliferation over Aurora A inhibition alone. More specifically, the Aurora A inhibitor MLN8237 cooperated with the Cdk inhibitor flavopiridol to reduce mitotic entry, the Plk1 inhibitor BI2536 to induce apoptosis, and the radiosensitizer IUdR to increase DNA damage.

MLN8237 and flavopiridol reduced proliferation due to a mitotic entry delay during G2. It was previously known that both Aurora A and Cdk1 have roles in mitotic entry; however, it was somewhat surprising that the effect would be greater than either individual treatment since the kinases appear to function in the same pathway (Lindqvist *et al.*, 2009).

For example, Cdk1 phosphorylation of Bora, increases the activity of Plk1. Likewise, Aurora A also increases Plk1 activity through direct phosphorylation of Plk1's T-loop. It is possible that reduced active Aurora A and Cdk1 combine to reduce active Plk1 in an additive fashion. Even still, inhibition of these kinases in combination could also decrease mitotic entry through other pathways such as suppressing Aurora A-mediated Cdk1 activation. Aurora A phosphorylation of Cdc25B, stimulates the phosphatase to remove the inhibitory phosphorylation on Cdk1 (Dutertre *et al.*, 2004). In this way, reduced Aurora A could decrease Cdk1 activity. To resolve these questions, it will be necessary to monitor the extent of Plk1 activation, the phosphorylation status of Plk1 substrates, and the phosphorylation status of Cdc25 (S353).

Additionally, flavopridol is a pan-Cdk inhibitor so it's likely some of the effects seen could develop from inhibition of a kinase other than Cdk1 (Losiewicz *et al.*, 1994; Bible and Kaufmann, 1996; Carlson B.A. *et al.*, 1996; Filgueira de Azevedo *et al.*, 2002; Baumli *et al.*, 2008; Zeidner and Karp, 2015; Roskoski, 2016). To resolve this question, the phosphorylation status of substrate proteins could be monitored. Although this is not a particularly restrictive concern for clinical use, the phenotypes observed more closely match those associated with Cdk1 (granted, not all relevant phenotypes were probed). In any case, if effects were mediated through inhibition of Cdk9, phenotypes associated with transcription, such as delays in S phase, would have been expected (Chao and Price, 2001); instead, a G2 and mitotic entry delay was observed (Figure 3-5B and 3-6). Concurrently, I also did not detect an induction of apoptosis, as seen in various studies (Bible and Kaufmann, 1996; König *et al.*, 1997; Parker *et al.*, 1998). These findings exemplify the idea that using drugs in combination, can not only give old drugs new life in the clinic but also may reveal secondary pathways utilized by a particular drug.

In combination, MLN8237 and BI2536 caused an increased incidence of cells in early apoptosis. There is precedent for inhibition or reduction of these kinases to cause an increase in this mechanism for cell death. In cells with reduced Plk1 expression, there was an increase in the G2/M population with a significant fraction undergoing apoptosis (Lei and Erikson, 2008; Maire *et al.*, 2013; Matthess *et al.*, 2014). Aurora A inhibition also increased the incidence of apoptosis (Scharer *et al.*, 2008; Li *et al.*, 2010; Ding *et al.*, 2015; Niu *et al.*, 2015), although in some cases, this induction was hypothesized to be due to prolonged mitotic arrest (Zhou *et al.*, 2013). In my experiments, however, this does not appear to follow a prolonged or errored mitosis as there was no increase in the mitotic index, mitotic errors, or time in mitosis (Figure 3-2 and Figure 3-4 and Supplemental Figure 3-4A). Additionally, when the G2/M population identified by flow cytometry was separated out, the delay was identified to be in G2 and not mitosis (Figure 3-5B). It would be expected to see an increase in DNA damage in apoptosis, however, the events associated with early apoptosis, such as phosphatidylserine externalization, precede any nuclear changes (Wlodkowic *et al.*, 2011). This phospholipid exposure signals macrophages to initiate phagocytosis, however, these cells were not co-cultured *in vitro* with other cell types. To demonstrate translatability, it would be interesting to test whether co-culturing would lead to macrophage activation and increased cell death in the combination-treated epithelial cells. It is also important to further examine the induction of apoptosis as one experiment does not finalize this conclusion (Blagosklonny, 2000; Wlodkowic *et al.*, 2011). To help reconcile this and provide a mechanism, probing for players involved in apoptotic signaling or assessing mitochondrial membrane potential may further elucidate this phenotype. Additionally, cellular membranes in apoptotic cells become penetrable by cyanine dyes prior to larger cations such as PI or 7-AAD, and cellular incorporation of these dyes would lend credence to this line of reasoning (Idziorek *et al.*, 1995; Wlodkowic *et al.*, 2011).

Additionally, since the effects are subtle, it may be necessary to increase the dosage to heighten the response. This may also be sufficient to push the cells into later stages of apoptosis.

This analysis reveals that Plk1 and Aurora A co-inhibition potentiates the effect of either individual treatment. This could have important clinical applications; if the required dosages can be reduced there is the potential to also reduce off-target and side effects. BI2536, however, has the least promise clinically since low intratumoral levels are characteristic with treatment (Haupenthal *et al.*, 2012). Conversely, The Plk1 inhibitor BI6727 has been shown to have even greater pharmacokinetics and improved clinical activity (Rudolph *et al.*, 2009; Schöffski *et al.*, 2012; Yim, 2013); therefore, for clinical applications, combination studies with BI6727 and MLN8237 should be performed. Notwithstanding, additional *in vitro* combination studies may expose new signaling networks and identify novel drug collaborations.

MLN8237 and IUdR co-treatment increases the presence of DNA damage in cultured cells. IUdR is used clinically as a radiosensitizer and has been shown to induce damage on its own (Figure 3-8B) (Sedelnikova *et al.*, 2002); however usage in combination with Aurora inhibition is novel. Aurora A has been shown to be involved in the DNA repair machinery and its inhibition could impede this response (Wang *et al.*, 2014). Moreover, IUdR treatment has also been hypothesized to reduce DNA damage repair and could further potentiate the accumulation of damage. To this end, mismatch repair (MMR) deficient cells incorporate more IUdR than MMR proficient cells (Berry *et al.*, 1999, 2000; Yan *et al.*, 2006). Similar results were also seen in assessments of base-excision repair (BER) (Taverna *et al.*, 2003). To help resolve this, the recruitment and activity of these repair mechanisms should be analyzed. For example, quantification of Rad51 foci would gauge the recruitment of repair

machinery (Zhang *et al.*, 2005), while the phosphorylation status of ATM-Chk2/ATR-Chk1 would assess the activation of signaling pathways.

Alternatively, Aurora A inhibition may increase DNA damage through mitotic defects associated with erroneous spindle structure and lagging chromosomes. Errors in mitosis have been shown to cause DNA damage (Hoffelder *et al.*, 2004; Janssen *et al.*, 2011; Crasta *et al.*, 2012; Ganem and Pellman, 2012; Zhang *et al.*, 2015) and since MDA-MB-231s are cancer cells containing mutated p53 (Olivier *et al.*, 2002), it's possible that some of these errors would go uncorrected. The persistence of these errors in combination with those induced by IUdR could result in an overall increase that's larger than either individual insult. However, if this is the mechanism of action, IUdR treatment should further increase the presence of mitotic errors since DNA damage prior to mitosis has been shown to cause mitotic errors (Hayashi and Karlseder, 2013; Bakhoum *et al.*, 2014). In disagreement, IUdR did not potentiate mitotic errors, even following 4 days of treatment (Figure 3-4). Additionally, p53 mutant MDA-MB-231s and MDA-MB-468s did not show increased sensitivity over p53 WT lines Cal51s and MCF10As (Supplemental Figure 3-2).

MLN8237 and IUdR is an intriguing combination particularly because the IUdR prodrug IPdR is already approved for clinical use. Though IPdR is used as a radiosensitzer, I've shown that combining IUdR and MLN8237 can induce DNA damage, without the need for radiation. This could have important clinical implications because it could omit, or greatly reduce the need for patient radiation exposure. To further support its applicability for use in patients, it's necessary to confirm the presence of DNA damage in tissues. To this end, work is underway to test this in the mouse xenograft models treated with the varying drug conditions (Control, IPdR, MLN8237, or IPdR, MLN combination). The abundance of γH2AX in epithelial tumor cells (identified by pan-cytokeratin antibody) will be quantified

and compared across treatment groups; nevertheless, these xenograft tumors were only collected at one time point and the window for observable damage may be missed. If the damage occurs early and results in cell death, the tissues could be probed for markers for apoptosis, autophagocytosis, or necrosis (Krysko *et al.*, 2008; Christofferson and Yuan, 2010), however this would not confirm DNA damage as the mechanism for their demise. Even still, since it's believed that IUdR is incorporated during S-phase and incorporation is confined to proliferating tissues, it's conceivable that there would be selectivity for growing tumors over normal tissue (Fornace *et al.*, 1990; Kinsella *et al.*, 1994, 2000; Seo *et al.*, 2005). This may also provide an opportunity for personalized medicine as patients with proliferative disease may benefit more. The translatability of this combination makes it particularly exciting. IPdR has FDA approval and I've shown that this combination is effective in mouse models; to support this idea, more investigation *in vivo* needs to be performed to verify efficacy and confirm low toxicities.

Overall, I've shown that MLN8237 in combination with other drugs is able to reveal new insights into kinase signaling networks and may have identified new clinical targets. With a focus on cell cycling pathways, this has the potential to be especially true for those with proliferative disease. Although many of the effects are subtle, they have the potential to make big impacts in patients. Incidentally, these inhibitors likely target multiple kinases even at the low concentrations used for our experiments. This could have advantages and disadvantages. On one hand, it complicates analysis of signaling pathways of a particular kinase; however, in cells there is extensive overlap and compensation built into signaling pathways. It's plausible that these small-molecule/ATP-competitive inhibitors off-targetly affect similar kinases and may ultimately target the same pathway. Additionally, in clinical applications, it's unlikely that a tumor has evolved to take advantage of a single pro-growth pathway; therefore, targeting growth from multiple angles may prove more effective. Going

forward, additional investigation of *in vitro* and *in vivo* combinations of kinase altering drugs will further expand our understanding of the interconnectedness of these networks and may identify combinations with even larger responses.

Outlook

This thesis has uncovered the intricacies of kinase regulation and novel overlap in kinase mediated pathways. This analysis is valuable collectively because if we know how kinases are regulated, we can better anticipate the effects of targeting them therapeutically. Additionally, this may identify new means for perturbing these pathways. Rather than modifying whole kinase activity, we may be able to more specifically target a particular function of that kinase. If phosphorylation sites that control specific functions can be identified and targeted, we gain precise control over effects in cells. Then, when used in combination with other therapies, these subtle effects can potentiate clinical responses.

Figure 4-1

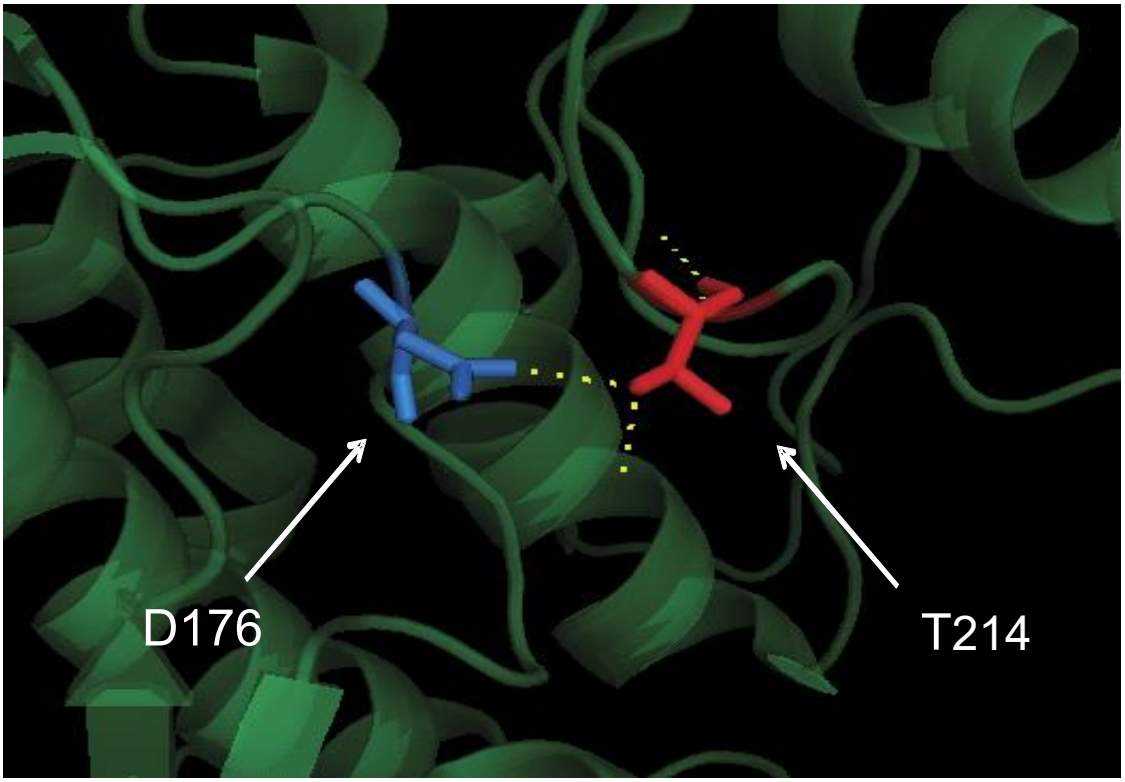

Figure 4-1: Resolved Plk1 crystal structure for Plk1 showing proposed hydrogen bond between threonine 214 and aspartic acid 176(Elling *et al.*, 2008)**.**

Table 4-1

Kinase	
Plk1	RKKTLCG**T**PNYIAPE
Aurora A	RRTTLCG**T**LDYLPPE
Aurora B	RRKTMCG**T**LDYLPPE
Nek1	LARTCIG**T**PYYLSPE
Nek2	FAKTFVG**T**PYYMSPE
Nek6	AAHSLVG**T**PYYMSPE
Nek9	MAETLVG**T**PYYMSPE
Nek11	LATTLTG**T**PHYMSPE
LATS 1/2	LAHSLVG**T**PNYIAPE
Greatwall	DDGRILG**T**PDYLAPE
Citron	NAKLPIG**T**PDYMAPE
ROCK 1/2	YEMLVGD**T**PFYADSL

Figure 4-1: T-loop conservation adjacent to Plk1 T214

Plk1 T214 or analogous threonine residues in other kinases are in bold.

References

Alvarado-Kristensson, M., Melander, F., Leandersson, K., Rönnstrand, L., Wernstedt, C., and Andersson, T. (2004). p38-MAPK signals survival by phosphorylation of caspase-8 and caspase-3 in human neutrophils. J. Exp. Med. *199*, 449–458.

American Type Culture Collection (2012). Thawing, Propagating, and Cryopreserving Protocol.

Aspinall, C. F., Zheleva, D., Tighe, A., and Taylor, S. S. (2015). Mitotic entry : Non-genetic requirement for Plk1 heterogeneity exposes the requirement for Plk1. Oncotarget *6*, 36472–36488.

Asteriti, I. A., Cesare, E. Di, Mattia, F. De, Hilsenstein, V., Neumann, B., Cundari, E., Lavia, P., and Guarguaglini, G. (2014). The Aurora-A inhibitor MLN8237 affects multiple mitotic processes and induces dose-dependent mitotic abnormalities and aneuploidy. Oncotarget *5*, 6229–6242.

Asteriti, I. A., De Mattia, F., and Guarguaglini, G. (2015). Cross-Talk between AURKA and Plk1 in Mitotic Entry and Spindle Assembly. Front. Oncol. *5*, 1–9.

Asteriti, I. a, Giubettini, M., Lavia, P., and Guarguaglini, G. (2011). Aurora-A inactivation causes mitotic spindle pole fragmentation by unbalancing microtubule-generated forces. Mol. Cancer *10*, 131.

Bakhoum, S. F., Kabeche, L., Murnane, J. P., Zaki, B. I., and Compton, D. a (2014). DNA damage response during mitosis induces whole chromosome mis-segregation. Cancer Discov. *4*, 1281–1289.

Bassermann, F., Frescas, D., Guardavaccaro, D., Busino, L., Peschiaroli, A., and Pagano, M. (2008). The Cdc14B-Cdh1-Plk1 axis controls the G2 DNA-damage-response checkpoint. Cell *134*, 256–267.

Baumli, S., Lolli, G., Lowe, E. D., Troiani, S., Rusconi, L., Bullock, A. N., Debreczeni, J. E. É. E., Knapp, S., and Johnson, L. N. (2008). The structure of P-TEFb (CDK9/cyclin T1), its complex with flavopiridol and regulation by phosphorylation. EMBO J. *27*, 1907–1918.

Bayliss, R., Fry, A., Haq, T., and Yeoh, S. (2012). On the molecular mechanisms of mitotic kinase activation. Open Biol. *2*.

Beck, J. *et al.* (2013). Ubiquitylation-dependent localization of PLK1 in mitosis. Nat. Cell Biol. *15*, 430–439.

Berdnik, D., and Knoblich, J. A. (2002). Drosophila Aurora-A is required for centrosome maturation and actin-dependent asymmetric protein localization during mitosis. Curr. Biol. *12*, 640–647.

Berry, S. E., Davis, T. W., Schupp, J. E., Hwang, H. S., De Wind, N., and Kinsella, T. J. (2000). Selective radiosensitization of drug-resistant MutS homologue-2 (MSH2) mismatch repair-deficient cells by halogenated thymidine (dThd) analogues: Msh2 mediates dThd analogue DNA levels and the differential cytotoxicity and cell cycle effects of the dThd a. Cancer Res. *60*, 5773–5780.

Berry, S. E., Garces, C., Hwang, H. S., Kunugi, K., Meyers, M., Davis, T. W., Boothman, D. A., and Kinsella, T. J. (1999). The mismatch repair protein, hMLH1, mediates 5-substituted halogenated thymidine analogue cytotoxicity, DNA incorporation, and radiosensitization in human colon cancer cells. Cancer Res. *59*, 1840–1845.

Bible, K. C., and Kaufmann, S. H. (1996). Flavopiridol: A cytotoxic flavone that induces cell death in noncycling A549 human lung carcinoma cells. Cancer Res. *56*, 4856–4861.

Bischoff, J. R., and Plowman, G. D. (1999). The Aurora/Ipl1p kinase family: Regulators of chromosome segregation and cytokinesis. Trends Cell Biol. *9*, 454–459.

Bishop, A. C. *et al.* (2000). A chemical switch for inhibitor-sensitive alleles of any protein kinase. Nature *407*, 395–401.

Blachly, J. S., and Byrd, J. C. (2013). Emerging drug profile: cyclin-dependent kinase inhibitors. Leuk. Lymphoma *54*, 2133–2143.

Blagosklonny, M. (2000). Spotlight on apoptosis. Leukemia *14*, 1500–1501.

Blangy, A. *et al.* (1995). Phosphorylation by p34cdc2 regulates spindle association of human Eg5, a kinesin-related motor essential for bipolar spindle formation in vivo. Cell *83*, 1159–1169.

Borgne, A., and Meijer, L. (1996). Sequential Dephosphorylation of p34 cdc2 on Thr-14 and Tyr-15 at the Prophase / Metaphase Transition. *271*, 27847–27854.

Boyle, P. (2012). Triple-negative breast cancer: Epidemiological considerations and recommendations. Ann. Oncol. *23*, 8–13.

Bruinsma, W., Macůrek, L., Freire, R., Lindqvist, A., and Medema, R. H. (2014). Bora and Aurora-A continue to activate Plk1 in mitosis. J. Cell Sci. *127*, 801–811.

Burkard, M. E. *et al.* (2009). Plk1 self-organization and priming phosphorylation of HsCYK-4 at the spindle midzone regulate the onset of division in human cells. PLoS Biol. *7*, 1–16.

Burkard, M. E., Randall, C. L., Larochelle, S., Zhang, C., Shokat, K. M., Fisher, R. P., and Jallepalli, P. V (2007). Chemical genetics reveals the requirement for Polo-like kinase 1 activity in positioning RhoA and triggering cytokinesis in human cells. PNAS *104*, 4383–4388.

Burkard, M. E., Santamaria, A., and Jallepalli, P. V (2012). Enabling and disabling polo-like kinase 1 inhibition through chemical genetics. ACS Chem. Biol. *7*, 978–981.

Cahu, J., Olichon, A., Hentrich, C., Schek, H., Drinjakovic, J., Zhang, C., Doherty-Kirby, A., Lajoie, G., and Surrey, T. (2008). Phosphorylation by Cdk1 increases the binding of Eg5 to microtubules In Vitro and in Xenopus egg extract spindles. PLoS One *3*, 1–10.

Carlson B.A., Dubay, M. M., Sausville, E. a, Brizuela, L., and Worland, P. J. (1996). Flavopridfol induces G1 arrest with inhibition of cyclin-dependent kinase (CDK)2 and CDK4 in human breast carcinoma cells. Cancer Res. *56*, 2973–2978.

Carmena, M. *et al.* (2012). The Chromosomal Passenger Complex Activates Polo Kinase at Centromeres. PLoS Biol. *10*, 1–15.

Casenghi M, Meraldi P, Weinhart U, Duncan PI, Körner R, Nigg, E. (2003). Polo-like kinase 1 regulates Nlp, a centrosome protein involved in microtubule nucleation. Dev Cell *5*, 113–125.

Castro, A., Arlot-Bonnemains, Y., Vigneron, S., Labbé, J. C., Prigent, C., and Lorca, T. (2002a). APC/Fizzy-Related targets Aurora-A kinase for proteolysis. EMBO Rep. *3*, 457–462.

Castro, A., Vigneron, S., Bernis, C., Labbé, J. C., Prigent, C., and Lorca, T. (2002b). The D-Box-activating domain (DAD) is a new proteolysis signal that stimulates the silent D-Box sequence of Aurora-A. EMBO Rep. *3*, 1209–1214.

Cervigni, R. I., Barretta, M. L., Persico, A., Corda, D., and Colanzi, A. (2011). The role of Aurora-A kinase in the Golgi-dependent control of mitotic entry. *1*, 61–65.

Chang, D. C., Xu, N., and Luo, K. Q. (2003). Degradation of cyclin B is required for the onset of anaphase in mammalian cells. J. Biol. Chem. *278*, 37865–37873.

Chang, L., and Karin, M. (2001). Mammalian MAP kinase signalling cascades. Nature *410*, 37–40.

Chao, S. H., and Price, D. H. (2001). Flavopiridol Inactivates P-TEFb and Blocks Most RNA Polymerase II Transcription in Vivo. J. Biol. Chem. *276*, 31793–31799.

Chou, T. *et al.* (2010). Flavonoid–flavonoid interaction and its effect on their antioxidant activity. J. Food Compos. Anal. *67*, 621–681.

Chou, T. C. (2010). Drug combination studies and their synergy quantification using the chou-talalay method. Cancer Res. *70*, 440–446.

Chou, T. C., and Talalay, P. (1984). Quantitative analysis of dose-effect relationships: the combined effects of multiple drugs or enzyme inhibitors. Adv. Enzyme Regul. *22*, 27–55.

Chow, J. P. H., Poon, R. Y. C., and Ma, H. T. (2011). Inhibitory phosphorylation of cyclin-dependent kinase 1 as a compensatory mechanism for mitosis exit. Mol. Cell. Biol. Biol. *31*, 1478–1491.

Christofferson, D. E., and Yuan, J. (2010). Cyclophilin A release as a biomarker of necrotic cell death. Cell Death Differ. *17*, 1942–1943.

Clay, F. J., McEwen, S. J., Bertoncello, I., Wilks, A. F., and Dunn, A. R. (1993). Identification and cloning of a protein kinase-encoding mouse gene, Plk, related to the polo gene of

Drosophila. Proc. Natl. Acad. Sci. U. S. A. *90*, 4882–4886.

Colevas, A. D., Blaylock, B., and Gravell, A. E. (2002). Current Clinical Trials of Flavopiridol. Oncology, 1–9.

Crasta, K., Ganem, N. J., Dagher, R., Lantermann, A. B., Ivanova, E. V, Pan, Y., Nezi, L., Protopopov, A., Chowdhury, D., and Pellman, D. (2012). DNA breaks and chromosome pulverization from errors in mitosis. Nature *482*, 53–58.

Cursi, S. *et al.* (2006). Src kinase phosphorylates Caspase-8 on Tyr380: a novel mechanism of apoptosis suppression. EMBO J. *25*, 1895–1905.

D'Assoro, A. B., Haddad, T., and Galanis, E. (2016). Aurora-A Kinase as a Promising Therapeutic Target in Cancer. Front. Oncol. *5*, 1–8.

Daub, H., Olsen, J. V, Bairlein, M., Gnad, F., Oppermann, F. S., Körner, R., Greff, Z., Kéri, G., Stemmann, O., and Mann, M. (2008). Kinase-selective enrichment enables quantitative phosphoproteomics of the kinome across the cell cycle. Mol. Cell *31*, 438–448.

Dees, E. C. *et al.* (2011). Phase 1 study of MLN8054, a selective inhibitor of Aurora A kinase in patients with advanced solid tumors. Cancer Chemother. Pharmacol. *67*, 945–954.

Degenhardt, Y., and Lampkin, T. (2010). Targeting polo-like kinase in cancer therapy. Clin. Cancer Res. *16*, 384–389.

Deibler, R. W., and Kirschner, M. W. (2010). Quantitative Reconstitution of Mitotic CDK1 Activation in Somatic Cell Extracts. Mol. Cell *37*, 753–767.

Dephoure, N., Zhou, C., Villén, J., Beausoleil, S. a, Bakalarski, C. E., Elledge, S. J., and Gygi, S. P. (2008). A quantitative atlas of mitotic phosphorylation. Proc. Natl. Acad. Sci. U. S. A. *105*,

10762–10767.

Ding, Y.-H. *et al.* (2015). Alisertib, an Aurora kinase A inhibitor, induces apoptosis and autophagy but inhibits epithelial to mesenchymal transition in human epithelial ovarian cancer cells. Drug Des. Devel. Ther. *9*, 425–464.

Dodson, C. A., and Bayliss, R. (2012). Activation of Aurora-A kinase by protein partner binding and phosphorylation are independent and synergistic. J. Biol. Chem. *287*, 1150–1157.

DuBois, S. G. *et al.* (2016). Phase I study of the aurora A kinase inhibitor alisertib in combination with irinotecan and temozolomide for patients with relapsed or refractory neuroblastoma: A nant (new approaches to neuroblastoma therapy) trial. J. Clin. Oncol. *34*, 1368–1375.

Dutertre, S. *et al.* (2004). Phosphorylation of CDC25B by Aurora-A at the centrosome contributes to the G2-M transition. J. Cell Sci. *117*, 2523–2531.

Elia, A. E. H., Cantley, L. C., and Yaffe, M. B. (2003a). Proteomic screen finds pSer/pThr-binding domain localizing Plk1 to mitotic substrates. Science (80-.). *299*, 1228–1231.

Elia, A. E. H. H., Rellos, P., Haire, L. F., Chao, J. W., Ivins, F. J., Hoepker, K., Mohammad, D., Cantley, L. C., Smerdon, S. J., and Yaffe, M. B. (2003b). The molecular basis for phosphodependent substrate targeting and regulation of Plks by the Polo-box domain. Cell *115*, 83–95.

Elling, R. A., Fucini, R. V., and Romanowski, M. J. (2008). Structures of the wild-type and activated catalytic domains of Brachydanio rerio Polo-like kinase 1 (Plk1): Changes in the active-site conformation and interactions with ligands. Acta Crystallogr. Sect. D Biol.

Crystallogr. *64*, 909–918.

Ellis, P. M., Chu, Q. S., Leighl, N., Laurie, S. A., Fritsch, H., Gaschler-Markefski, B., Gyorffy, S., and Munzert, G. (2013). A phase i open-label dose-escalation study of intravenous BI 2536 together with pemetrexed in previously treated patients with non-small-cell lung cancer. Clin. Lung Cancer *14*, 19–27.

Elowe, S., Hümmer, S., Uldschmid, A., Li, X., and Nigg, E. a (2007). on BubR1 regulates the stability of kinetochore – microtubule interactions. Genes Dev. *21*, 2205–2219.

Filgueira de Azevedo, W., Canduri, F., and Freitas da Silveira, N. J. (2002). Structural basis for inhibition of cyclin-dependent kinase 9 by flavopiridol. Biochem. Biophys. Res. Commun. *293*, 566–571.

Floyd, S., Pines, J., and Lindon, C. (2008). APC/CCdh1 Targets Aurora Kinase to Control Reorganization of the Mitotic Spindle at Anaphase. Curr. Biol. *18*, 1649–1658.

Fode, C., Motro, B., Yousefi, S., Heffernan, M., and Dennis, J. W. (1994). Sak, a murine protein-serine/threonine kinase that is related to the Drosophila polo kinase and involved in cell proliferation. Proc. Natl. Acad. Sci. U. S. A. *91*, 6388–6392.

Fornace, A. J., Dobson, P. P., and Kinsella, T. J. (1990). Enhancement of radiation damage in cellular dna following unifilar substitution with iododeoxyuridine. Int. J. Radiat. Oncol. Biol. Phys. *18*, 873–878.

Frost, A., Mross, K., Steinbild, S., Hedbom, S., Unger, C., Kaiser, R., Trommeshauser, D., and Munzert, G. (2012). Phase I study of the Plk1 inhibitor BI 2536 administered intravenously on three consecutive days in advanced solid tumours. Curr. Oncol. *19*, 28–35.

Fu, J., Bian, M., Jiang, Q., and Zhang, C. (2007). Roles of Aurora kinases in mitosis and tumorigenesis. Mol. Cancer Res. *5*, 1–10.

Ganem, N. J., and Pellman, D. (2012). Linking abnormal mitosis to the acquisition of DNA damage. J. Cell Biol. *199*, 871–881.

Gavet, O., and Pines, J. (2010). Progressive activation of CyclinB1-Cdk1 coordinates entry to mitosis. Dev. Cell *18*, 533–543.

Gelmon, K., Dent, R., Mackey, J. R., Laing, K., Mcleod, D., and Verma, S. (2012). Targeting triple-negative breast cancer: Optimising therapeutic outcomes. Ann. Oncol. *23*, 2223–2234.

Glotzer, M., Murray, A. W., and Kirschner, M. W. (1991). Cyclin is degraded by the ubiquitin pathway. Nature *349*, 132–138.

Glover, D. M., Hagan, I. M., and Tavares, Á. A. M. (1998). Polo-like kinases: A team that plays throughout mitosis. Genes Dev. *12*, 3777–3787.

Glover, D. M., Leibowitz, M. H., McLean, D. A., and Parry, H. (1995). Mutations in aurora prevent centrosome separation leading to the formation of monopolar spindles. Cell *81*, 95–105.

Gnad, F., Gunawardena, J., and Mann, M. (2011). PHOSIDA 2011: the posttranslational modification database. Nucleic Acids Res. *39*, D253–D260.

Goepfert, T. M., and Brinkley, B. R. (2000). The centrosome-associated Aurora/Ipl-like kinase family. Curr Top Dev Biol *49*, 331–342.

Golsteyn, R. M., Lane, H. A., Mundt, K. E., Arnaud, L., and Nigg, E. A. (1996). The family of polo-like kinases. Progress. Cell Cycle Res. *2*, 107–114.

Golsteyn, R. M., Schultz, S. J., Bartek, J., Ziemiecki, A., Ried, T., and Nigg, E. A. (1994). Cell cycle analysis and chromosomal localization of human Plk1, a putative homologue of the mitotic kinases Drosophila polo and Saccharomyces cerevisiae Cdc5. J Cell Sci *107 (Pt 6*, 1509–1517.

Gopalan, G., Chan, C. S. M., and Donovan, P. J. (1997). A novel mammalian, mitotic spindle-associated kinase is related to yeast and fly chromosome segregation regulators. J. Cell Biol. *138*, 643–656.

Graff, J. N., Higano, C. S., Hahn, N. M., Taylor, M. H., Zhang, B., Zhou, X., Venkatakrishnan, K., Leonard, E. J., and Sarantopoulos, J. (2016). Open-label, multicenter, phase 1 study of alisertib (MLN8237), an aurora A kinase inhibitor, with docetaxel in patients with solid tumors. Cancer *122*, 2524–2533.

Gregan, J., Polakova, S., Zhang, L., Tolić-Nørrelykke, I. M., and Cimini, D. (2011). Merotelic kinetochore attachment: Causes and effects. Trends Cell Biol. *21*, 374–381.

Gurkan, E., Schupp, J. E., Aziz, M. a., Kinsella, T. J., and Loparo, K. a. (2007). Probabilistic modeling of DNA mismatch repair effects on cell cycle dynamics and iododeoxyuridine-DNA incorporation. Cancer Res. *67*, 10993–11000.

Hamanaka, R., Maloid, S., Smith, M. R., O'Connell, C. D., Longo, D. L., and Ferris, D. K. (1994). Cloning and characterization of human and murine homologues of the Drosophila polo serine-threonine kinase. Cell Growth Differ *5*, 249–257.

Hanisch, A., Wehner, A., Nigg, E. A., Sillje, H. H. W., and Silljé, H. H. W. (2006). Different Plk1 functions show distinct dependencies on Polo-Box domain-mediated targeting. Mol. Biol. Cell *17*, 448–459.

Hannak, E., Kirkham, M., Hyman, A. A., and Oegema, K. (2001). Aurora-A kinase is required for centrosome maturation in Caenorhabditis elegans. J. Cell Biol. *155*, 1109–1115.

Haren, L., Stearns, T., and Lüders, J. (2009). Plk1-dependent recruitment of γ-tubulin complexes to mitotic centrosomes involves multiple PCM components. PLoS One *4*.

Haroon, A. (1998). PubMed (http://www.ncbi.nlm.nih.gov/PubMed). Lancet, SI16.

Harris, L. N. *et al.* (2006). Molecular subtypes of breast cancer in relation to paclitaxel response and outcomes in women with metastatic disease: results from CALGB 9342. Breast Cancer Res. *8*, R66.

Haupenthal, J. *et al.* (2012). Reduced efficacy of the Plk1 inhibitor BI 2536 on the progression of hepatocellular carcinoma due to low intratumoral drug levels. Neoplasia *14*, 410–419.

Hayashi, M. T., and Karlseder, J. (2013). DNA damage associated with mitosis and cytokinesis failure. Oncogene *32*, 4593–4601.

Heald, R., McLoughlin, M., and McKeon, F. (1993). Human wee1 maintains mitotic timing by protecting the nucleus from cytoplasmically activated cdc2 kinase. Cell *74*, 463–474.

Hershko, A. (1999). Mechanisms and regulation of the degradation of cyclin B. Philos. Trans. R. Soc. Lond. B. Biol. Sci. *354*, 1571-5-6.

Hoar, K., Chakravarty, A., Rabino, C., Wysong, D., Bowman, D., Roy, N., and Ecsedy, J. a (2007). MLN8054, a small-molecule inhibitor of Aurora A, causes spindle pole and chromosome congression defects leading to aneuploidy. Mol. Cell. Biol. *27*, 4513–4525.

Hoffelder, D. R., Luo, L., Burke, N. a, Watkins, S. C., Gollin, S. M., and Saunders, W. S. (2004).

Resolution of anaphase bridges in cancer cells. Chromosoma *112*, 389–397.

Hofheinz, R. D., Al-Batran, S. E., Hochhaus, A., Jäger, E., Reichardt, V. L., Fritsch, H., Trommeshauser, D., and Munzert, G. (2010). An open-label, phase I study of the polo-like kinase-1 inhibitor, BI 2536, in patients with advanced solid tumors. Clin. Cancer Res. *16*, 4666–4674.

Holtrich, U. W. E., Wolf, G., Brauninger, A., Karnq, T., Bohme, B., Rjbsamen-waigmann, H., and Strebhardt, K. (1994). Induction and down-regulation of PLK, a human serine/threonine kinase expressed in proliferating cells and tumors. Biochemistry *91*, 1736–1740.

Honda, K., Mihara, H., Kato, Y., Yamaguchi, a, Tanaka, H., Yasuda, H., Furukawa, K., and Urano, T. (2000). Degradation of human Aurora2 protein kinase by the anaphase-promoting complex-ubiquitin-proteasome pathway. Oncogene *19*, 2812–2819.

Van Horn, R. D. *et al.* (2010). Cdk1 activity is required for mitotic activation of aurora A during G2/M transition of human cells. J. Biol. Chem. *285*, 21849–21857.

Hornbeck, P. V, Kornhauser, J. M., Tkachev, S., Zhang, B., Skrzypek, E., Murray, B., Latham, V., and Sullivan, M. (2012). PhosphoSitePlus: a comprehensive resource for investigating the structure and function of experimentally determined post-translational modifications in man and mouse. Nucleic Acids Res. *40*, D261–D270.

Huang, T. T., Nijman, S. M. B., Mirchandani, K. D., Galardy, P. J., Cohn, M. a, Haas, W., Gygi, S. P., Ploegh, H. L., Bernards, R., and D'Andrea, A. D. (2006). Regulation of monoubiquitinated PCNA by DUB autocleavage. Nat. Cell Biol. *8*, 339–347.

Hudis, C. A., and Gianni, L. (2011). Triple-Negative Breast Cancer: An Unmet Medical Need. Oncologist *16*, 1–11.

Huse, M., and Kuriyan, J. (2002). The conformational plasticity of protein kinases. Cell *109*, 275–282.

Hyun, S.-Y. Y., Hwan, H.-I. I., and Jang, Y.-J. J. (2014). Polo-like kinase-1 in DNA damage response. BMB Rep. *47*, 249–255.

Idziorek, T., Estaquier, J., De Bels, F., and Ameisen, J. C. (1995). YOPRO-1 permits cytofluorometric analysis of programmed cell death (apoptosis) without interfering with cell viability. J. Immunol. Methods *185*, 249–258.

Jackman, M., Lindon, C., Nigg, E. a, and Pines, J. (2003). Active cyclin B1-Cdk1 first appears on centrosomes in prophase. Nat. Cell Biol. *5*, 143–148.

Jang, Y.-J., Ma, S., Terada, Y., and Erikson, R. L. (2002). Phosphorylation of threonine 210 and the role of serine 137 in the regulation of mammalian polo-like kinase. J. Biol. Chem. *277*, 44115–44120.

Janssen, A., van der Burg, M., Szuhai, K., Kops, G. J. P. L., and Medema, R. H. (2011). Chromosome Segregation Errors as a Cause of DNA Damage and Structural Chromosome Aberrations. Science (80-.). *333*, 1895–1898.

Johmura, Y., Soung, N., Park, J., Yu, L., Zhou, M., Bang, J. K., and Kim, B. (2011). Regulation of microtubule-based microtubule nucleation by mammalian polo-like kinase 1. PNAS *108*, 11446–11451.

Johnson, L. N., Noble, M. E. M., and Owen, D. J. (1996). Active and inactive protein kinases: Structural basis for regulation. Cell *85*, 149–158.

Joukov, V., De Nicolo, A., Rodriguez, A., Walter, J. C., and Livingston, D. M. (2010).

Centrosomal protein of 192 kDa (Cep192) promotes centrosome-driven spindle assembly by engaging in organelle-specific Aurora A activation. Proc. Natl. Acad. Sci. U. S. A. *107*, 21022–21027.

Joukov, V., Walter, J. C., and De Nicolo, A. (2014). The Cep192-Organized Aurora A-Plk1 Cascade Is Essential for Centrosome Cycle and Bipolar Spindle Assembly. Mol. Cell *55*, 578–591.

Karp, J. E. *et al.* (2011). Phase 1 and pharmacokinetic study of bolus-infusion flavopiridol followed by cytosine arabinoside and mitoxantrone for acute leukemias. Blood *117*, 3302–3310.

Karsenti, E. (1991). Mitotic spindle morphogenesis in animal cells. Semin. Cell Biol. *2*, 251–260.

Karthigeyan, D., Prasad, S. B. B., Shandilya, J., Agrawal, S., and Kundu, T. K. (2011). Biology of Aurora A kinase: implications in cancer manifestation and therapy. Med. Res. Rev. *31*, 757–793.

Kasahara, K., Goto, H., Izawa, I., Kiyono, T., Watanabe, N., Elowe, S., Nigg, E. A., and Inagaki, M. (2013). PI 3-kinase-dependent phosphorylation of Plk1-Ser99 promotes association with 14-3-3γ and is required for metaphase-anaphase transition. Nat. Commun. *4*, 1–12.

Kassam, F., Enright, K., Dent, R., Dranitsaris, G., Myers, J., Flynn, C., Fralick, M., Kumar, R., and Clemons, M. (2009). Survival Outcomes for Patients with Metastatic Triple-Negative Breast Cancer: Implications for Clinical Practice and Trial Design. Clin. Breast Cancer *9*, 29–33.

Katayama, H. *et al.* (2013). Aurora Kinase-A Inactivates DNA Damage Induced Apoptosis and Spindle Assembly Checkpoint Response Functions of p73. *21*, 196–211.

Katayama, H., Brinkley, W. R., and Sen, S. (2003). The Aurora kinases: role in cell transformation and tumorigenesis. Cancer Met. Rev. *22*, 451–464.

Katayama, H., Zhou, H., Li, Q., Tatsuka, M., and Sen, S. (2001). Interaction and Feedback Regulation between STK15/BTAK/Aurora-A Kinase and Protein Phosphatase 1 through Mitotic Cell Division Cycle. J. Biol. Chem. *276*, 46219–46224.

Khoury, G. a, Baliban, R. C., and Floudas, C. a (2011). Proteome-wide post-translational modification statistics: frequency analysis and curation of the swiss-prot database. Sci. Rep. *1*, 1–5.

Kimura, M., Kotani, S., Hattori, T., Sumi, N., Yoshioka, T., Todokoro, K., and Okano, Y. (1997). Cell cycle-dependent expression and spindle pole localization of a novel human protein kinase, aik, related to aurora of Drosophila and yeast Ipl1. J. Biol. Chem. *272*, 13766–13771.

Kinsella, J., Vielhuber, A., and Fitzsimmons, E. (1998). Preclinical Prodrug Mouse for and Evaluation Human Radiosensitization as a in 5-Iodo-2 ' -deoxyuridine-mediated. *4*, 99–109.

Kinsella, T. J., Kinsella, M. T., Hong, S., Johnson, J. P., Burback, B., and Tosca, P. J. (2008). Toxicology and pharmacokinetic study of orally administered 5-iodo-2-pyrimidinone-2 ` deoxyribose (IPdR) x 28 days in Fischer-344 rats: impact on the initial clinical phase I trial design of IPdR-mediated radiosensitization. Cancer Chemother. Pharmacol. *61*, 323–334.

Kinsella, T. J., Kunugi, K. A., Vielhuber, K. A., McCulloch, W., Liu, S. H., and Cheng, Y. C. (1994). An in vivo comparison of oral 5-Iodo-2′-deoxyuridine and 5-iodo-2-pyrimidinone-2′-deoxyribose toxicity, pharmacokinetics, and DNA incorporation in athymic mouse tissues and the human colon cancer xenograft, HCT-116. Cancer Res. *54*, 2695–2700.

Kinsella, T. J., Vielhuber, K. A., Kunugi, K. A., Xenografts, G., Schupp, J., Davis, T. W., and Sands,

H. (2000). Preclinical Toxicity and Efficacy Study of a 14-day Schedule of Oral 5-Iodo-2-pyrimidinone-2′-deoxyribose as a Prodrug for 5-Iodo-2′-deoxyuridine Radiosensitization in U251 Human Glioblastoma Xenografts Preclinical Toxicity and Efficacy Study of a 14-. Clin. Cancer Res. *6*, 1468–1475.

Knighton, D., Zheng, J., Ten Eyck, L., Ashford, V., Xuong, N., Taylor, S., and Sowadski, J. (1991). Crystal structure of the catalytic subunit of cyclic adenosine monophosphate-dependent protein kinase. Science (80-.). *253*, 407–414.

Kollareddy, M., Zheleva, D., Dzubak, P., Brahmkshatriya, P. S., Lepsik, M., and Hajduch, M. (2012). Aurora kinase inhibitors: Progress towards the clinic. Invest. New Drugs *30*, 2411–2432.

Komlodi-Pasztor, E., Sackett, D. L., and Fojo, A. T. (2012). Inhibitors targeting mitosis: Tales of how great drugs against a promising target were brought down by a flawed rationale. Clin. Cancer Res. *18*, 51–63.

König, A., Schwartz, G. K., Mohammad, R. M., Al-Katib, A., and Gabrilove, J. L. (1997). The Novel Cyclin-Dependent Kinase Inhibitor Flavopiridol Downregulates Bcl-2 and Induces Growth Arrest and Apoptosis in Chronic B-Cell Leukemia Lines. Blood *90*, 4307–4312.

Krysko, D. V., Berghe, T. Vanden, Parthoens, E., D'Herde, K., and Vandenabeele, P. (2008). Chapter 16 Methods for Distinguishing Apoptotic from Necrotic Cells and Measuring Their Clearance. In: Methods in Enzymology, 307–341.

Kummar, S. *et al.* (2013). First-in-human phase 0 trial of oral 5-iodo-2-pyrimidinone-2'-deoxyribose in patients with advanced malignancies. Clin. Cancer Res. *19*, 1852–1857.

Lake, R. J., and Jelinek, W. R. (1993). Cell cycle- and terminal differentiation-associated

regulation of the mouse mRNA encoding a conserved mitotic protein kinase. Mol Cell Biol *13*, 7793–7801.

Lampson, M. A., and Cheeseman, I. M. (2011). Sensing centromere tension: Aurora B and the regulation of kinetochore function. *21*, 133–140.

Lampson, M. A., Renduchitala, K., Khodjakov, A., and Kapoor, T. M. (2004). Correcting improper chromosome-spindle attachments during cell division. Nat Cell Biol *6*, 232–237.

Lanasa, M. C. *et al.* (2015). Final results of EFC6663: A multicenter, international, phase 2 study of alvocidib for patients with fludarabine-refractory chronic lymphocytic leukemia. Leuk. Res. *39*, 495–500.

Lane, H. A., and Nigg, E. A. (1996). Antibody Microinjection Reveals an Essential Role for Human Polo-like Kinase 1 (Plkl) in the Functional Maturation of Mitotic Centrosomes. J. Cell Biol. *1*, 1701–1713.

Larochelle, S., Merrick, K. A., Terret, M.-E., Wohlbold, L., Barboza, N. M., Zhang, C., Shokat, K. M., Jallepalli, P. V., and Fisher, R. P. (2007). Requirements for Cdk7 in the assembly of Cdk1/cyclin B and activation of Cdk2 revealed by chemical genetics in human cells. *25*, 839–850.

Lasek, A. L., McPherson, B. M., Trueman, N. G., and Burkard, M. E. (2016). The functional significance of posttranslational modifications on polo-like kinase 1 revealed by chemical genetic complementation. PLoS One *11*, 1–17.

Lee, K.-J., Shang, Z.-F., Lin, Y.-F., Sun, J., Morotomi-Yano, K., Saha, D., and Chen, B. P. C. (2015). The Catalytic Subunit of DNA-Dependent Protein Kinase Coordinates with Polo-Like Kinase 1 to Facilitate Mitotic Entry. Neoplasia *17*, 329–338.

Lee, K., and Rhee, K. (2011). PLK1 phosphorylation of pericentrin initiates centrosome maturation at the onset of mitosis. J. Cell Biol. *195*, 1093–1101.

Lee, K. S., Grenfell, T. Z., Yarm, F. R., and Erikson, R. L. (1998). Mutation of the polo-box disrupts localization and mitotic functions of the mammalian polo kinase Plk. Proc. Natl. Acad. Sci. U. S. A. *95*, 9301–9306.

Lee, K. S., Park, J. E., Kang, Y. H., Zimmerman, W., Soung, N. K., Seong, Y. S., Kwak, S. J., and Erikson, R. L. (2008). Mechanisms of mammalian polo-like kinase 1 (Plk1) localization: Self- versus non-self-priming. Cell Cycle *7*, 141–145.

Lehmann, B. D. B., Bauer, J. a J., Chen, X., Sanders, M. E., Chakravarthy, a B., Shyr, Y., and Pietenpol, J. a (2011). Identification of human triple-negative breast cancer subtypes and preclinical models for selection of targeted therapies. J. Clin. Invest. *121*, 2750–2767.

Lei, M., and Erikson, R. L. (2008). Plk1 depletion in nontransformed diploid cells activates the DNA-damage checkpoint. Oncogene *27*, 3935–3943.

Lenart, P., Petronczki, M., Steegmaier, M., Di Fiore, B., Lipp, J. J., Hoffmann, M., Rettig, W. J., Kraut, N., and Peters, J. M. (2007). The Small-Molecule Inhibitor BI 2536 Reveals Novel Insights into Mitotic Roles of Polo-like Kinase 1. Curr. Biol. *17*, 304–315.

Lera, R. F., and Burkard, M. E. (2012). High mitotic activity of Polo-like kinase 1 is required for chromosome segregation and genomic integrity in human epithelial cells. J. Bol. Chem. *287*, 42812–42825.

Li, B., Ouyang, B., Pan, H., Peter, T., Slamon, D. J., Arceci, R., Lu, L., Dai, W., and Reissmann, P. T. (1996). prk , a Cytokine-inducible Human Protein Serine/Threonine Kinase Whose Expression Appears to be Down-regulated in Lung Carcinomas. *271*, 19402–19408.

Li, M., Jung, A., Ganswindt, U., Marini, P., Friedl, A., Daniel, P. T., Lauber, K., Jendrossek, V., and Belka, C. (2010). Aurora kinase inhibitor ZM447439 induces apoptosis via mitochondrial pathways. Biochem. Pharmacol. *79*, 122–129.

Lim, S., and Kaldis, P. (2013). Cdks, cyclins and CKIs: roles beyond cell cycle regulation. Development *140*, 3079–3093.

Lindon, C., and Pines, J. (2004). Ordered proteolysis in anaphase inactivates Plk1 to contribute to proper mitotic exit in human cells. J. Cell Bol. *164*, 233–241.

Lindqvist, A., Rodríguez-bravo, V., and Medema, R. H. (2009). The decision to enter mitosis : feedback and redundancy in the mitotic entry network. *185*, 193–202.

Lindqvist, A., Van Zon, W., Rosenthal, C. K., and Wolthuis, R. M. F. (2007). Cyclin B1-Cdk1 activation continues after centrosome separation to control mitotic progression. PLoS Biol. *5*, 1127–1137.

Littlepage, L. E., and Ruderman, J. V. (2002). Identification of a new APC/C recognition domain, the A box, which is required for the Cdh1-dependent destruction of the kinase Aurora-A during mitotic exit. Genes Dev. *16*, 2274–2285.

Liu, D., Davydenko, O., and Lampson, M. a. (2012). Polo-like kinase-1 regulates kinetochore-microtubule dynamics and spindle checkpoint silencing. J. Cell Biol. *198*, 491–499.

Liu, X., and Erikson, R. L. (2002). Activation of Cdc2/cyclin B and inhibition of centrosome amplification in cells depleted of Plk1 by siRNA. Proc Natl Acad Sci U S A *99*, 8672–8676.

Liu, X., Lei, M., and Erikson, R. L. (2006). Normal Cells , but Not Cancer Cells , Survive Severe Plk1 Depletion. Mol. Cell. Biol. *26*, 2093–2108.

Llamazares, S., Moreira, A., Tavares, A., Girdham, C., Spruce, B. A., Gonzalez, C., Karess, R. E., Glover, D. M., and Sunkel, C. E. (1991). polo encodes a protein kinase homolog required for mitosis in Drosophila. Genes Dev. *5*, 2153–2165.

Lobjois, V., Jullien, D., Bouché, J. P., and Ducommun, B. (2009). The polo-like kinase 1 regulates CDC25B-dependent mitosis entry. Biochim. Biophys. Acta - Mol. Cell Res. *1793*, 462–468.

Losiewicz, M. D., Carlson, B. A., Kaur, G., Sausville, E. A., and Worland, P. J. (1994). Potent inhibition of CDC2 kinase activity by the flavonoid L86-8275. Biochem. Biophys. Res. Commun. *201*, 589–595.

Lowe, E. D., Noble, M. E. M., Skamnaki, V. T., Oikonomakos, N. G., Owen, D. J., and Johnson, L. N. (1997). The crystal structure of a phosphorylase kinase peptide substrate complex: kinase substrate recognition. EMBO J. *16*, 6646–6658.

Lowery, D. M., Lim, D., and Yaffe, M. B. (2005). Structure and function of Polo-like kinases. Oncogene *24*, 248–259.

Lu, L.-Y., Wood, J. L., Minter-Dykhouse, K., Ye, L., Saunders, T. L., Yu, X., and Chen, J. (2008). Polo-like kinase 1 is essential for early embryonic development and tumor suppression. Mol. Cell. Biol. *28*, 6870–6876.

De Luca, M., Brunetto, L., Asteriti, I. a, Giubettini, M., Lavia, P., and Guarguaglini, G. (2008). Aurora-A and ch-TOG act in a common pathway in control of spindle pole integrity. Oncogene *27*, 6539–6549.

De Luca, M., Lavia, P., and Guarguaglini, G. (2006). A functional interplay between Aurora-A, Plk1 and TPX2 at spindle poles: Plk1 controls centrosomal localization of Aurora-A and

TPX2 spindle association. Cell Cycle *5*, 296–303.

MacCorkle, R. a, and Tan, T.-H. (2005). Mitogen-activated protein kinases in cell-cycle control. Cell Biochem. Biophys. *43*, 451–461.

Macůrek, L., Lindqvist, A., Lim, D., Lampson, M. A., Klompmaker, R., Freire, R., Clouin, C., Taylor, S. S., Yaffe, M. B., and Medema, R. H. (2008). Polo-like kinase-1 is activated by aurora A to promote checkpoint recovery. Nature *455*, 119–123.

Mahankali, M., Henkels, K. M., Speranza, F., and Gomez-Cambronero, J. (2014). A non-mitotic role for aurora kinase A as a direct activator of cell migration upon interaction with PLD, FAK and Src. J. Cell Sci. *128*, 516–526.

Maire, V. *et al.* (2013). Polo-like kinase 1: A potential therapeutic option in combination with conventional chemotherapy for the management of patients with triple-negative breast cancer. Cancer Res. *73*, 813–823.

Malumbres, M. (2014). Cyclin-dependent kinases. Genome Biol. *15*, 122.

Malumbres, M., and Pérez de Castro, I. (2014). Aurora kinase A inhibitors: promising agents in antitumoral therapy. Expert Opin. Ther. Targets *18*, 1377–1393.

Margadant, C., Cremers, L., Sonnenberg, A., and Boonstra, J. (2013). MAPK uncouples cell cycle progression from cell spreading and cytoskeletal organization in cycling cells. Cell. Mol. Life Sci. *70*, 293–307.

Martin, S. J., Reutelingsperger, C. P., McGahon, a J., Rader, J. a, van Schie, R. C., LaFace, D. M., and Green, D. R. (1995). Early redistribution of plasma membrane phosphatidylserine is a general feature of apoptosis regardless of the initiating stimulus: inhibition by

overexpression of Bcl-2 and Abl. J. Exp. Med. *182*, 1545–1556.

Marumoto, T., Honda, S., Hara, T., Nitta, M., Hirota, T., Kohmura, E., and Saya, H. (2003). Aurora-A Kinase Maintains the Fidelity of Early and Late Mitotic Events in HeLa Cells. J. Biol. Chem. *278*, 51786–51795.

Marumoto, T., Zhang, D., and Saya, H. (2005). Aurora-A - a guardian of poles. Nat. Rev. Cancer *5*, 42–50.

Marzo, I., and Naval, J. (2013). Antimitotic drugs in cancer chemotherapy: Promises and pitfalls. Biochem. Pharmacol. *86*, 703–710.

Matsumoto, T., Wang, P.-Y., Ma, W., Sung, H. J., Matoba, S., and Hwang, P. M. (2009). Polo-like kinases mediate cell survival in mitochondrial dysfunction. PNAS *106*, 14542–14546.

Matthess, Y., Raab, M., Knecht, R., Becker, S., and Strebhardt, K. (2014). Sequential Cdk1 and Plk1 phosphorylation of caspase-8 triggers apoptotic cell death during mitosis. Mol. Oncol. *8*, 596–608.

Matthess, Y., Raab, M., Sanhaji, M., Lavrik, I. N., and Strebhardt, K. (2010). Cdk1/cyclin B1 controls Fas-mediated apoptosis by regulating caspase-8 activity. Mol. Cell. Biol. *30*, 5726–5740.

Matulonis, U. A. *et al.* (2012). Phase II study of MLN8237 (alisertib), an investigational Aurora A kinase inhibitor, in patients with platinum-resistant or -refractory epithelial ovarian, fallopian tube, or primary peritoneal carcinoma. Gynecol. Oncol. *127*, 63–69.

Melichar, B. *et al.* (2015). Safety and activity of alisertib, an investigational aurora kinase A inhibitor, in patients with breast cancer, small-cell lung cancer, non-small-cell lung cancer,

head and neck squamous-cell carcinoma, and gastro-oesophageal adenocarcinoma: a five-arm ph. Lancet Oncol. *16*, 395–405.

Miyoshi, Y., Iwao, K., Egawa, C., and Noguchi, S. (2001). Association of Centrosomal Kinase STK15/BTAK mRNA Expression with Chromosomal Instability in Human Breast Cancers. Int. J. Cancer *92*, 370–373.

Morgan, D. O. (1995). Principles of CDK regulation. Nature *374*, 131–134.

Mortensen, E. M., Haas, W., Gygi, M., Gygi, S. P., and Kellogg, D. R. (2005). Cdc28-dependent regulation of the Cdc5/Polo kinase. Curr. Biol. *15*, 2033–2037.

Mross, K. *et al.* (2012). A randomised phase II trial of the Polo-like kinase inhibitor BI 2536 in chemo-naïve patients with unresectable exocrine adenocarcinoma of the pancreas - a study within the Central European Society Anticancer Drug Research (CESAR) collaborative network. Br. J. Cancer *107*, 280–286.

Mross, K., Frost, A., Steinbild, S., Hedbom, S., Rentschler, J., Kaiser, R., Rouyrre, N., Trommeshauser, D., Hoesl, C. E., and Munzert, G. (2008). Phase I dose escalation and pharmacokinetic study of BI 2536, a novel Polo-like kinase 1 inhibitor, in patients with advanced solid tumors. J. Clin. Oncol. *26*, 5511–5517.

Murphy, C. G., and Dickler, M. N. (2015). The Role of CDK4/6 Inhibition in Breast Cancer. Oncologist *20*, 483–490.

Murray, a W., Solomon, M. J., and Kirschner, M. W. (1989). The role of cyclin synthesis and degradation in the control of maturation promoting factor activity. Nature *339*, 280–286.

Nadler, Y., Camp, R. L., Schwartz, C., Rimm, D. L., Kluger, H. M., and Kluger, Y. (2008).

Expression of Aurora A (but not Aurora B) is predictive of survival in breast cancer. Clin. Cancer Res. *14*, 4455–4462.

National Cancer Institute (2009). Cancer Statistics Review 1975-2009 (Vintage 2009 Populations): Introduction. SEER Cancer Stat. Rev. *2009*.

National Cancer Institute (NCI) Ropidoxuridine in Treating Patients With Advanced Gastrointestinal Cancer Undergoing Radiation Therapy.

Naviglio, S., Matteucci, C., Matoskova, B., Nagase, T., Nomura, N., Di Fiore, P. P., and Draetta, G. F. (1998). UBPY: A growth-regulated human ubiquitin isopeptidase. EMBO J. *17*, 3241–3250.

Neef, R., Gruneberg, U., Kopajtich, R., Li, X., Nigg, E. A., Sillje, H., and Barr, F. A. (2007). Choice of Plk1 docking partners during mitosis and cytokinesis is controlled by the activation state of Cdk1. Nat. Cell Biol. *9*, 436–444.

Neef, R., Preisinger, C., Sutcliffe, J., Kopajtich, R., Nigg, E. A., Mayer, T. U., and Barr, F. A. (2003). Phosphorylation of mitotic kinesin-like protein 2 by polo-like kinase 1 is required for cytokinesis. J. Cell Biol. *162*, 863–875.

Nigg, E. a, Blangy, a, and Lane, H. a (1996). Dynamic changes in nuclear architecture during mitosis: on the role of protein phosphorylation in spindle assembly and chromosome segregation. Exp. Cell Res. *229*, 174–180.

Nikonova, A. S., Astsaturov, I., Serebriiskii, I. G., Jr., R. L. D., and Golemis, E. A. (2013). Aurora-A kinase (AURKA) in normal and pathological cell growth. Cell Mol Life Sci *70*, 661–687.

Nishida, E., and Gotoh, Y. (1993). The MAP kinase cascade is essential for diverse signal

transduction pathways. Trends Biochem. Sci. *18*, 128–131.

Nishimura, K., Fukagawa, T., Takisawa, H., Kakimoto, T., and Kanemaki, M. (2009). An auxin-based degron system for the rapid depletion of proteins in nonplant cells. Nat. Methods *6*, 917–922.

Niu, N. K. *et al.* (2015). Pro-apoptotic and pro-autophagic effects of the aurora kinase A inhibitor alisertib (MLN8237) on human osteosarcoma U-2 OS and MG-63 cells through the activation of mitochondria-mediated pathway and inhibition of p38 MAPK/PI3K/Akt/mTOR signaling pathway. Drug Des. Devel. Ther. *9*, 1555–1584.

Nolen, B., Taylor, S., and Ghosh, G. (2004). Regulation of protein kinases: Controlling activity through activation segment conformation. Mol. Cell *15*, 661–675.

Nurse, P. (1990). Universal control mechanism regulating onset of M-phase. Nature *344*, 503–508.

O'Connor, A., Maffini, S., Rainey, M. D., Kaczmarczyk, A., Gaboriau, D., Musacchio, A., and Santocanale, C. (2015). Requirement for PLK1 kinase activity in the maintenance of a robust spindle assembly checkpoint. Biol. Open *1*, 11–19.

Olivier, M., Eeles, R., Hollstein, M., Khan, M. A., Harris, C. C., and Hainaut, P. (2002). The IARC TP53 database: New online mutation analysis and recommendations to users. Hum. Mutat. *19*, 607–614.

Oppermann, F. S., Grundner-Culemann, K., Kumar, C., Gruss, O. J., Jallepalli, P. V, and Daub, H. (2012). Combination of chemical genetics and phosphoproteomics for kinase signaling analysis enables confident identification of cellular downstream targets. Mol. Cell. Proteomics *11*, 1–12.

Parker, B. W., Kaur, G., Nieves-Neira, W., Taimi, M., Kohlhagen, G., Shimizu, T., Losiewicz, M. D., Pommier, Y., Sausville, E. a, and Senderowicz, a M. (1998). Early induction of apoptosis in hematopoietic cell lines after exposure to flavopiridol. Blood *91*, 458–465.

Paschal, C. R., Maciejowski, J., and Jallepalli, P. V. (2012). A stringent requirement for Plk1 T210 phosphorylation during K-fiber assembly and chromosome congression. Chromosoma *121*, 565–572.

Patra, D., and Dunphy, W. G. (1998). Xe-p9, a Xenopus Suc1/Cks protein,is essential for the Cdc2-dependent phosphorylation of the anaphase- promoting complex at mitosis. *15*, 2549–2559.

Paull, T. T., Rogakou, E. P., Yamazaki, V., Kirchgessner, C. U., Gellert, M., and Bonner, W. M. (2000). A critical role for histone H2AX in recruitment of repair factors to nuclear foci after DNA damage. Curr. Biol. *10*, 886–895.

Peng, C., Cho, Y. Y., Zhu, F., Zhang, J., Wen, W., Xu, Y., Yao, K., Ma, W. Y., Bode, A. M., and Dong, Z. (2011). Phosphorylation of caspase-8 (Thr-263) by ribosomal S6 kinase 2 (RSK2) mediates caspase-8 ubiquitination and stability. J. Biol. Chem. *286*, 6946–6954.

Petronczki, M., Glotzer, M., Kraut, N., and Peters, J. M. (2007). Polo-like Kinase 1 Triggers the Initiation of Cytokinesis in Human Cells by Promoting Recruitment of the RhoGEF Ect2 to the Central Spindle. Dev. Cell *12*, 713–725.

Potapova, T. A., Daum, J. R., Byrd, K. S., and Gorbsky, G. J. (2009). Fine Tuning the Cell Cycle : Activation of the Cdk1 Inhibitory Phosphorylation Pathway during Mitotic Exit. Mol. Biol. Cell *20*, 1737–1748.

Potapova, T. a, Daum, J. R., Pittman, B. D., Hudson, J. R., Jones, T. N., Satinover, D. L.,

Stukenberg, P. T., and Gorbsky, G. J. (2006). The reversibility of mitotic exit in vertebrate cells. Nature *440*, 954–958.

Qi, W., Tang, Z., and Yu, H. (2006). Phosphorylation- and Polo-Box–dependent Binding of Plk1 to Bub1 Is Required for the Kinetochore Localization of Plk1. Mol. Biol. Cell *17*, 3705–3716.

Rape, M., Reddy, S. K., and Kirschner, M. W. (2006). The processivity of multiubiquitination by the APC determines the order of substrate degradation. Cell *124*, 89–103.

Reboutier, D., Benaud, C., and Prigent, C. (2015). Aurora A's Functions During Mitotic Exit: The Guess Who Game. Front. Oncol. *5*, 1–7.

Reboutier, D., Troadec, M. B., Cremet, J. Y., Chauvin, L., Guen, V., Salaun, P., and Prigent, C. (2013). Aurora a is involved in central spindle assembly through phosphorylation of ser 19 in P150Glued. J. Cell Biol. *201*, 65–79.

Robinson, M. J., and Cobb, M. H. (1997). Mitogen-activated protein kinase pathways. Curr. Opin. Cell Biol. *9*, 180–186.

Romé, P., Montembault, E., Franck, N., Pascal, A., Glover, D. M., and Giet, R. (2010). Aurora A contributes to p150glued phosphorylation and function during mitosis. J. Cell Biol. *189*, 651–659.

Roskoski, R. (2016). Cyclin-dependent protein kinase inhibitors including palbociclib as anticancer drugs. Pharmacol. Res. *107*, 249–275.

Rudner, A. D., Hardwick, K. G., and Murray, A. W. (2000). Cdc28 activates exit from mitosis in budding yeast. J. Cell Biol. *149*, 1361–1376.

Rudolph, D., Steegmaier, M., Hoffmann, M., Grauert, M., Baum, A., Quant, J., Haslinger, C., Garin-Chesa, P., and Adolf, G. R. (2009). BI 6727, a polo-like kinase inhibitor with improved pharmacokinetic profile and broad antitumor activity. Clin. Cancer Res. *15*, 3094–3102.

Russo, a a, Jeffrey, P. D., and Pavletich, N. P. (1996). Structural basis of cyclin-dependent kinase activation by phosphorylation. Nat. Struct. Biol. *3*, 696–700.

Saif, M. W., Berk, G., Cheng, Y.-C., and Kinsella, T. J. (2007). IPdR: a novel oral radiosensitizer. Expert Opin. Investig. Drugs *16*, 1415–1424.

Santamaria, A., Wang, B., Elowe, S., Malik, R., Zhang, F., Bauer, M., Schmidt, A., Silljé, H. H. W., Körner, R., and Nigg, E. a (2011). The Plk1-dependent phosphoproteome of the early mitotic spindle. Mol. Cell. Proteomics *10*, M110.004457.

Sawin, K. E., and Mitchison, T. J. (1995). Mutations in the kinesin-like protein Eg5 disrupting localization to the mitotic spindle. Proc. Natl. Acad. Sci. U. S. A. *92*, 4289–4293.

Scharer, C. D., Laycock, N., Osunkoya, A. O., Logani, S., McDonald, J. F., Benigno, B. B., and Moreno, C. S. (2008). Aurora kinase inhibitors synergize with paclitaxel to induce apoptosis in ovarian cancer cells. J. Transl. Med. *6*, 79.

Schöffski, P. (2009). Polo-like kinase (PLK) inhibitors in preclinical and early clinical development in oncology. Oncologist *14*, 559–570.

Schöffski, P. *et al.* (2010). Multicentric parallel phase II trial of the polo-like kinase 1 inhibitor BI 2536 in patients with advanced head and neck cancer, breast cancer, ovarian cancer, soft tissue sarcoma and melanoma. The first protocol of the European Organization for Research . Eur. J. Cancer *46*, 2206–2215.

Schöffski, P., Awada, A., Dumez, H., Gil, T., Bartholomeus, S., Wolter, P., Taton, M., Fritsch, H., Glomb, P., and Munzert, G. (2012). A phase I, dose-escalation study of the novel Polo-like kinase inhibitor volasertib (BI 6727) in patients with advanced solid tumours. Eur. J. Cancer *48*, 179–186.

von Schubert, C., Cubizolles, F., Bracher, J. M., Sliedrecht, T., Kops, G. J. P. L., and Nigg, E. A. (2015). Plk1 and Mps1 Cooperatively Regulate the Spindle Assembly Checkpoint in Human Cells. Cell Rep. *12*, 66–78.

Schumacher, J. M., Ashcroft, N., Donovan, P. J., and Golden, A. (1998). A highly conserved centrosomal kinase, AIR-1, is required for accurate cell cycle progression and segregation of developmental factors in Caenorhabditis elegans embryos. Development *125*, 4391–4402.

Schwartz, G. K. *et al.* (2002). Phase I study of the cyclin-dependent kinase inhibitor flavopiridol in combination with paclitaxel in patients with advanced solid tumors. J. Clin. Oncol. *20*, 2157–2170.

Sebastian, M. *et al.* (2010). The efficacy and safety of BI 2536, a novel Plk-1 inhibitor, in patients with stage IIIB/IV non-small cell lung cancer who had relapsed after, or failed, chemotherapy: results from an open-label, randomized phase II clinical trial. J. Thorac. Oncol. *5*, 1060–1067.

Sedelnikova, O. A., Rogakou, E. P., Panyutin, I. G., and Bonner, W. M. (2002). Quantitative detection of (125)IdU-induced DNA double-strand breaks with gamma-H2AX antibody. Radiat. Res. *158*, 486–492.

Sedlacek, H. H. (2001). Mechanisms of action of flavopiridol. Crit. Rev. Oncol. Hematol. *38*, 139–170.

Seki, A., Coppinger, J. A., Jang, C.-Y., Yates, J. R., and Fang, G. (2008). Bora and the kinase Aurora a cooperatively activate the kinase Plk1 and control mitotic entry. Science (80-.). *320*, 1655–1658.

Sells, T. B. *et al.* (2015). MLN8054 and Alisertib (MLN8237): Discovery of Selective Oral Aurora A Inhibitors. ACS Med. Chem. Lett. *6*, 630–634.

Senderowicz, A. M. (1999). Flavopiridol: the first cyclin-dependent kinase inhibitor in human clinical trials. Invest. New Drugs, 313–320.

Seo, Y., Yan, T., Schupp, J. E., Radivoyevitch, T., and Kinsella, T. J. (2005). Schedule-dependent drug effects of oral 5-iodo-2-pyrimidinone-2'- deoxyribose as an in vivo radiosensitizer in U251 human glioblastoma xenografts. Clin. Cancer Res. *11*, 7499–7507.

Seo, Y., Yan, T., Schupp, J. E., Yamane, K., Radivoyevitch, T., and Kinsella, T. J. (2006). The interaction between two radiosensitizers: 5-Iododeoxyuridine and caffeine. Cancer Res. *66*, 490–498.

Simeonov, A. (2013). Recent developments in the use of differential scanning fluorometry in protein and small molecule discovery and characterization. Expert Opin. Drug Discov. *8*, 1071–1082.

Smith, E. *et al.* (2011). Differential control of Eg5-dependent centrosome separation by Plk1 and Cdk1. Embo J *30*, 2233–2245.

Smits, V. A., Klompmaker, R., Arnaud, L., Rijksen, G., Nigg, E. A., and Medema, R. H. (2000). Polo-like kinase-1 is a target of the DNA damage checkpoint. Nat. Cell Biol. *2*, 672–676.

Song, B., Liu, X. S., Davis, K., and Liu, X. (2011). Plk1 phosphorylation of Orc2 promotes DNA

replication under conditions of stress. Mol. Cell. Biol. *31*, 4844–4856.

Song, L., and Rape, M. (2008). Reverse the curse-the role of deubiquitination in cell cycle control. Curr. Opin. Cell Biol. *20*, 156–163.

Sourisseau, T., Maniotis, D., Mccarthy, A., Tang, C., Lord, C. J., Ashworth, A., and Linardopoulos, S. (2010). Aurora-A expressing tumour cells are deficient for homology-directed DNA double strand-break repair and sensitive to PARP inhibition. EMBO Mol. Med. *2*, 130–142.

Steegmaier, M. *et al.* (2007). BI 2536, a Potent and Selective Inhibitor of Polo-like Kinase 1, Inhibits Tumor Growth In Vivo. Curr. Biol. *17*, 316–322.

Stegmeier, F. *et al.* (2007). Anaphase initiation is regulated by antagonistic ubiquitination and deubiquitination activities. Nature *446*, 876–881.

Sumara, I., Gime, J. F., Gerlich, D., Hirota, T., Kraft, C., Torre, C. De, Ellenberg, J., and Peters, J. (2004). Roles of Polo-like Kinase 1 in the Assembly of Functional Mitotic Spindles. Curr. Biol. *14*, 1712–1722.

Sun, H., Wang, Y., Wang, Z., Meng, J., Qi, Z., and Yang, G. (2014). Aurora-A controls cancer cell radio- and chemoresistance via ATM/Chk2-mediated DNA repair networks. Biochim. Biophys. Acta - Mol. Cell Res. *1843*, 934–944.

Sundell-Berman, S., and Johanson, K. J. (1992). DNA Strand Breaks in IUdR Containing Cells After Irradiation with Low-Energy X Rays. 080–090.

Sunkel, C. E., and Glover, D. M. (1988). polo, a mitotic mutant of Drosophila displaying abnormal spindle poles. J. Cell Sci. *89*, 25–38.

Sur, S., Pagliarini, R., Bunz, F., Rago, C., Diaz, L. a, Kinzler, K. W., Vogelstein, B., and Papadopoulos, N. (2009). A panel of isogenic human cancer cells suggests a therapeutic approach for cancers with inactivated p53. Proc. Natl. Acad. Sci. U. S. A. *106*, 3964–3969.

Takizawa, C. G., and Morgan, D. O. (2000). Control of mitosis by changes in the subcellular location of cyclin-B1-Cdk1 and Cdc25C. Curr. Opin. Cell Biol. *12*, 658–665.

Tanaka, T., Kimura, M., and Matsunaga, K. (1999). Centrosomal Kinase AIK1 Is Overexpressed in Invasive Ductal Carcinoma of the Breast Advances in Brief Centrosomal Kinase AIK1 Is Overexpressed in Invasive Ductal Carcinoma. Cancer, 2041–2044.

Tang, J., Yang, X., and Liu, X. (2008). Phosphorylation of Plk1 at Ser326 regulates its functions during mitotic progression. Oncogene *27*, 6635–6645.

Taverna, P., Hwang, H. shin, Schupp, J. E., Radivoyevitch, T., Session, N. N., Reddy, G., Zarling, D. A., and Kinsella, T. J. (2003). Inhibition of base excision repair potentiates iododeoxyuridine-induced cytotoxicity and radiosensitization. Cancer Res. *63*, 838–846.

Thomas, Y. *et al.* (2016). Cdk1 Phosphorylates SPAT-1/Bora to Promote Plk1 Activation in C. elegans and Human Cells. Cell Rep. *15*, 510–518.

Tsvetkov, L. M., Tsekova, R. T., Xu, X., and Stern, D. F. (2005). The Plk1 Polo Box Domain Mediates a Cell Cycle and DNA Damage Regulated Interaction with Chk2. Cell Cycle *4*, 609–617.

Tsvetkov, L., and Stern, D. F. (2005). Phosphorylation of Plk1 at S137 and T210 is Inhibited in Response to DNA Damage. Cell Cycle *4*, 166–171.

U.S. National Institutes of Health (2013). ClinicalTrials.gov.

Vose, J. M., Friedberg, J. W., Waller, E. K., Cheson, B. D., Juvvigunta, V., Fritsch, H., Petit, C., Munzert, G., and Younes, A. (2013). The Plk1 inhibitor BI 2536 in patients with refractory or relapsed non-Hodgkin lymphoma: a phase I, open-label, single dose-escalation study. Leuk. Lymphoma *54*, 708–713.

van Vugt, M. A. T. M. *et al.* (2010). A mitotic phosphorylation feedback network connects Cdk1, Plk1, 53BP1, and Chk2 to inactivate the G(2)/M DNA damage checkpoint. PLoS Biol. *8*, 1–20.

van Vugt, M. A. T. M., van de Weerdt, B. C. M., Vader, G., Janssen, H., Calafat, J., Klompmaker, R., Wolthuis, R. M. F., and Medema, R. H. (2004). Polo-like kinase-1 is required for bipolar spindle formation but is dispensable for anaphase promoting complex/Cdc20 activation and initiation of cytokinesis. J. Biol. Chem. *279*, 36841–36854.

Walter, A. O., Seghezzi, W., Korver, W., Sheung, J., and Lees, E. (2000). The mitotic serine / threonine kinase Aurora2 / AIK is regulated by phosphorylation and degradation. 4906–4916.

Wang, X. X., Liu, R., Jin, S. Q., Fan, F. Y., and Zhan, Q. M. (2006). Overexpression of Aurora-A kinase promotes tumor cell proliferation and inhibits apoptosis in esophageal squamous cell carcinoma cell line. Cell Res. *16*, 356–366.

Wang, Y., and Iliakis, G. (1992). Effects of 5'-iododeoxyuridine on the repair of radiation induced potentially lethal damage interphase chromatin breaks and DNA double strand breaks in chinese hamster ovary cells. Int. J. Radiat. Oncol. Biol. Phys. *23*, 353–360.

Wang, Y., Sun, H., Wang, Z., Liu, M., Qi, Z., Meng, J., Sun, J., and Yang, G. (2014). Aurora-A: a potential DNA repair modulator. Tumor Biol. *35*, 2831–2836.

Watanabe, N., Arai, H., Nishihara, Y., Taniguchi, M., Watanabe, N., Hunter, T., and Osada, H. (2004). M-phase kinases induce phospho-dependent ubiquitination of somatic Wee1 by SCFbeta-TrCP. Proc. Natl. Acad. Sci. U. S. A. *101*, 4419–4424.

van de Weerdt, B. C. M., Vugt, M. A. T. M. Van, Lindon, C., Kauw, J. J. W., Rozendaal, M. J., Klompmaker, R., Wolthuis, R. M. F., and Medema, R. H. (2005). Uncoupling Anaphase-Promoting Complex / Cyclosome Activity from Spindle Assembly Checkpoint Control by Deregulating Polo-Like Kinase 1. Mol. Cell. Biol. *25*, 2031–2044.

Wickliffe, K., Williamson, A., Jin, L., and Rape, M. (2009). The Multiple Layers of Ubiquitin-Dependent Cell Cycle Control. Chem. Rev. *109*, 1537–1548.

Williams, D. M., and Cole, P. A. (2001). Kinase chips hit the proteomics era. Trends Biochem. Sci. *26*, 271–273.

Winer, E. P. *et al.* (2004). Failure of higher-dose paclitaxel to improve outcome in patients with metastatic breast cancer: Cancer and leukemia group B trial 9342. J. Clin. Oncol. *22*, 2061–2068.

Wlodkowic, D., Telford, W., Skommer, J., and Darzynkiewicz, Z. (2011). Apoptosis and Beyond: Cytometry in Studies of Programmed Cell Death. Methods Cell Biol *103*, 55–98.

Wolfe, B. A., Takaki, T., Petronczki, M., and Glotzer, M. (2009). Polo-like kinase 1 directs assembly of the HsCyk-4 RhoGAP/Ect2 RhoGEF complex to initiate cleavage furrow formation. PLoS Biol. *7*, 1–15.

Yamamoto, T., Ebisuya, M., Ashida, F., Okamoto, K., Yonehara, S., and Nishida, E. (2006). Continuous ERK Activation Downregulates Antiproliferative Genes throughout G1 Phase to Allow Cell-Cycle Progression. Curr. Biol. *16*, 1171–1182.

Yamamoto, Y., Ibusuki, M., Nakano, M., Kawasoe, T., Hiki, R., and Iwase, H. (2009). Clinical significance of basal-like subtype in triple-negative breast cancer. Breast Cancer *16*, 260–267.

Yan, T., Seo, Y., Schupp, J. E., Zeng, X., Desai, A. B., and Kinsella, T. J. (2006). Methoxyamine potentiates iododeoxyuridine-induced radiosensitization by altering cell cycle kinetics and enhancing senescence. Mol. Cancer Ther. *5*, 893–902.

Yim, H. (2013). Current clinical trials with polo-like kinase 1 inhibitors in solid tumors. Anticancer. Drugs *24*, 999–1006.

Yuan, J., and Chen, J. (2010). MRE11-RAD50-NBS1 complex dictates DNA repair independent of H2AX. J. Biol. Chem. *285*, 1097–1104.

Zeidner, J. F., and Karp, J. E. (2015). Clinical activity of alvocidib (flavopiridol) in acute myeloid leukemia. Leuk. Res. *39*, 1312–1318.

Zhai, S., Senderowicz, A. M., Sausville, E. A., and Figg, W. D. (2002). Flavopiridol, a novel cyclin-dependent kinase inhibitor, in clinical development. Ann. Pharmacother. *36*, 905–911.

Zhang, C.-Z., Spektor, A., Cornils, H., Francis, J. M., Jackson, E. K., Liu, S., Meyerson, M., and Pellman, D. (2015). Chromothripsis from DNA damage in micronuclei. Nature *522*, 179–184.

Zhang, J., Ma, Z., Treszezamsky, A., and Powell, S. N. (2005). MDC1 interacts with Rad51 and facilitates homologous recombination. Nat. Struct. Mol. Biol. *12*, 902–909.

Zhang, N., Fu, J. N., and Chou, T. C. (2016). Synergistic combination of microtubule targeting anticancer fludelone with cytoprotective panaxytriol derived from panax ginseng against

MX-1 cells in vitro: Experimental design and data analysis using the combination index method. Am. J. Cancer Res. *6*, 97–104.

Zhou, N. *et al.* (2013). The investigational aurora kinase A inhibitor MLN8237 induces defects in cell viability and cell-cycle progression in malignant bladder cancer cells in vitro and in vivo. Clin. Cancer Res. *19*, 1717–1728.

Zhu, C., Lau, E., Schwarzenbacher, R., Bossy-Wetzel, E., and Jiang, W. (2006). Spatiotemporal control of spindle midzone formation by PRC1 in human cells. Proc. Natl. Acad. Sci. U. S. A. *103*, 6196–6201.

Zorba, A., Buosi, V., Kutter, S., Kern, N., Pontiggia, F., Cho, Y. J., and Kern, D. (2014). Molecular mechanism of Aurora A kinase autophosphorylation and its allosteric activation by TPX2. Elife *2014*, 1–24.

Appendix

Peptide array to investigate upstream kinases of kinase T-loops and other proteins of interest

Figure 1

Spot Location	Peptide Sequence	Protein or Corresponding Control
A1	SDLNLDDSFVDTWFS	Plk1-Control
A2	QANSRRISLCIPKDR	Aurora A-Control
A3	KGSTRRKSLVGKIPP	Aurora B-Control
A4	EGPSLPGSPVKKKAR	Cdk1-Control
A5	TGPSPPLSPPPPPSP	ERK1-Control
A6	TPTPPPLSPTPPGPA	ERK2-Control
A7	DSGFCLDSPGPLDSK	Nek11-Control
A8	DDFFLGFSYNRPTVG	Nek6-Control
A9	MKKNFAYSFIKMKKK	Nek2-Control
A10	NKAMPIASPKFSRNT	Bub1-Control
A11	EAAGPAPsPMRAANR	Bub1/BubR1-Control
A12	VKLNKNTTPNKKLNK	TTK/Mps1-Control
B1	KGQKYFDSGDYNMAK	Gwl/MASTL-Control
B2	MARTKQTARKS	Haspin/GSG2-Control
B3	VEYDGERKKTLCGTPNYI	Plk1
B4	ERKKTLCGTPNYIAPEVL	Plk1
B5	PPEQRKKTICGTPNYVAP	Plk3
B6	PHEKHYTLCGTPNYISEI	Plk4
B7	APSSRRTTLCGTLDYLPP	Aurora A
B8	VHAPSLRRKTMCGTLDYL	Aurora B
B9	RRKTMCGTLDYLPPEMIE	Aurora B
B10	HDTSFAKTFVGTPYYMSP	Nek2 (NIMA)
B11	FSSETTAAHSLVGTPYYM	Nek6
B12	FFSSKTTAAHSLVGTPYY	Nek7
C1	MGSCDLATTLTGTPHYMS	Nek11
C2	LNSEYSMAETLVGTPYYM	Nek9
C3	LNSTVELARTICGTPYYL	Nek1
C4	TIFTAKCETSGFQCVEML	Bub1
C5	QLDVFTLSGFRTVQILEG	BubR1
C6	ANQMQPDTTSVVKDSQVG	TTK/Esk (MPS1)
C7	HQRCLAHSLVGTPNYIAP	MEN/SIN Kinases- LATS1/2
C8	HPEHAFYEFTFRRFFDDN	MEN/SIN Kinases- LATS1
C9	DINMMDILTTPSMAKPRQ	Gwl
C10	MVNAKLPIGTPDYMAPEV	Citron Kinase
C11	FLYEMLVGDTPFYADSLV	ROCK1/2
C12	KPDRKKRYTVVGNPYWM	LIML1/2
D1	LTDTMAkRNTVIGTPFWM	STK3/MST2
D2	HVADNDITPYLVSRFYRA	PRP4
D3	VVFCDVSMDEDLFTGDGD	Haspin/GSG2
D4	MAMDSSLQARLFPGLAIK	MCAK 1-18
D5	LAIKIQRSNGLIHSANVR	MCAK 15-32
D6	ANVRTVNLEKSCVSVEWA	MCAK 29-46
D7	VEWAEGGATKGKEIDFDD	MCAK 42-59
D8	LPLQENVTIQKQKRRSVN	MCAK 80-97
D9	IQKQKRRSVNSKIPAPKE	MCAK 88-105
D10	APKESLRSRSTRMSTVSE	MCAK 102-119
D11	STRMSTVSELRITAQEND	MCAK 111-128
D12	PAAANSRKQFSVPPAPTR	MCAK 134-151
E1	FSVPPAPTRPSCPAVAEI	MCAK 143-160
E2	AEIPLRMVSEEMEEQVHS	MCAK 158-175
E3	EEQVHSIRGSSSANPVNS	MCAK 170-187
E4	SANPVNSVRRKSCLVKEV	MCAK 181-198
E5	REEKKAQNSEMRMKRAQE	MCAK 205-222
E6	KRAQEYDSSFPNWEFARM	MCAK 218-235
E7	EFRATLECHPLTMTDPIE	MCAK 238-255
E8	KEIDVISIPSKCLLLVHE	MCAK 266-283
E9	EPKLKVDLTKYLENQAFC	MCAK 283-300
E10	FDFAFDETASNEVVYRFT	MCAK 301-318
E11	VVYRFTARPLVQTIFEGG	MCAK 313-329
E12	EGGKATCFAYGQTGSGKT	MCAK 325-345
F1	GSGKTHTMGGDLSGKAQN	MCAK 341-358
F2	KAQNASKGIYAMASRDVF	MCAK 355-372
F3	KLGLEVYVTFFEIYNGKL	MCAK 372-399
F4	GLQEHLVNSADDVIKMID	MCAK 433-450
F5	IDMGSACRTSGQTFANSN	MCAK 449-466
F6	GQTFANSNSSRSHACFQI	MCAK 459-476
F7	KGRMHGKFSLVDLAGNER	MCAK 481-498
F8	RGADTSSADRQTRMEGAE	MCAK 498-515
F9	MEGAEINKSLLALKECIR	MCAK 511-528
F10	PFRESKLTQVLRDSFIGE	MCAK 538-555
F11	IGENSRTCMIATISPGIS	MCAK 553-570
F12	SPGISSCEYTLNTLRYAD	MCAK 566-583
G1	RVKELSPHSGPSGEQLIQ	MCAK 584-601
G2	IQMETEEMEACSNGALIP	MCAK 600-617
G3	PGNLSKEEEELSSQMSSF	MCAK 617-634
G4	ELSSQMSSFNEAMTQIRE	MCAK 626-643
G5	GPDWLELSEMTEQPDYDL	MCAK 659-676
G6	DYDLETFVNKAESALAQQ	MCAK 673-690
G7	LAQQAKHFSALRDVIKAL	MCAK 687-704
G8	MQLEEQASRQISSKKRPQ	MCAK 708-725
G9	VPRAESGDSLGSEDRDLL	Anillin 616-633
G10	EDRDLLYSIDAYRSQRFK	Anillin 628-645
G11	QRFKETERPSIKQVIVRK	Anillin 642-659
G12	LLLIATGKRTLLIDELNK	Anillin 725-742
H1	GPQRKNKASPQSEFMPSK	Anillin 747-764
H2	MPSDKTIGGGDDSFNTFF	Tuba1B 36-53
H3	GGDDSFNTFFSETGAGKH	Tuba1B 44-61
H4	AVFVDLEPTVIDEVRTGT	Tuba1B 65-82
H5	ERLSVDYGKKSKLEFSIY	Tuba1B 155-172
H6	TTHTTLEHSDCAFMVDNE	Tuba1B 190-207
H7	RNLDIERPTYTNLNRLIS	Tuba1B 215-232
H8	DGALNVDLTEFQTNLVPY	Tuba1B 245-262
H9	EQLSVAEITNACFEPANQ	Tuba1B 284-301
H10	IATIKTKRSIQFVDWCPT	Tuba1B 332-349
H11	EGMEEGEFSEAREDMAAL	Tuba1B 411-428
H12	DYEEVGVDSVEGEGEEEG	Tuba1B 431-448

Figure 1: List of peptides included on array slide.

Sequences for A1-D3 were chosen to assay for the upstream kinases of phosphorylation sites in kinase T-loops. All other peptides span regions of interest for MCAK, Anillin, or α-Tubulin 1B.

Figure 2

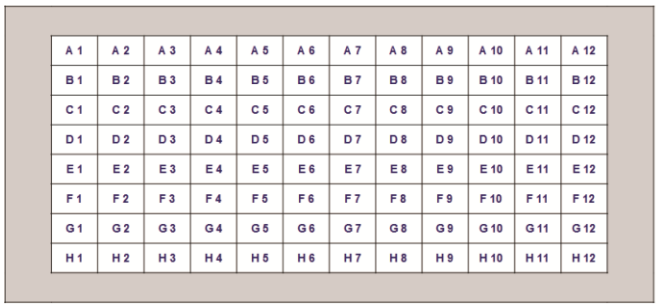
A 1 A 2 A 3 A 4 A 5 A 6 A 7 A 8 A 9 A 10 A 11 A 12
B 1 B 2 B 3 B 4 B 5 B 6 B 7 B 8 B 9 B 10 B 11 B 12
C 1 C 2 C 3 C 4 C 5 C 6 C 7 C 8 C 9 C 10 C 11 C 12
D 1 D 2 D 3 D 4 D 5 D 6 D 7 D 8 D 9 D 10 D 11 D 12
E 1 E 2 E 3 E 4 E 5 E 6 E 7 E 8 E 9 E 10 E 11 E 12
F 1 F 2 F 3 F 4 F 5 F 6 F 7 F 8 F 9 F 10 F 11 F 12
G 1 G 2 G 3 G 4 G 5 G 6 G 7 G 8 G 9 G 10 G 11 G 12
H 1 H 2 H 3 H 4 H 5 H 6 H 7 H 8 H 9 H 10 H 11 H 12

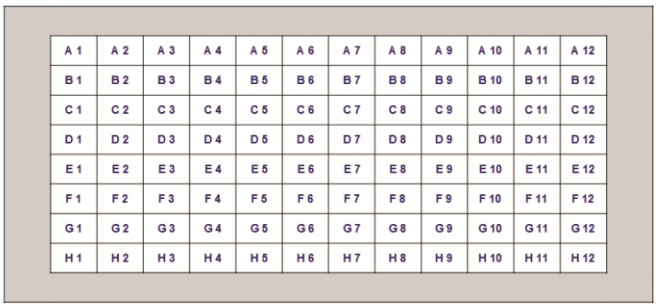
A 1 A 2 A 3 A 4 A 5 A 6 A 7 A 8 A 9 A 10 A 11 A 12
B 1 B 2 B 3 B 4 B 5 B 6 B 7 B 8 B 9 B 10 B 11 B 12
C 1 C 2 C 3 C 4 C 5 C 6 C 7 C 8 C 9 C 10 C 11 C 12
D 1 D 2 D 3 D 4 D 5 D 6 D 7 D 8 D 9 D 10 D 11 D 12
E 1 E 2 E 3 E 4 E 5 E 6 E 7 E 8 E 9 E 10 E 11 E 12
F 1 F 2 F 3 F 4 F 5 F 6 F 7 F 8 F 9 F 10 F 11 F 12
G 1 G 2 G 3 G 4 G 5 G 6 G 7 G 8 G 9 G 10 G 11 G 12
H 1 H 2 H 3 H 4 H 5 H 6 H 7 H 8 H 9 H 10 H 11 H 12

Figure 2: Peptide placement on slide arrays.

Letter-number combination corresponds to indicated peptide on peptide list

Figure 3

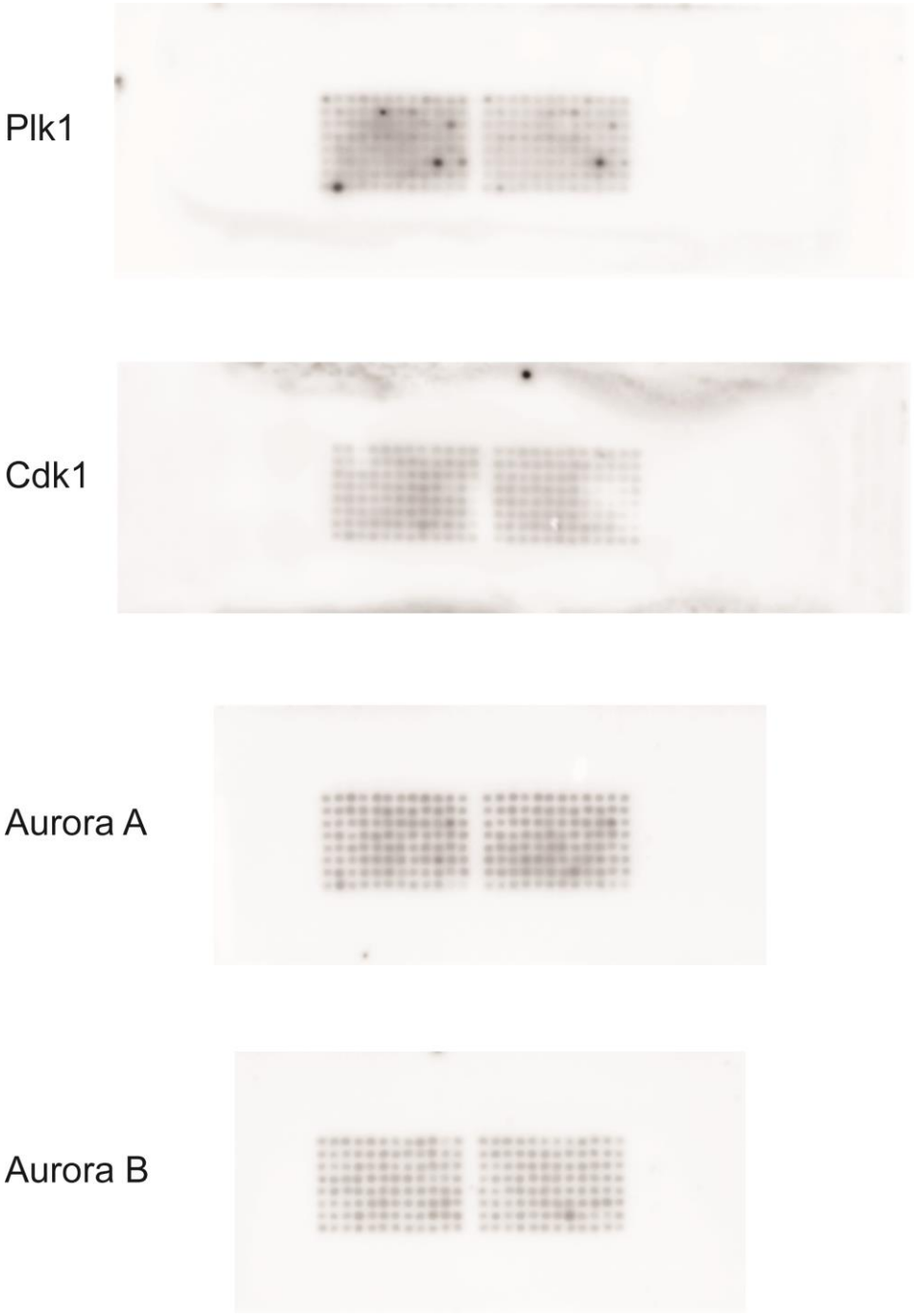

Figure 3: Results of peptide arrays incubated with indicated kinase

Figure 4

Spot Location	Peptide Sequence	Protein or Corresponding Control
A1	SDLNLDDSFVDTWFS	Plk1-Control
B6	PHEKHYTLCGTPNYISEI	Plk4
B8	VHAPSLRRKTMCGTLDYL	Aurora B
C11	FLYEMLVGDTPFYADSLV	ROCK1/2
D3	FCDVSMDEDLFTGDGD	Haspin/GSG2
D6	ANVRTVNLEKSCVSVEWA	MCAK 29-46
F10	PFRESKLTQVLRDSFIGE	MCAK 538-555
F12	SPGISSCEYTLNTLRYAD	MCAK 566-583
G5	GPDWLELSEMTEQPDYDL	MCAK 659-676
G9	VPRAESGDSLGSEDRDLL	Anillin 616-633
H2	MPSDKTIGGGDDSFNTFF	Tuba1B 36-53
H8	DGALNVDLTEFQTNLVPY	Tuba1B 245-262

Figure 4: Results of peptide array incubated with recombinant Plk1

Summarized results of peptide array incubated with GST-Plk1 kinase domain (Amino Acids 1-352)

Figure 5

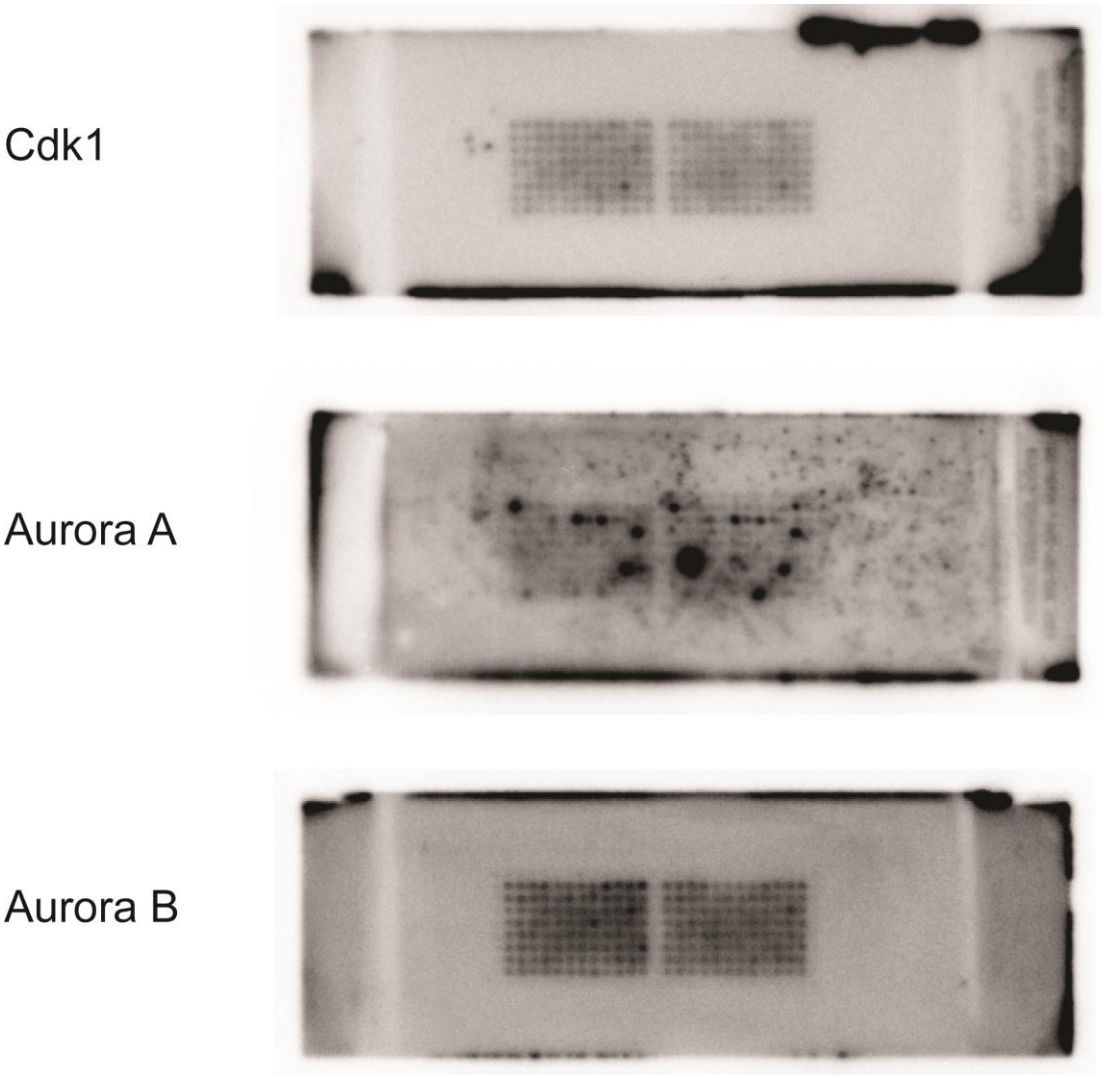

Figure 5: Results of peptide arrays incubated with indicated kinase following blocking step

Methods

Adapted from JPT protocol:
https://www.jpt.com/fileadmin/user_upload/Protocol_Random_Kinase_Peptide_Microarray.pdf

Reaction Mixture

Applicable kinase buffer- up to 350µl

Kinase- 1Unit (for recombinant Plk1 that I purified, I used 20µg)

1µM cold ATP

1mM DTT

50µCi [32P] ATP

Procedure:

1. Set heat block so that humidity chamber is at 30°C (monitor with thermometer, 31°C worked for me)
2. Create humidity chamber (heat up ahead of time) and array sandwich.
    a. Soak thick filter paper in 1:1 PBS:ddH2O
    b. Suggested humidity chamber: medium petri dish inside large petri dish. However, other formats may work.
    c. Lay peptide array face up inside humidity chamber. If surface is glass, lay peptide array on filter paper to reduce glass-glass sticking
    d. Place spacers on each short side of array and place dummy slide on top
3. Optional blocking step
    a. Kinase buffer, cold ATP, DTT, GTP (1mM), BSA (2%)
    b. 30°C, 2+ hous
    c. Open in beaker of PBS
4. Create reaction mixture and pipette carefully between slides. Watch for dry gaps. Detergent may help. Record dry areas in notebook so can compare to resulting image
5. Incubate for 3-5 hours
6. Open slides in beaker of PBS, to reduce surface tension that could pull peptides off the slide
7. Wash slides in 0.1M Phosphoric Acid 5X, 3-4 minutes each (I did wash steps inside medium petri dish on orbital shaker).
8. Wash slides in ddH2O 5X, 3-4 minutes each
9. Wash slides in methanol 1X-alllow slide to dry
10. For exposure and development
    a. Place slides in cassette, place film on top

b. I placed flexible rubber and then a piece of hard plastic (borrowed from Beebe lab) on top to help get slide as close to the film as possible
c. Close cassette and place weights on top (again to get the slide as close to the film as possible)
d. Expose overnight, develop as usual